UCRL-10634

University of California

Ernest O. Lawrence Radiation Laboratory

BIO-ORGANIC CHEMISTRY QUARTERLY REPORT

September through November 1962

TWO-WEEK LOAN COPY

This is a Library Circulating Copy which may be borrowed for two weeks. For a personal retention copy, call Tech. Info. Division, Ext. 5545

DISCLAIMER

This document was prepared as an account of work sponsored by the United States Government. While this document is believed to contain correct information, neither the United States Government nor any agency thereof, nor the Regents of the University of California, nor any of their employees, makes any warranty, express or implied, or assumes any legal responsibility for the accuracy, completeness, or usefulness of any information, apparatus, product, or process disclosed, or represents that its use would not infringe privately owned rights. Reference herein to any specific commercial product, process, or service by its trade name, trademark, manufacturer, or otherwise, does not necessarily constitute or imply its endorsement, recommendation, or favoring by the United States Government or any agency thereof, or the Regents of the University of California. The views and opinions of authors expressed herein do not necessarily state or reflect those of the United States Government or any agency thereof or the Regents of the University of California.

UCRL-10634
UC-4 Chemistry
TID-4500 (18th Ed.)

UNIVERSITY OF CALIFORNIA
Lawrence Radiation Laboratory
Berkeley, California

Contract No. W-7405-eng-48

BIO-ORGANIC CHEMISTRY QUARTERLY REPORT

September through November 1962

January 18, 1963

Printed in USA. Price $2.50. Available from the
Office of Technical Services
U. S. Department of Commerce
Washington 25, D.C.

BIO-ORGANIC CHEMISTRY QUARTERLY REPORT

September through November 1962

Contents

1. Carbon-14 and Nitrogen-15 Tracer Studies of Amino Acid Synthesis during Photosynthesis by Chlorella (Bassham, Kirk, and Crowley) 1

2. Some Properties of a Subunit of the Higher Plant Chloroplast Lamella (Biggins and Park) 13

3. Depolarization of Light-Scattering and of Fluorescence by Spinach Quantasomes (Sauer) 23

4. Effect of α-Pyridyl-hydroxymethane-sulfonic Acid on ^{14}C Fixation in Chloroplasts (Ullrich) 42

5. On the Use of the Nuclear Activation Reaction $^{18}O(\alpha, \eta)\ ^{21}Ne$ for ^{18}O Analysis (Shneour) 49

6. Photo-Induced Absorption Changes. I. Instrumentation (Kuntz) 56

7. Microspectrophotometric Studies of Some Organic Solids (Ilten and Sauer) 69

8. Isotopic Studies on the Radiation Decomposition of Crystalline Choline Chloride (Smith and Lemmon) 78

9. Synthesis of Organic Compounds by Electric Discharges (Oró) . 84

10. Synthesis of Organic Compounds by High-Energy Electrons (Oró) 102

11. Ultraviolet-Absorbing Compound(s) Reported Present in the Murray Meteorite (Oró) 114

* Preceding Quarterly Reports: UCRL-10479, UCRL-10350.

BIO-ORGANIC CHEMISTRY QUARTERLY REPORT

September through November 1962

M. Calvin, Director

Lawrence Radiation Laboratory and Department of Chemistry
University of California, Berkeley, California

January 18, 1963

1. CARBON-14 AND NITROGEN-15 TRACER STUDIES OF AMINO ACID SYNTHESIS DURING PHOTOSYNTHESIS BY CHLORELLA

James A. Bassham, Martha Kirk, and Gerald J. Crowley

In a previous quartely report[1] we described modifications and improvements in the steady-state photosynthesis apparatus that were made to enable us to carry out dual tracer experiments on the synthesis of amino acids by Chlorella. These modifications were designed to permit us to employ simultaneously carbon 14 in the form of $^{14}CO_2$ and $H^{14}CO_3^-$, and ^{15}N in the form of $^{15}NH_4^+$ as tracers to study the biosynthesis of amino acids. In the same report[2] we described methods that we were developing for the conversion of the amino acids to nitrogen gas and analysis of the ^{15}N content with the mass spectrometer. Also, we described analysis of the total content of amino acids by using a colorimetric method.

During the past year we have encountered great difficulties in perfecting these methods to a point where they could be used for an experiment. These difficulties have stemmed from several sources: (a) The mass spectrometer, which we were attempting to push to its limit of sensitivity, at first had a great many electronic defects which, over the course of the year, have been gradually corrected. (b) The analysis by mass spectrometer of very small amounts of nitrogen gas is inherently difficult because of the problem of air contamination. (c) The ninhydrin estimation of total amino acid content is easily thrown off by contaminating ions such as chloride, while at the same time the quantitative recovery of amino acids from paper chromatograms following two dimensional paper chromatography is made difficult by (a) the tendency of some amino acids to break down during chromatography and (b) by the ease with which the papers can be contaminated with ninhydrin positive substances. Individually, each of these problems has been overcome. However, the probability of doing a complete experiment and having all of the various analyses work at the same time has remained low. Nevertheless, some results have now been obtained which are of interest and will be reported.

---

1. Martha Kirk and J. A. Bassham, in Bio-Organic Chemistry Quarterly Report, UCRL-9772, March 1961, p. 97.

2. Ibid., p. 102.

Procedure for Photosynthetic Experiment

Chlorella pyrenoidosa grown in continuous-culture tubes[3] were centrifuged and resuspended in medium to 2-1/2% wet-packed cells/suspension volume. Sixty milliliters of this algae suspension was placed in the cell of the steady-state apparatus.[1] The nutrient medium used was the same as that reported in the preceding quarterly report.[4] The pH was set at 6 and the temperature at 20° C. The illumination by a bank of fluorescent tubes and by an incandescent lamp was the same as that described in the preceding quarterly report.[4] The algae were allowed to photosynthesize in the presence of 1.9% CO_2-in-air for 24 h, except for an 8-h period during the night when the lights were automatically turned off. About 25 min before the start of the experiment, the pH control was turned off and the algae were allowed to deplete the medium of ammonium ion. This was considered accomplished when the pH of the medium would not go any lower than 4.2.

At this time (time zero) the gas phase of the system was opened to the large reservoir of 2% $^{14}CO_2$ in air (about 6 μC/μM) and enough $NaH^{14}CO_3$ solution (24 μM, 0.5 mC) was injected into the solution through a rubber plug to bring the specific activity of the suspension immediately to that of the gas phase. Also injected at the same instant was 0.5 ml of a 0.1M solution of $^{15}NH_4OH$ or more as necessary to bring the pH to 6; further amounts were injected from time to time to control the pH at that level. Samples were withdrawn at predetermined times by means of the sampling valve, and were killed in 80% methanol contained in preweighed tubes.

Analysis of Amino Acids

Samples of two sizes were taken—those which contained about 1 ml of algae suspension (25 mg of wet-packed algae) and those which contained about 5 ml of suspension (125 mg wet-packed algae).

Aliquot portions of the smaller samples were concentrated and placed, without extraction, on chromatograms, which were then developed in the usual manner. After radioautography, the ^{14}C content of the individual amino acids in each sample was determined. Later the amino acid areas were eluted from the paper and rechromatographed in 1 dimension (ascending) by using butanol-acetic acid-water as developing solvent. These rechromatographed amino acids were used in the subsequent ninhydrin determination of the total amino acid content. Throughout this procedure radioactivity determinations were made to follow the losses of animo acids.

The larger samples were extracted with 80% alcohol, 20% alcohol, and then water, and the combined extracts were concentrated. Each sample was divided and applied to 15 different chromatographic papers, which were developed in the usual two dimensions (phenol-water and butanol-propionic acid-water). After radioautography, the amino acids from these papers

---

3. J. A. Bassham and M. Calvin, The Path of Carbon in Photosynthesis (Prentice-Hall Inc., Englewood Cliffs, New Jersey, 1957).
4. J. A. Bassham and Martha Kirk, in Bio-Organic Chemistry Quarterly Report, UCRL-10479, September 1962, p.3.

were eluted and the eluates containing a given amino acid from a given point were recombined and taken to dryness in vacuo, after which the amino acid was taken up and placed on a strip for ascending chromatography in butanol-acetic acid-water.

Analysis of ^{15}N

Following this second chromatography the strip was eluted and 0.1 ml of 0.5N NaOH was added. The contents of the tubes were then frozen by immersion in liquid nitrogen, placed in a desiccator over H_2SO_4, and evacuated with a pump to dryness. When dry, the residue was reconstituted in 0.5 ml of deionized water, and 0.1 ml of 0.8N citric acid solution was added, which, together with the sodium hydroxide already present, buffered the sample at pH 5.0. Then 0.4 ml of ninhydrin-KCN reagent[2] was added, the tubes were covered with glass marbles and placed in a boiling-water bath for 20 min to develop the ninhydrin color. After cooling in an ice bath, 2 or 3 drops of constant-boiling HCl was added to the solution until the color disappeared. In this way, the DYDA (diketohydrindine-diketohydrinamine) color complex was decomposed, releasing ammonium ion. This solution containing ammonium ion was then transferred into the oxidation apparatus shown in Fig. 1-1. The solution was placed in bulb A, and 0.5 ml of BrO^- solution (made up as in reference 2) was placed in bulb B. The apparatus was then attached to a vacuum line and evacuated at room temperature until a pressure of about 100 μ was recorded on the vacuum gauge. The solution was then frozen in liquid nitrogen and the evacuation continued until the vacuum gauge registered 0 μ. The contents of the flask were then allowed to thaw during continued pumping and once again were frozen. After the second freezing the flask was further evacuated until zero pressure was recorded. The stopcock connecting the flask to the vacuum line was then closed and the apparatus removed from the vacuum line. The contents of the flasks were thawed and the BrO^- solution in bulb B was poured into bulb A by tilting the entire apparatus, thus causing the oxidation of the ammonium ion to N_2. The course of the reaction could be observed by the bubbling which took place under the partial vacuum.

The apparatus was then taken to the vacuum line of the mass spectrometer and connected by means of ball joints. The mass-spectrometer inlet system was evacuated, and meanwhile the contents of the reaction flask were again frozen in liquid nitrogen. At this point a test was made of the possible leakage of the system, by closing the taps on the mass spectrometer that evacuate the expansion volume. If the vacuum held, the sample from the reaction flask was admitted to the mass spectrometer, then analysis of the mass peaks from mass 12 to 40 was carried out.

Since it was found that there is always some contamination by air as revealed by the height of the mass-32 peak, it was necessary to devise a method for calculating the $^{15}N/^{14}N+^{15}N$ ratio, which does not depend on the mass-28 peak. For this purpose we used the formula $F = 1/(1+2R)$, where R is the ratio of the mass-30 peak to the mass-29 peak and F is the fraction of $^{14}N/^{14}N+^{15}N$. The fraction of ^{15}N is then given by $1 - F$.

One correction to the 29 peak was made on the following basis: The mass-12 peak was used to calculate the mass-28 and -29 peak contributions

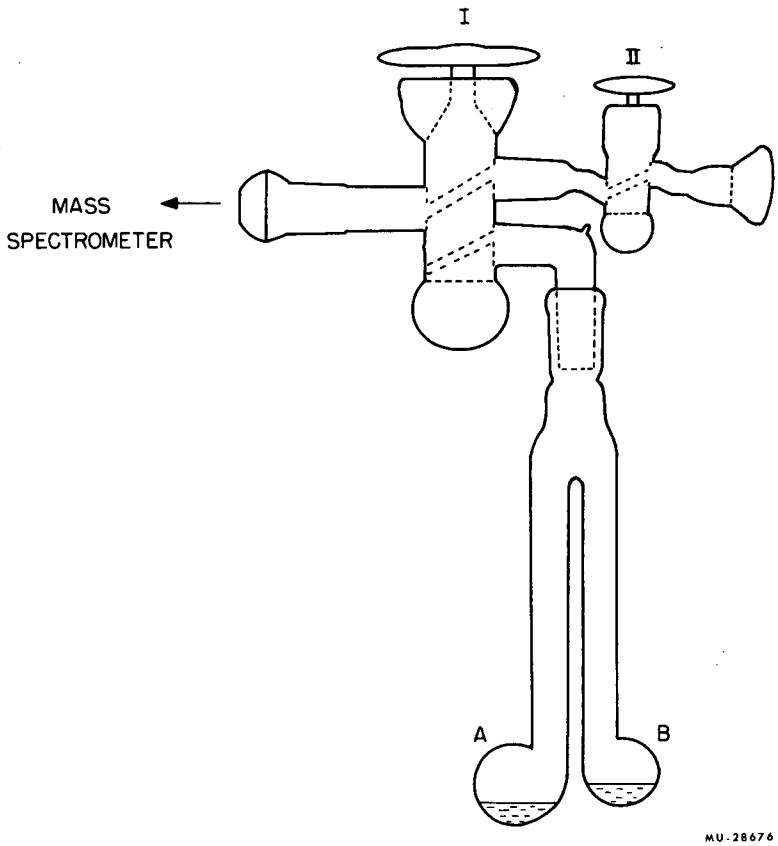

Fig. 1-1. Apparatus used for oxidation of $^{15}NH_4^+$ ion to $^{15}N_2$ for measurement of ^{15}N enrichment by mass spectrometry.

according to the ratio 29/28/12 = 1.1/100/3.2. In addition, each 100 units of 28 due to CO gives 0.25 units of 30, which therefore also must be corrected.

Another correction to mass 29 is based upon the air correction. The mass 28 due to air is assumed to be equal to 5.5 times the number of units of mass 32 (O_2). Then the correction of the peak height at 29 is 0.88 times the peak height 28 due to air. Thus, this correction for the peak height is given by 5.5×peak height 32×0.88/100.

It should be noted that the mass-32 peak could also be contributed to by O_2 arising from NaOBr breakdown. However, this possibility was obviated by the addition of KI to the NaOBr solution when it was prepared.[5]

Procedure for the Estimation of Total Amount of Amino Acid

The purification of amino acids for estimation of their total content followed the same chromatographic procedure as just described for the ^{15}N analysis—that is, a two-dimensional chromatography in the usual solvents, followed by an ascending one-dimensional chromatography in butanol-acetic acid-water. As in the ^{15}N estimation, the amino acids were eluted and 0.1 ml of 0.5N sodium hydroxide was added, after which the solution was taken to dryness in a dessicator over H_2SO_4. Then 0.1 ml of 0.8N citric acid solution and 0.5 ml of deionized water were added to bring the amino acid back into solution in a total volume of 0.6 ml. To each sample was then added 0.4 ml of ninhydrin KCN reagent (see reference 2), and the tubes were stoppered with glass marbles and boiled for 20 min in a boiling-water bath to develop the color. After boiling, the tubes were cooled for 5 min in an ice-water bath diluted to 2 ml with 60% isopropanol in water. The absorption at 570 mμ was then read on the Beckman DU spectrophotometer. The absorption was read against a blank which contained all reagents except the amino acids, and then was compared against the standard curve obtained by reading a series of samples of known amounts of glutamic acid. The total amounts of amino acids were then corrected for the amount of algae material originally extracted to give the amino acid spot, and the amount of amino acid was then calculated for 1 cc of wet-packed cells.

Results

As in previous experiments[6,7] we first calculated the micromoles of carbon in the actively turning-over reservoirs of amino acids by taking the saturation values of ^{14}C in the amino acids (when they were no longer increasing in radioactivity) and dividing by the ratio of ^{14}C to total carbon. We continuously obtained this ratio from the ionization-chamber and infrared-analyzer readings that were plotted on our multipoint recorder. The micromoles of ^{14}C were then divided by the number of atoms of carbon per molecule

5. A. P. Sims and E. C. Cocking, Nature 181, 474 (1958).
6. J. A. Bassham and Martha Kirk, Biochim. Biophys. Acta 43, 447 (1960).
7. D. C. Smith, J. A. Bassham, and Martha Kirk, Biochim. Biophys. Acta 48, 299 (1961).

to give micromoles of compound in the actively turning-over reservoir. This number could then be compared with the total micromoles of amino acids as determined by the ninhydrin estimation (Table 1-I). It should be mentioned that the total estimation of amino acids is still subject to some uncertainty, and that the values given represent only an approximate value (± 20%) based on the average of what we consider to be the best of several points. The general result is in agreement with our previous report[6], in which it was found that the actively turning-over reservoir of carbon was of the order of 1/3 to 1/4 the total pool of amino acids. Dividing the micromoles of ^{14}C at each time during the experiment by the total micromoles of amino acid, we get the percentage labeling of the carbon skeleton. These percentages of ^{14}C labeling are compared with the measured percentages of ^{15}N labeling in Fig. 1-2 through 1-5 for alanine, glutamic acid, aspartic acid, and glutamine, respectively. In the case of glutamine, it is not certain whether the ^{15}N percentage represents (a) both the amino group and the amide group, (b) only the amino group, or (c) some intermediate value. Presumably the ninhydrin reaction will affect only the amino group, converting it to DYDA. However, we suspect that the subsequent oxidation with hypobromite may oxidize not only the ammonium ion that was liberated from DYDA upon treatment with HCl, but also may oxidize the amide nitrogen to some extent.

Table 1-I. ^{14}C saturation level and total pool size of amino acid pools.

Amino acid	μM/ml wet-packed algae		% saturation
	Total	^{14}C level	
Glutamic	37	12.3	33.3
Aspartic	14	3.1	22.0
Glutamine	18	2.8	15.6
Alanine	25	.5	20.0

One result which stands out clearly from these experiments is the fact that the amino groups of the greater part of the total amino acid pools become labeled, unlike the carbon skeletons which become saturated at from 1/3 to 1/4 of the total pools of the amino acids. Thus, we can conclude that besides the synthesis of amino acids (presumably in the chloroplast) from radioactive carbon skeletons, there is simultaneous synthesis of amino acids (presumably outside the chloroplast) from unlabeled carbon skeletons. The source of these unlabeled carbon skeletons can only be surmised. (Presumably there may be a continuous breakdown and resynthesis of cellular protein.) If so, the large reservoir of unlabeled protein in the cell may be supplying the carbon skeletons for the synthesis of new amino acids. A consequence of this would be the dilution of the labeled nitrogen with unlabeled nitrogen from the breakdown of the proteins. Indeed, this appears to be the case, because the maximum labeling approached after 5 h was only about 70%.

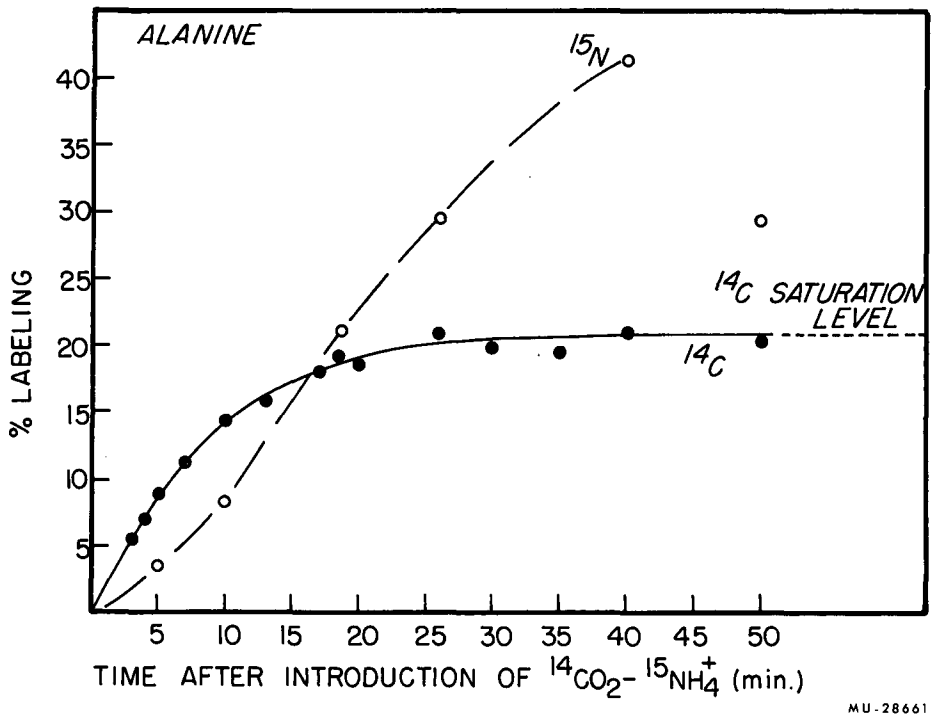

Fig. 1-2. Comparison of labeling of alanine with ^{15}N and ^{14}C during photosynthesis by Chlorella.

The ^{14}C labeling is based on a comparison of "micromoles of ^{14}C" found in the compound at a given time after introduction of $^{14}CO_2$ with the total micromoles of alanine (times 3) reported in Table 1-I. "Micromoles of ^{14}C" is calculated in in the usual way[6] by dividing the ^{14}C found in the compound by the ratio of $^{14}C/(^{14}C+^{12}C)$ of the carbon dioxide being taken up by the plant. Thus "micromoles of ^{14}C" is equal to the true micromoles of ^{14}C which would be found in the compound if 100% $^{14}CO_2$ were administered to the algae. The percentage labeling with ^{15}N is the actual labeling ratio ($\times$ 100) of $^{15}N/(^{15}N+^{14}N)$ as determined with the mass spectrometer described in the text.

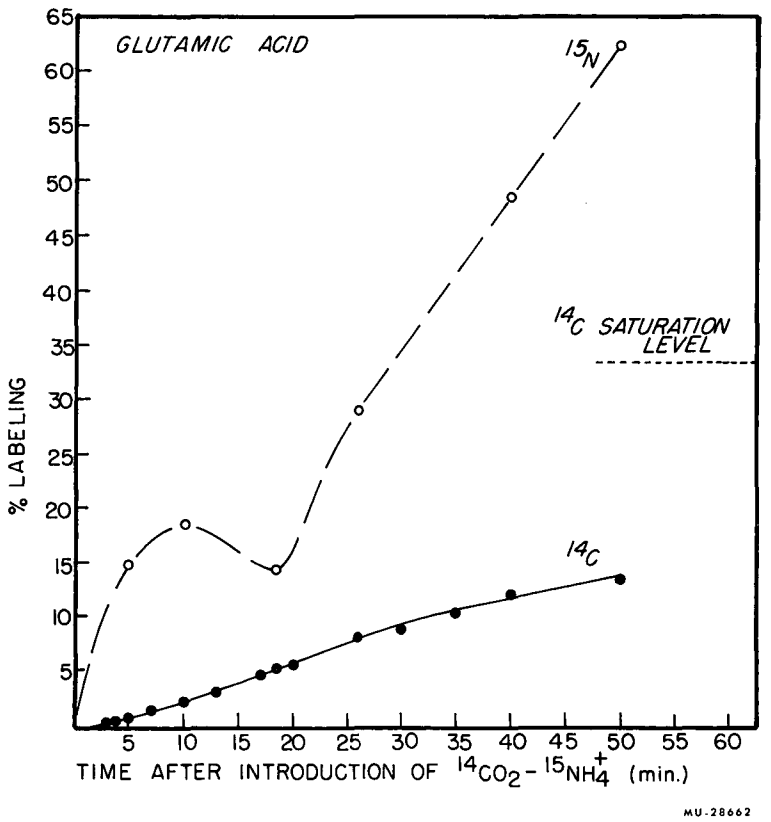

Fig. 1-3. Comparison of labeling of glutamic acid with ^{15}N and ^{14}C during photosynthesis by Chlorella. (For explanation see Fig. 1-2.)

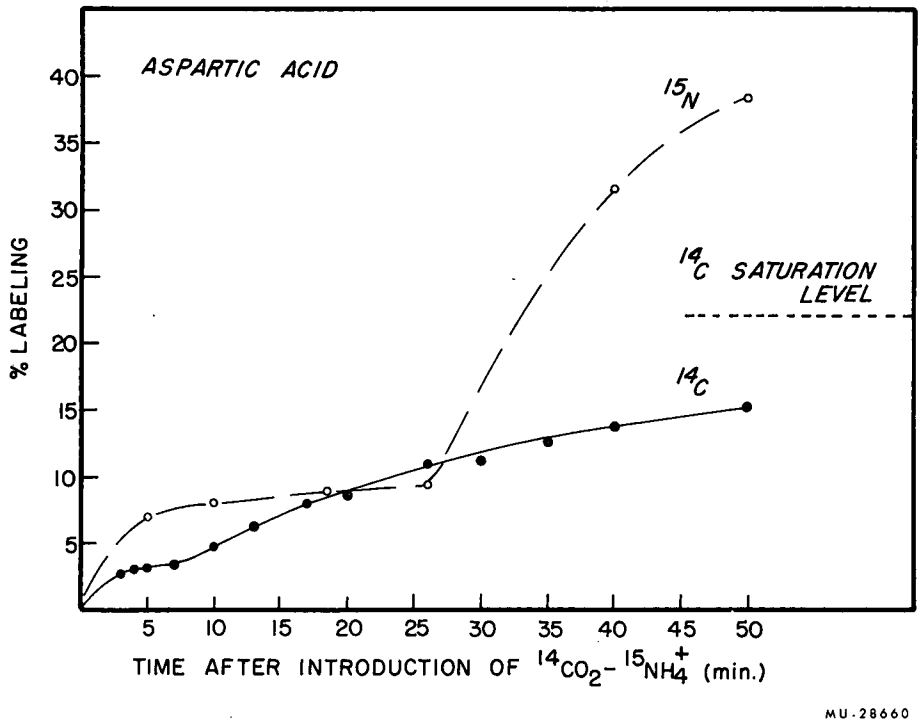

Fig. 1-4. Comparison of labeling of aspartic acid with ^{15}N and ^{14}C during photosynthesis by Chlorella. (For explanation see Fig. 1-2.)

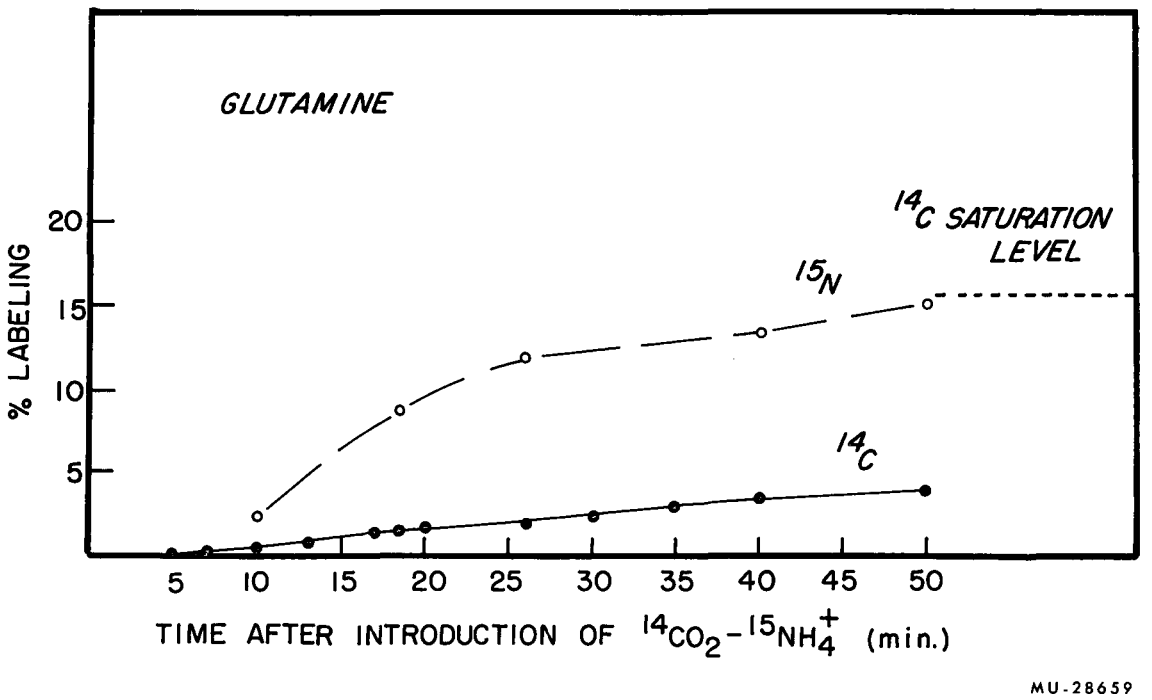

Fig. 1-5. Comparison of labeling of glutamine with ^{15}N and ^{14}C during photosynthesis by Chlorella. (For explanation see Fig. 1-2.)

An important objective of this work was to learn, if possible, the relative importance of initial points of entry of amino nitrogen into the biosynthetic pathways. The very rapid labeling of alanine, in particular, had suggested the possibility that there might be a direct incorporation of amino nitrogen into alanine by some reductive amination of pyruvic acid or even of phosphoenolpyruvic acid.[8] Unfortunately, the results given here do not permit an unequivocal answer to this question.

It may be that the simultaneous synthesis of amino acids at two different sites, suggested above, masks the situation at the photosynthetic site, where carbon skeletons formed from the carbon reduction cycle of photosynthesis are aminated. In Fig. 1-6, the relative rates of labeling are compared, in terms of percentage labeling of the total pools. Clearly, in these terms, the most rapidly ^{15}N-labeled amino acid is glutamic acid, followed by aspartic acid, and then by alanine. From the shapes of the labeling curves it appears that the depletion of NH_4^+ ion has had some non-steady-state effect. It may be that during this prelabeling period there was an accumulation of keto-acids due to protein breakdown in the absence of NH_4^+. The subsequent rapid labeling of certain amino acids such as glutamic and aspartic acids with ^{15}N upon addition of $^{15}NH_4^+$ would then most probably be of the non-photosynthetic type described above. Alanine labeling with ^{15}N does not exhibit such "non-steady-state" behavior, however. Perhaps pyruvic acid from protein breakdown is metabolized too rapidly and does not accumulate. In any event, the alanine ^{15}N labeling that is observed, though not as rapid as that in glutamic acid, could still represent direct amination of phosphoenolpyruvic acid. Alternatively, such alanine labeling could also result from transamination by glutamic acid (or aspartic acid) in a small pool, whose amino groups are rapidly labeled by reductive amination.

---

8. J. A. Bassham and M. Calvin, The Photosynthesis of Carbon Compounds, (W. A. Benjamin, Inc., New York, 1962).

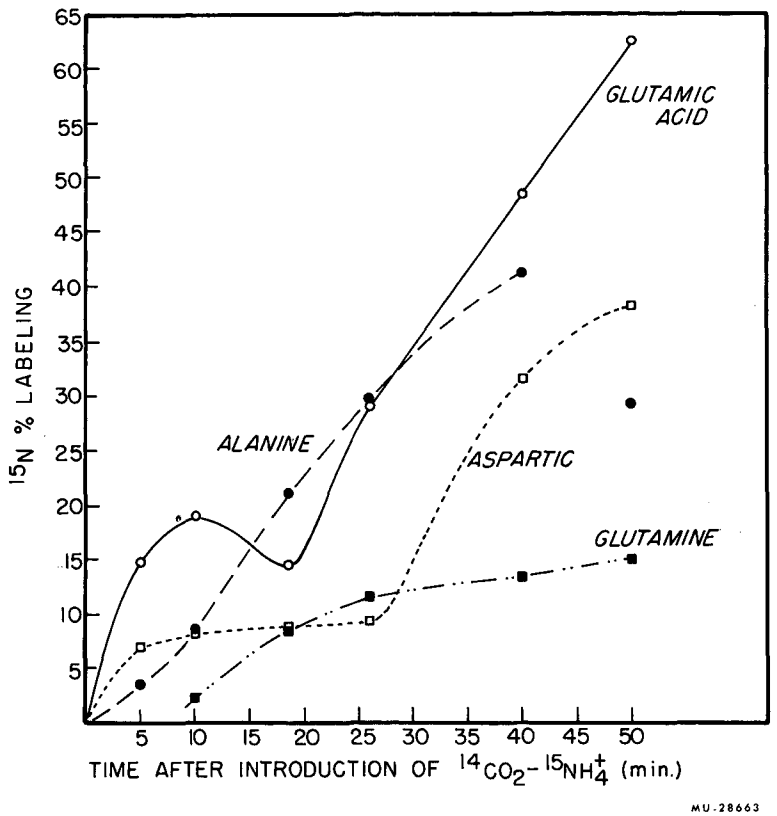

Fig. 1-6. Comparison of the ^{15}N labeling of alanine, glutamic acid, aspartic acid, and glutamine during photosynthesis by Chlorella.

2. SOME PROPERTIES OF A SUBUNIT OF THE HIGHER PLANT CHLOROPLAST LAMELLA

John Biggins and Roderic B. Park

Recently we developed a technique for the fragmentation of chloroplast lamellae that yielded a preparation of subunits which appeared homogeneous in the ultracentrifuge.[1] We now report a more extensive physical characterization of this particle and discuss its relation to the photosynthetic unit.

Methods

Preparation

The subunits were prepared by cysteine treatment of the sonicated insoluble fraction of washed chloroplasts as described previously.[1] One-tenth of one percent $HS \cdot CH_2 \cdot CH_2OH$ was found to be equally effective in the fragmentation.

Analytical Ultracentrifugation

A Spinco Model E ultracentrifuge was used with a standard 4° single sector cell. Measurements were made by an absorption technique using a 435-mμ filter instead of the normal chlorine-bromine filter on the uv optical system. This technique measured chlorophyll absorption in the Soret band. For studies of density gradient sedimentation equilibrium, both schlieren and absorption techniques were used. Absorption photographs were scanned by means of a microdensitometer. The rotor temperature was controlled during experiments by an RTIC system.

Results

Sedimentation Velocity

By use of the absorption technique and by virtue of the high molecular extinction of chlorophyll, determinations were carried out on very dilute solutions of the subunits. The sedimentation coefficient of the subunit is 86 Svedbergs (see Figs. 2-1 and 2-2). Full use of the sedimentation-velocity data was made by rigorous analysis of the boundary for polydispersity.[2]

The function

$$g(s) = \frac{dc/dx}{co}\left(\frac{x}{x_m}\right)^2 x\omega^2 t$$

was computed for every value of s for three boundary positions during a single centrifugation. The plot g(s) against s then represents a distribution of sedimentation coefficients in a preparation of subunits (Fig. 2-3).

---

1. J. Biggins and R. B. Park, in Bio-Organic Chemistry Quarterly Report, UCRL-10350, July 1962, p. 48.

2. J. B. Shumaker and H. K. Schachman, Biochim. Biophys. Acta 23, 630 (1957).

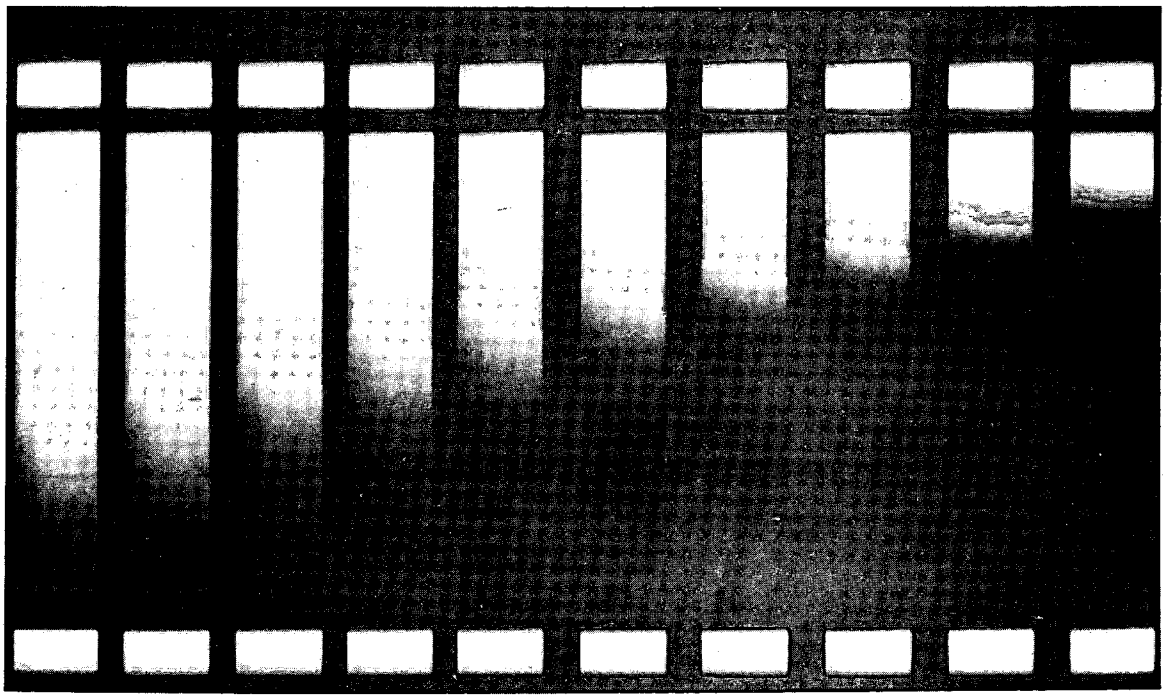

ZN-3545

Fig. 2-1. Absorption photograph taken during the sedimentation of spinach chloroplast subunits. Concentration A_{675} = 0.71; speed, 39,460 rpm; temp., 18.8° C; 1/10 ionic strength NaCl; 2-min intervals between exposures.

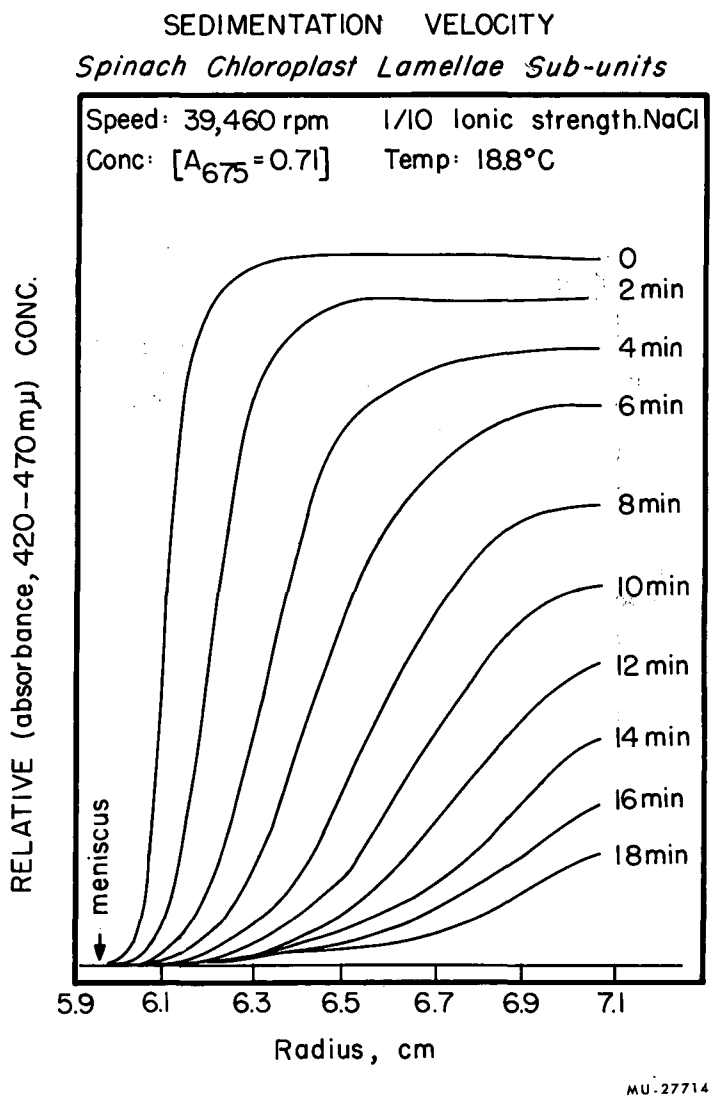

Fig. 2-2. Densitometer tracing of an absorption photograph taken during a centrifugation of chloroplast lamallae subunits. The subunits are 86 Svedbergs if 50% concentration points are used.

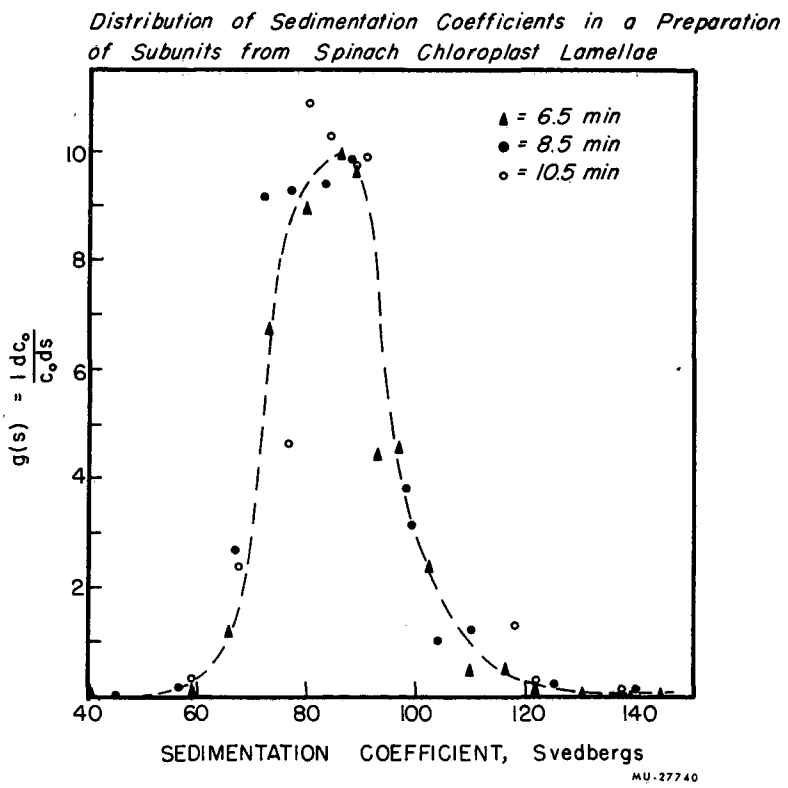

Fig. 2-3. Distribution of sedimentation coefficients in a preparation of subunits from spinach chloroplast lamellae.

Although the contribution due to diffusion is not yet known from an independent measurement, it is likely that the boundary spreading is due to polydispersity of the subunit preparation. However, the half-width at half maximum is within 15% of $g(s)_{max}$. This polydispersity could probably be accounted for on the basis of variation for a particle of this size and multimolecular complexity.

Density Gradient Sedimentation Equilibrium

As high electrolyte concentrations lead to aggregation of the subunits, the use of cesium chloride as a compound for forming a density gradient by centrifugal distribution was prohibited.[3] Sucrose was used instead and it was found that at least 72 h was necessary to form a linear density gradient along the rotational radius.

Twenty microliters of a subunit preparation ($A_{675} = 0.7$) was added to 1 ml of 0.45 g sucrose/ml and centrifuged for 3 days at 56,100 rpm at 3° C. As the equilibrium condition for sucrose was approached, the subunits migrated centrifugally from the meniscus and centripetally from the cell bottom and formed a discrete band where the buoyancy term was zero.

The subunit band (Fig. 2-4) was shown to be a Gaussian distribution by obtaining a linear plot of log concentration vs band width^2 (Fig. 2-5). Hence, the preparation is likely to be homogeneous with respect to density corresponding to 1.175 g/cc, which is expected for a particle containing 50% lipid and 50% protein. This value refers to the effective density of the subunits under these conditions. As 1.13M sucrose was used, it is probable that the particle dehydration occurred during the experiment, leading to an effective density greater than the real density.

Approach to Sedimentation Equilibrium

Excessive precession of the 8-lb standard rotor at very low speed rendered accurate determination of the molecular weight impossible. However, operation at slightly higher speed (3,617 rpm) and employing Archibald's method for treatment of data during the approach to sedimentation equilibrium gave a mean $M = 1.76 \times 10^6$. A partial specific volume of 0.85 was assumed.

Electron Microscopy

A sample of the subunit preparation was observed by negative staining with 1% phosphotungstic acid. Figure 2-6 corroborates the suggestion that the preparation is nonuniform, although not to a considerable extent. The variation in particle diameter is from 100 to 400 Å, and the subunits appear spherical.

Hill Reaction Using Ferricyanide

Excess cysteine and alkaline buffer was removed from a subunit preparation by means of gel filtration with Sephadex G-75 coarse. A column

3. M. S. Meselson, F. W. Stahl, and J. Vinograd, Proc. Nat. Acad Sci. U. S. 43, 328 (1958).

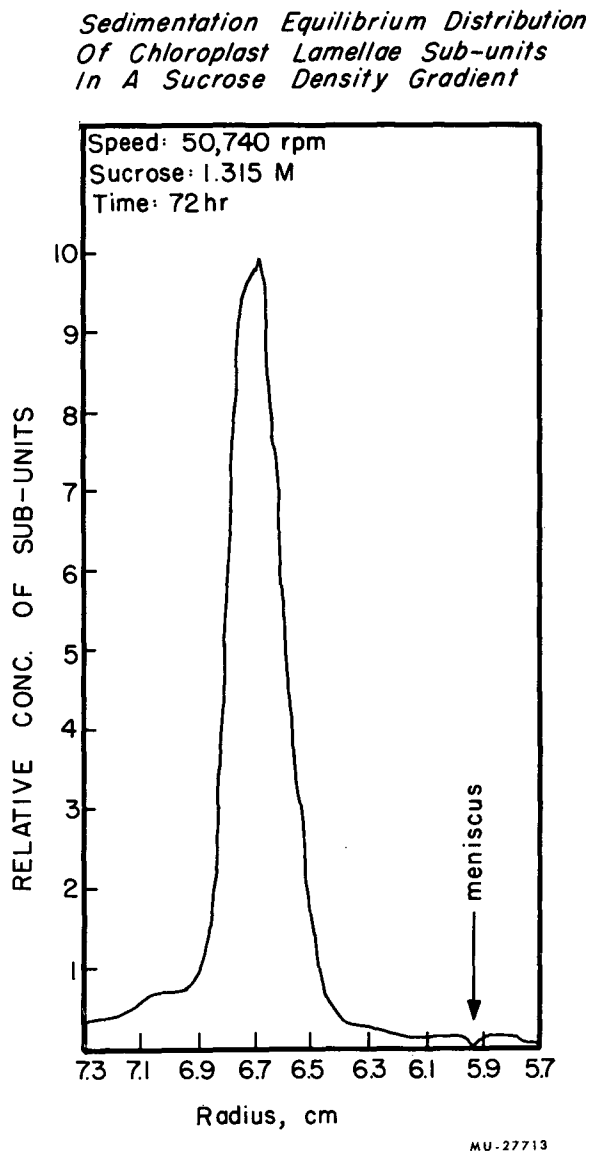

Fig. 2-4. Densitometer tracing of an absorption photograph taken at sedimentation equilibrium of lamellae subunits in a sucrose density gradient.

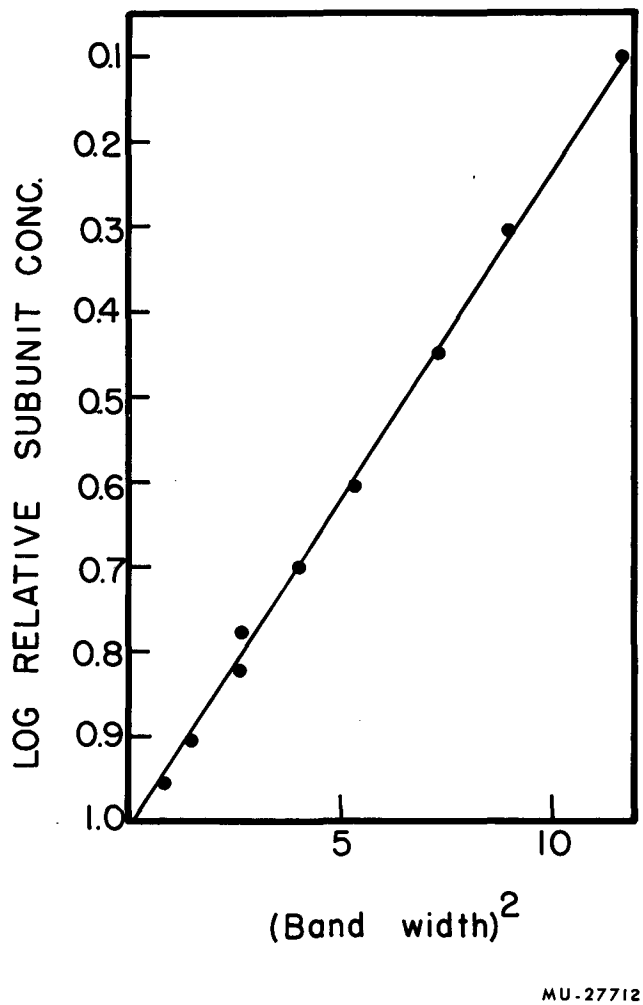

Fig. 2-5. Log relative concentration of lamellae subunits vs (band width)^2 of the equilibrium distribution of subunits in a sucrose density gradient.

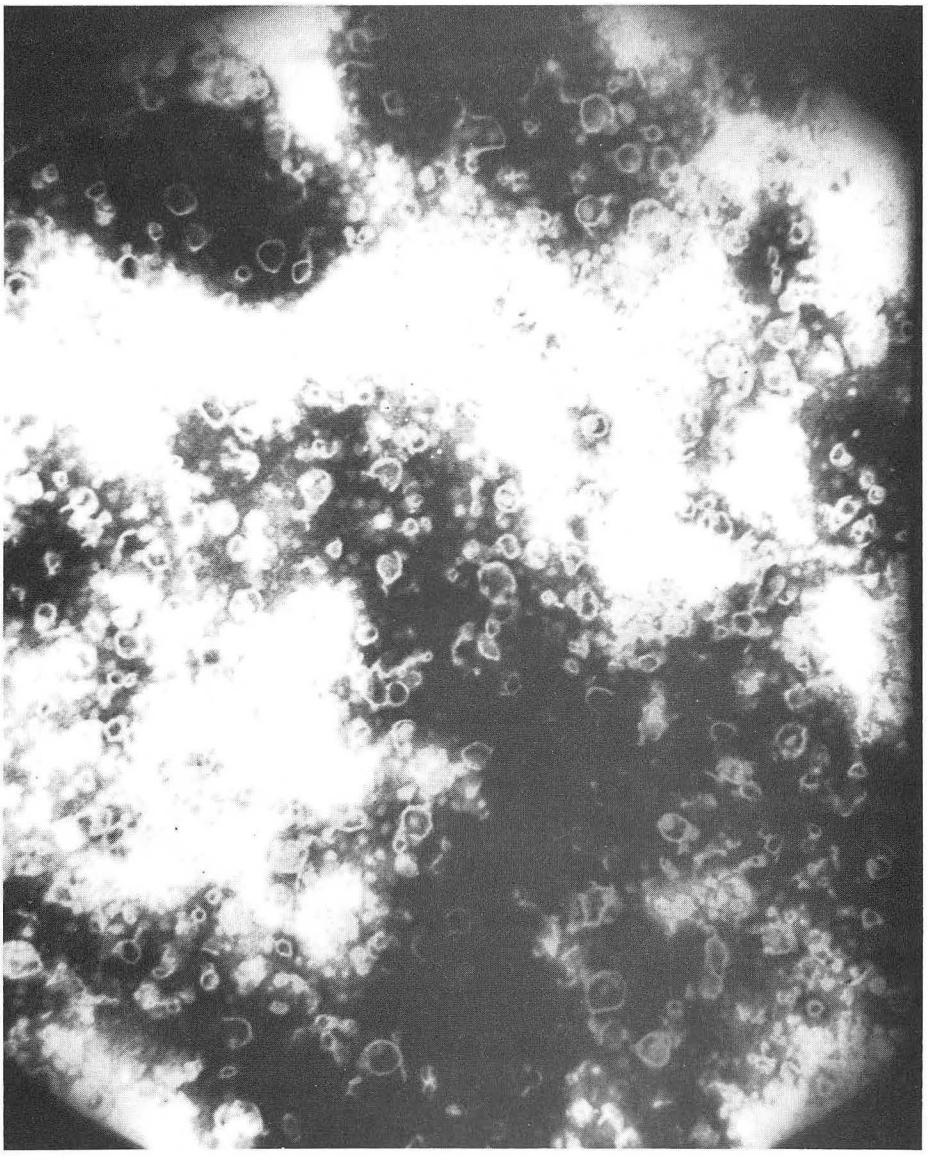

ZN-3544

Fig. 2-6. Negative staining of lamellae subunits.

50×2 cm equilibrated with 10^{-2}M potassium phosphate at pH 7.6 and 0.01% KCl was used and 3 ml of subunits eluted. By manometry, using standard Warburg vessels, ferricyanide was reduced in the light (60 μM ferricyanide per mg chlorophyll per hour) by this preparation.

Discussion

From electron-microscope studies Park and Pon[4] proposed a model for the substructure of the chloroplast lamella. They observed a particulate system which appeared to be composed of 100×200 Å oblate spheroids. They showed that by utilizing a suitable packing arrangement of the particles the double membrane system in all photosynthetic structures in green plants could consist of such subunits. The 100×200 Å oblate spheroid has been termed a quantasome and Park[5] has suggested that it may be the morphological expression of the physiological photosynthetic unit first formulated by Emerson and Arnold.[6] Such a unit contains on the order of 200 chlorophyll molecules.

Chemical analysis of purified lamellae show that the ratio of lipid to non-lipid is 1:1. Twenty percent by weight of the lipid fraction is chlorophyll; the non-lipid fraction is chiefly protein. In addition to protein, iron, manganese, and copper appear in the molar ratio 6:1:3. As Mn is essential for O_2 evolution in photosynthesis, there must be at least one Mn per photosynthetic unit. On the basis of their analytical data, Park and Pon[7] have calculated the minimum molecular weight of a photosynthetic unit as 9.6×10^6 for a one-Mn unit. This calculated unit contains 115 chlorophylls.

The test of the concept of a photosynthetic unit would be the isolation of an active homogeneous subunit that no longer yields two or more active subunits when fragmented. Sonic preparations of chloroplast lamellae yielding aggregations of up to eight quantasomes are active in Hill reaction. Their rates of quantum conversion are similar to unbroken lamellae, but the preparations are physically nonuniform. Such polydispersity impedes precise physical measurements and obscures the detection of the activity of the smallest particles present.

The subunit described in this report satisfies some criteria necessary for the photosynthetic unit. The absorption spectrum is similar to that of unbroken lamellae, whole chloroplasts, and whole leaves, as measured by spectrophotometers with light-scattering attachments. The molecular weight of the subunit preparation from sedimentation data, size, and density is on the order of 2 million. This molecular weight corresponds to twice the calculated minimum molecular weight on the basis of one Mn per unit. These subunits contain about 200 chlorophylls, and they are of a similar particle size and shape. They are active in the Hill reaction when ferricyanide is used as oxidant.

---

4. R. B. Park and N. Pon, J. Mol. Biol. 3, 1 (1961).
5. R. B. Park, J. Chem. Educ. 39, 424 (1962).
6. R. Emerson and A. Arnold, J. Gen. Physiol. 16, 191 (1932).
7. R. B. Park and N. G. Pon, J. Mol. Biol. (in press).

Thus, these subunits appear to satisfy the requirements of the photosynthetic unit in terms of chlorophyll content and molecular weight, and also approximate the dimensions of the quantasome.

Summary

We have isolated a subunit from spinach chloroplast lamellae. Its absorption spectrum is similar to that of whole chloroplasts, and it is active in the Hill reaction. It has a sedimentation coefficient of 86 Svedbergs and has a molecular weight of 1.76×10^6, assuming a density of 1.175 g/cc.

It satisfies some criteria for the photosynthetic unit and the quantasome.

3. DEPOLARIZATION OF LIGHT-SCATTERING AND OF FLUORESCENCE BY SPINACH QUANTASOMES

Kenneth Sauer*

A study has been made of the light-scattering and fluorescence of various preparations of spinach quantasomes. From measurements of the depolarization of light scattered by small particles it is possible to estimate the anisotropy of the particle polarizability. In addition, fluorescence depolarization studies are of interest for materials of photosynthetic origin because of the attributed correlation between the extent of depolarization and the efficiency of the transfer of electronic excitation energy among pigment molecules. Furthermore, evidence bearing on the existence of specially oriented chlorophyll molecules may be expected from such studies.

Theoretical

The scattering of light by small particles has been described in some detail in books by van de Hulst[1] and by Stacey.[2] For our purposes it is worthwhile to list the basic assumptions underlying the theoretical equations which will be used. These assumptions are:

1. The particles under investigation are small in comparison with the wavelength of light used for the scattering measurements. Generally, the theory for Rayleigh scattering is felt to apply only to particles smaller than $\lambda/20$.

2. The particles do not absorb radiation at the wavelengths used. As a consequence, only the real components of the polarizability tensor need be considered.

3. The particle can be treated as a homogeneous sphere or ellipsoid. For such particles the field induced by the polarization and the total field are both constant inside the particle.

4. The solvent is isotropic and there are no correlations in orientation between the molecules of solute and those of solvent. It should be stated that in the case of each of these assumptions, theory has now been extended to cover systems not satisfying the requirements. These more elaborate treatments are either not required or are not justifiable in connection with the results of this study.

For small isotropic scattering particles, the scattering at 90 deg to the incident beam is completely plane polarized, regardless of the extent of polarization of the exciting beam. The electric vector of the scattered light

---

* U. S. Public Health Service Postdoctoral Fellow, 1960-63.

1. H. C. van de Hulst, Light Scattering by Small Particles (John Wiley and Sons, New York, 1957).

2. K. A. Stacey, Light Scattering in Physical Chemistry (Academic Press, New York, 1956).

lies in a plane normal to the direction of the exciting beam. For scattering particles with an anisotropic polarizability, the scattering of right angles is no longer completely plane polarized in the normal plane, but is reinforced by an additional component in the axial or beam direction.

In order to simplify the mathematical representation of the scattering depolarization analysis, let us assume that both the exciting beam and the direction of observation of light scattered at 90 deg both lie in the horizontal plane. (This corresponds to the experimental arrangement of this study, as will be described below.) Following the notation of Stacey,[2] we will designate the horizontal and vertical components of the scattered light intensity by H and V, respectively. The subscripts u, h, and v will be used to characterize the incident beam as unpolarized, horizontally plane polarized, or vertically plane polarized, respectively. Corresponding values for the depolarization, ρ, are defined by the relations

$$\rho_v = \frac{H_v}{V_v}; \quad \rho_h = \frac{V_h}{H_h}; \quad \rho_u = \frac{H_u}{V_u} = \frac{H_h + H_v}{V_h + V_v} . \tag{1}$$

Furthermore, the Rayleigh-Krishman relation requires $H_v = V_h$ in all cases.[3,4] For completely isotropic scattering particles

$$\begin{aligned} &V_v \neq 0; \quad H_v = V_h = H_h = 0 \\ &\rho_v = 0; \quad \rho_h = 1, \quad \rho_u = 0. \end{aligned} \tag{2}$$

For anisotropic particles

$$V_v \neq H_v = V_h \neq 0; \quad \rho_v \neq 0, \quad \rho_h = 1, \quad \rho_u \neq 0. \tag{3}$$

Rayleigh calculated the depolarization for the case of a polarizability ellipsoid [assumption (3), above] with principal components α, β, and γ directed along mutually perpendicular particle axes.[3] Following integration for all possible orientations of the scattering particles in the suspension, he obtained the result

$$\rho_u = \frac{(\alpha^2 + \beta^2 + \gamma^2 - \alpha\beta - \alpha\gamma - \beta\gamma)}{2(\alpha^2 + \beta^2 + \gamma^2 + \alpha\beta + \alpha\gamma + \beta\gamma)} . \tag{4}$$

In the case of an ellipsoid of revolution, where β = γ,

$$\rho_u = \frac{\alpha^2 - 2\alpha\beta + \beta^2}{2(\alpha^2 + 2\alpha\beta + 3\beta^2)} . \tag{5}$$

---

3. Lord Rayleigh, Phil. Mag 35, 373 (1918).
4. R. S. Krishman, Proc. Indian Acad. Sci. A1, 211 (1934); A2, 221 (1935); A3, 128 (1936).

These latter cases have been designated as Langevin. In addition, it is necessary to include Rayleigh's definitions of the average polarizability

$$\bar{\alpha} = \frac{(\alpha + \beta + \gamma)}{3} \tag{6}$$

and of the optical anisotropy

$$\delta^2 = \frac{1}{2} \frac{(\alpha - \beta)^2 + (\beta - \gamma)^2 + (\gamma - \alpha)^2}{(\alpha + \beta + \gamma)^2} . \tag{7}$$

Cabannes[5] has used these hypotheses to derive equivalent relationships:

$$\rho_u = \frac{6\delta^2}{5 + 7\delta^2} ; \qquad \delta^2 = \frac{5\rho_u}{6 - 7\rho_u} \tag{8}$$

It is essential to note that up to this point in the discussion the theory applies only to scattering particles in a vacuum.

The theory for anisotropic scattering resulting from particles suspended in a liquid medium has been developed by G. Weill.[6] By assuming there is no interaction between the solvent and the solute, the effect of the solvent, characterized by an average polarizability $\bar{\alpha}_0$, can be separated from the effect of the solute, characterized by the three pricipal polarizabilities $\Delta\alpha$, $\Delta\beta$, and $\Delta\gamma$. For Langevin molecules where $\Delta\beta = \Delta\gamma$, Weill found

$$\left.\begin{aligned} V_v &= \frac{8\pi^4}{\lambda^4} n \left[\left(\frac{\Delta\alpha + 2\Delta\beta}{3} \right)^2 + \frac{4}{5} \left(\frac{\Delta\alpha - \Delta\beta}{3} \right)^2 \right] \\ H_v &= \frac{8\pi^4}{\lambda^4} n \frac{3}{5} \left(\frac{\Delta\alpha - \Delta\beta}{3} \right)^2 \end{aligned}\right\} \tag{9}$$

for the supplementary scattering due to solute alone, where n is the number of molecules of solute per unit volume. The apparent anisotropy of the solution, by analogy with the Rayleigh case, is defined as

$$\Delta^2 = \frac{5\rho_u}{6 - 7\rho_u} . \tag{10}$$

The molecular anisotropy, δ^2, for the solute alone is then related to the apparent anisotropy by the equation

---

5. J. Cabannes, La diffusion moléculaire de la lumière, Paris (Les Presses universitaires de France, 1929).

6. G. Weill, Étude de l'anisotropie moléculaire par diffusion de la lumière. Application aux macromolécules en chaînes, Thesis, University of Strasbourg, 1961.

$$\delta^2 = \Delta^2 \times \left(\frac{\eta^2 - \eta_0^2}{\eta^2 - 1} \right)^2 , \qquad (11)$$

where η and η_0 are the refractive indices of the pure solute and the pure solvent, respectively.

Experimental

The measurements of light scattering and of fluorescence were carried out by using an Aminco-Bowman spectrophotofluorimeter (American Instrument Company, Silver Springs, Maryland). Light from the xenon arc source is dispersed by the excitation momochromator (single grating monochromator) and is incident on the sample cuvette through a system of slits and baffles. A Glan-Thompson prism polarizer or a supplementary wavelength filter can be introduced into the monochromatic excitation beam just before it reaches the sample. The fluorescent and scattered radiation passes through a second set of slits and baffles defining a beam at 90° to the direction of excitation. Optionally, a second polarizing element may be introduced at this point. The emergent beam passes through a second single-grating monochromator, then through an optional wavelength filter to the face of the photomultiplier detector. The instrument was provided with a special red sensitive detector, consisting of an RCA 7102 end-window photomultiplier in a housing that was cooled to dry-ice temperature. The photomultiplier operating voltage was 1500 V, unless otherwise quoted. The activation (action) spectra or emission (fluorescence plus scattering) spectra could be recorded as a function of activation wavelength λ_A, or of emission wavelength λ_F, by using a Sanborn XY-Oscillograph. Alternatively, output signals were read from a meter for fixed values of λ_A and λ_F. Photomultiplier output was read on a percent transmission scale, which was linear in intensity incident on the detector at any one wavelength. The readings (reported as "Relative Intensity" in the Results section below) are only relative values on an arbitrary scale of 100. As all the data, except where noted, were recorded by using the same instrument parameters, the relative intensities should give meaningful intercomparisons, so long as these are interpreted with due regard to the vagaries of the instrument. A description of the basic instrument optics has been published.[7]

The preparation of spinach quantasome aggregates has been described previously.[8, 9] The small- and medium-sized aggregates were prepared by sonication of chloroplasts from which soluble stroma substances had been removed by twofold extraction in distilled water. Following centrifugation at 45 000 g for 5 min, the precipitate was discarded. The supernatant was recentrifuged at 145 000 g for 15 min, and the small and medium aggregates

7. J. M. Price, M. Kaihara, and H. K. Howerton, Appl. Opt. 1, 521 (1962).
8. R. B. Park and N. G. Pon, J. Mol. Biol. 3, 1 (1961).
9. K. Sauer and M. Calvin, Biochim. Biophys. Acta 64, 324 (1962).

were obtained in the supernatant liquid and the resuspended precipitate, respectively.[9] Quantasome "monomers" were prepared from water-extracted chloroplasts which were then sonicated in a medium containing 0.1M glycine, 0.05M KOH, and 0.02M cysteine (pH 9). Some of the properties of this preparation have been described.[10]

Instrumental parameters were evaluated by using both laboratory distilled water and ethanolic solutions of rhodamine B base (Matheson, Coleman, and Bell, B 1193). In no case was any attempt made to remove dust particles from the solutions.

Results

A series of excitation spectra and emission spectra has been obtained from a variety of preparations and under a number of experimental conditions. Certain general features of these spectra characteristically appear and must be kept in mind. In addition to fluorescence and Rayleigh scattering, additional observed effects arise from Tyndall scattering, Raman scattering of the solvent, and scattering due to polarizability fluctuations in the solvent. Instrumental effects, such as higher-order grating transmissions in the monochromators, stray or white light from the monochromators, and light reflected at cuvette surfaces and elsewhere, all contribute observable anomalies under some circumstances. Beyond these, the variations with wavelength of the xenon arc emitted intensity, of the momochromator efficiencies, and of the detector sensitivity lead to very significant distortions of the activation and emission spectra. Source and detector noise and long-term instability are present and raise serious questions about the quantitative significance of the measurements. Polarizations that are a property of the instrument itself must be taken into account in evaluating the depolarization calculations. Concentration-dependent effects resulting in fluorescence self-absorption and multiple light scattering are also observed.

Before examining some of these instrumental parameters experimentally let us look at some typical emission and activation spectra for spinach quantasomes. Figure 3-1 shows polarized emission spectra activated at 500 mμ for two suspensions of small aggregates of quantasomes differing tenfold in concentration. Figure 3-2 shows action spectra of the polarized emission at 750 mμ for the same two suspensions. In each of these two cases the activating radiation is unpolarized. In Fig. 3-1 the spectrum of fluorescence excited by light at 500 mμ (absorbed primarily by carotenoids) exhibits a maximum in the red (near 700 mμ) and a shoulder at about 50 mμ to longer wavelengths. These are both characteristic of chlorophyll a fluorescence. The dilute suspension [Fig. 3-1 (b)] gives a fluorescence spectrum which is relatively undistorted. The spectrum of the tenfold-more concentrated suspension has its maximum shifted 23 mμ to longer wavelengths and is appreciably less than tenfold more intense. Both of these effects can be readily explained in terms of self-absorption by the more concentrated sample. The relationship between fluorescence intensity and polarizer

10. J. Biggins and R. B. Park, in Bio-Organic Chemistry Quarterly Report, UCRL-10350, June 1962, p. 48.

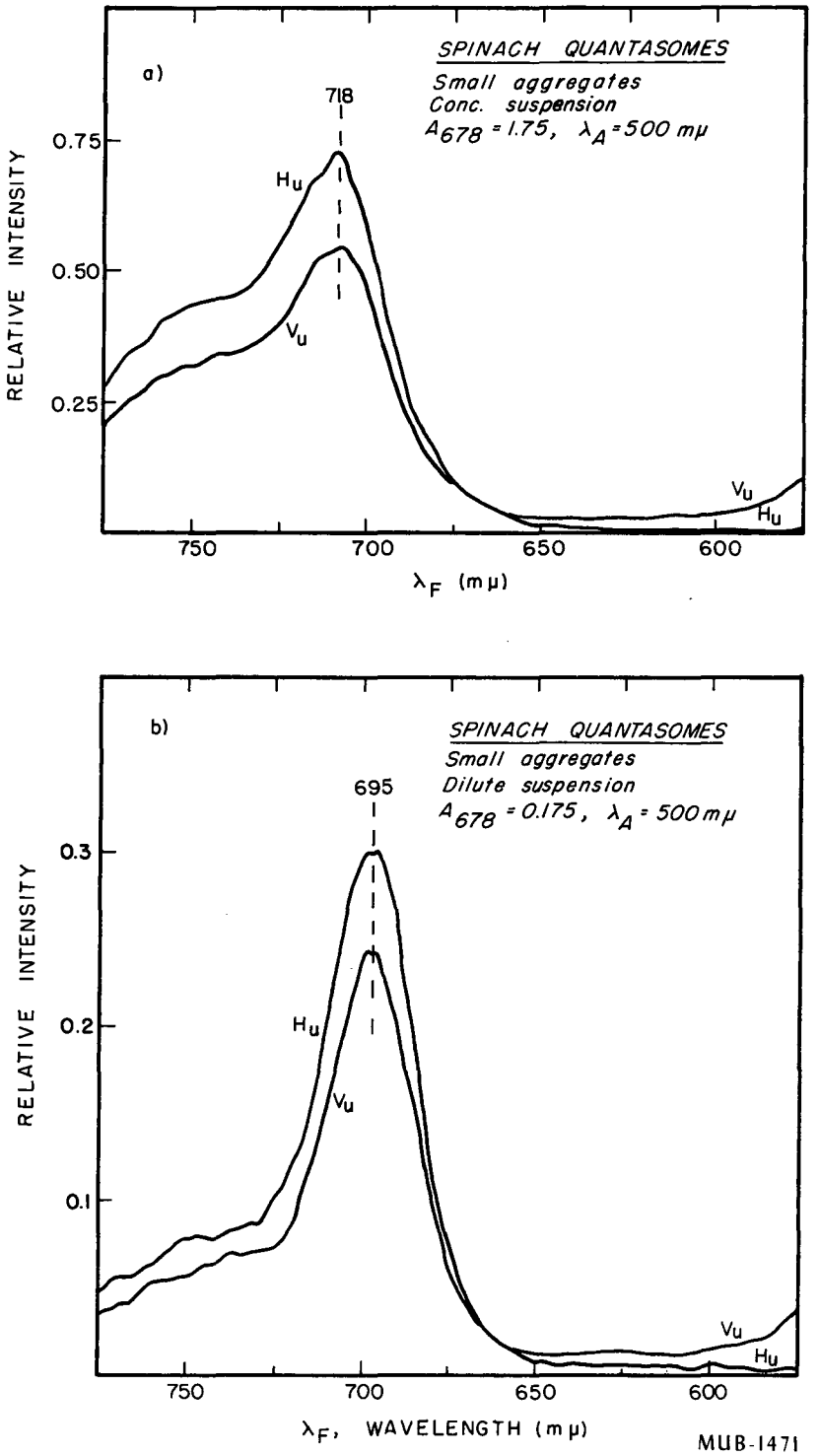

Fig. 3-1. Fluorescence spectra of spinach quantasomes: relative intensity emitted vs wave length of emitted light. Exciting wave length 500 mμ; unpolarized. Symbols V_u and H_u refer to emitted radiation polarized vertically and horizontally, respectively.

(a) Concentrated suspension; absorbance 1.75 at 678 mμ.

(b) Tenfold dilution; absorbance 0.175 at 678 mμ.

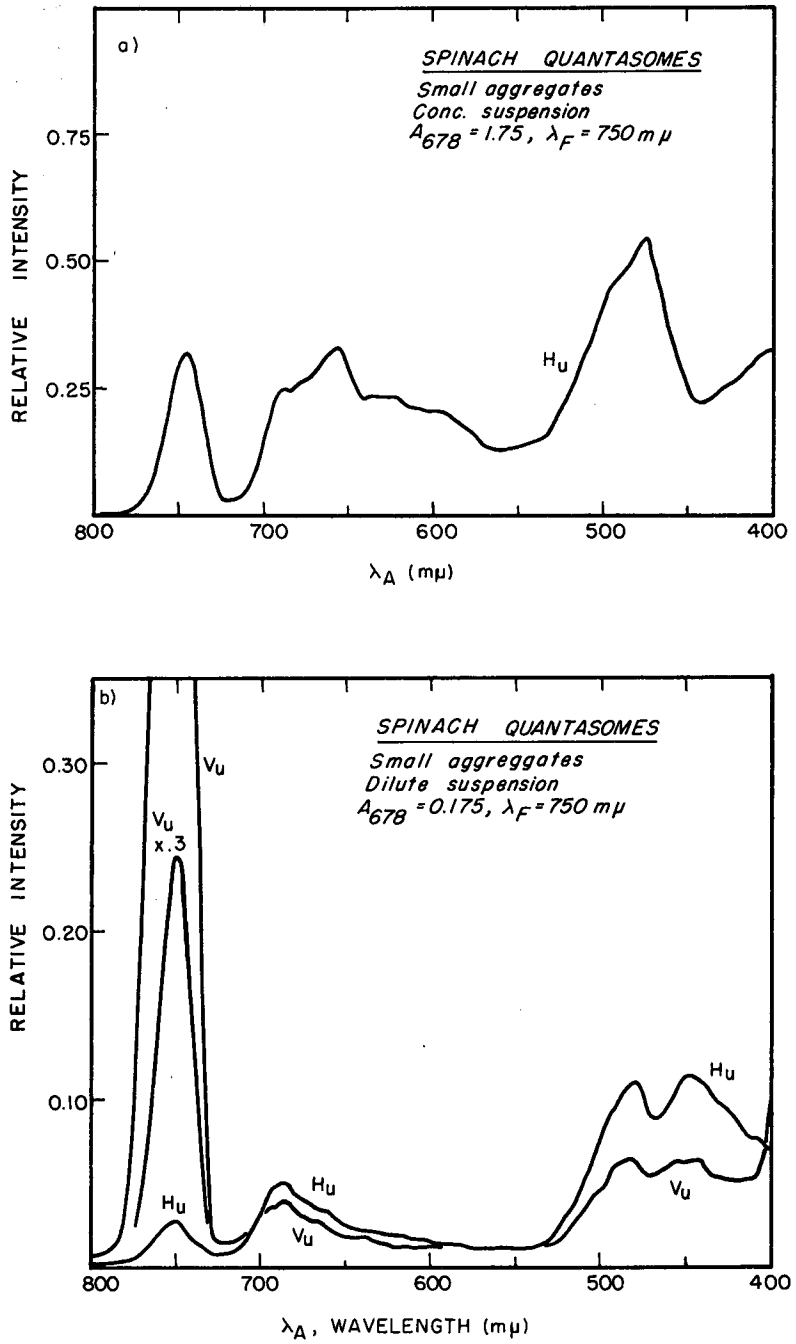

Fig. 3-2. Excitation spectra of spinach quantasomes: relative intensity emitted at 750 mμ vs wavelength of exciting light (unpolarized). For further details, see Fig. 1.

orientation is not that which is expected. For a sample exhibiting complete depolarization of fluorescence, the two intensities V_u and H_u would be expected to be the same. Where there is complete retention of orientation of the transition moment during the fluorescence lifetime, the intensity polarized vertically will generally be much stronger than that polarized horizontally. In the particular case shown, an alternative explanation is possible because the absorption and emission oscillators are different—even residing primarily in different molecules. Nevertheless, this is felt not to be the reason for the anomalous polarization; rather, evidence is available that the effect is an instrumental one. Polarized emission spectra of ethanolic solutions of rhodamine B were studied in order to test for instrumental irregularities. It is well documented that the time constant for rotational diffusion of rhodamine B in nonviscous solvents is short compared with its fluorescence lifetime.[11] Consequently the fluorescence is expected to be completely depolarized (i.e., $\rho = 1$. At worst, ρ is smaller than one in the case where rotational diffusion is not rapid enough, since under the conditions of this test study the same oscillator was responsible for absorption $\lambda_{max} = 550$ mμ, as for fluorescence, $\lambda_{max} = 580$ mμ). By using the Aminco instrument as described above, the component of rhodamine B fluorescence polarized horizontally is greater than that polarized vertically. The sample studied gave a polarization ratio $\rho_u = 1.21 \pm 0.03$. As this value is quite comparable to those observed from the quantasome fluorescence (see below), the attribution of the result to an instrumental effect is felt to be justified.

[The source of the instrumental effect is not altogether clear. In a separate experiment a piece of opal glass was placed in the sample chamber and was oriented at 45 deg to the beams in such a manner that the normal to its surface approximately bisected the angle between the excitation and emission beams. The opalescent surface was placed on the side of beam incidence. In this case the scattered light in the region 680 to 720 mμ exhibited no preference of polarization—i.e., $\rho = 1.00 \pm 0.05$. It would seem that this result is in direct contradiction with those from the solutions of fluorescent dye. It may be that specular reflection from the smooth opal glass surface introduced just enough elliptical polarization with long axis vertical (which is the direction to be expected) to virtually compensate the horizontal polarization induced by the exit monochromator system. This is a distinct possibility. Until further calibrations are made, it will be assumed that the exit monochromator introduces elliptical polarization with ellipticity of 1.21 with the long axis oriented horizontally. One further feature, related to the wavelength dependence of the ellipticity, will be mentioned below.]

An additional feature observable in the spectra of Fig. 3-1 is that the values of V_u become significantly greater than those for H_u at wavelengths below 600 mμ—i.e., in the region approaching the exciting wavelength at 500 mμ. This becomes understandable when it is noted that both the Rayleigh scattering and the Raman scattering from water (expected at $20\,000 - 3300 = 16\,700$ cm^{-1} or 600 mμ) are both strongly polarized in the vertical direction.

---

11. P. Pringsheim, Fluorescence and Phosphorescence (Interscience Publishers, New York, 1949).

As can be seen from Fig. 3-1(b), there is a significant amount of fluorescence from quantasomes at 750 mμ, although this is only about one-fourth of that at the maximum. Activation spectra for the 750-mμ fluorescence are shown in Fig. 3-2. Here, again, the distorting effects resulting from self-absorption at high concentrations are apparent in comparing Fig. 3-2(a) and 3-2(b). In general, if fluorescence occurs with a quantum yield that is independent of exciting wavelength, then the activation spectra are identical with the absorption spectra of the solutions.

Several factors serve to distort this relationship in Fig. 3-2(b). First, the strong maximum at 750 mμ, where the exciting and emission wavelengths are the same, results entirely from Rayleigh scattering. As has been shown previously, spinach quantasomes exhibit completely negligible absorption at 750 mμ.[8] Second, the displacement of the bands at 445 and 685 mμ from the positions of the quantasome absorption maxima at 437 and 678 mμ–and also the comparative enhancement of the blue relative to the red band in Fig. 3-2(b)–result, at least in part, from the greater sensitivity of the instrument to blue rather than to red wavelengths. The wavelength dependence of the instrument sensitivity, measured by means of scattering from an opalescent plate, is shown in Fig. 3-3. There is a difference of nearly threefold in the sensitivities at 437 vs 678 mμ. The sensitivity curve also gives us the probable explanation of a third distortion of the activation spectra [shown in Fig. 3-2(b) and exhibited in all other activation spectra] relative to the absorption spectra. The pronounced peak at about 480 mμ in the activation spectra has no counterpart in the quantasome absorption spectrum. It does, however, correspond to a peculiar pronounced submaximum in the sensitivity curve.

An activation peak at just this wavelength would be rather difficult to account for in terms of the known spectral properties of quantasomes. Nor can such a peak be satisfactorily explained in terms of Raman scattering or transmission in higher orders of the monochromator gratings. (The peak is present in action spectra even when a blocked interference filter is placed in series with the emission monochromator.) The origin of this instrument sensitivity maximum is not clear. The sensitivity of the photomultiplier detector actually exhibits a broad minimum just in that wavelength region. There may be a strong maximum in the emission from the xenon lamp. Alternatively, the effect could conceivably result from a polarization anomaly of the monochromator gratings as described by Wood.[12] In any case, the various distortions listed above should make it abundantly clear that the determination of true fluorescence action spectra with an instrument of the type used here involves forbiddingly painstaking procedures.

Light-Scattering Depolarization

A summary of the results obtained from the studies of the polarization of scattered light by various preparations of spinach quantasomes is given in Table 3-I. Data from all the experiments are included in order that some of the hazards associated with such measurements can be noted. Examination of the results shows, for example, that the use of 3×3 mm cuvettes is unsatisfactory with this instrument, owing to a spurious contribution of scattering, presumably from the walls and corners of the cuvettes. The contribution

12. R. W. Wood, Phys. Rev. 48, 928 (1935).

Table 3-I. Polarized components of light scattering from spinach quantasomes.[a]

	Sample age (days)	Concentration (absorbance at 678 mμ)	λ_F (mμ)	IF[b]	V_v	H_v	H_h	V_h	$\rho_v^{(+)}$
					Monomers				
(1)	1-2	0.94	720	+	$\gg$ 0.3	0.022	0.035	0.025	$\ll$ 0.07
(2)	2	0.94	711	+	$\gg$ 1.2	0.045	0.08	0.06	$\ll 0.03_7$
					V_u	H_u	$\rho_u^{(-)}$	$\rho_u^{(+)}$	
(3)[c]	15	0.78	725	-	0.092	0.004	0.043	--	
(4)	15	0.78	725	-	0.81	0.031	0.038	--	
(5)	15	0.78	750	-	0.65	0.021	0.032	--	
(6)	15	0.78	720	-	0.97	0.036	0.037	--	
					Small fragments				
(7)	1	1.75	725	-	7.3	0.39	0.053	--	
(8)	1	1.75	750	-	6.4	0.36	0.056	--	
(9)	1	1.75	750	-	7.1	0.73	(0.05)[d]	--	
(10)	2	1.75	750	-	5.3	0.85	(0.09)[d]	--	
(11)	2	1.75	740	-	--	0.86	--	--	
(12)	2	1.75	730	-	5.7	1.05	(0.12)[d]	--	
(13)	2	1.75	720	-	7.2	0.95	(0.08)[d]	--	
(14)	2	1.75	710	-	6.4	1.7[e]	--	--	
(15)	2	1.75	750	-	--	0.31	--	--	

(16)	2	0.175	750	-	0.80	0.020	0.025	--
(17)	2	0.175	740	-	--	0.020	--	--
(18)	2	0.175	730	-	0.96	0.020	0.021	--
(19)	2	0.175	720	-	1.12	0.025	0.022	--
(20)	2	0.350	720	+	1.2	0.032	--	0.027
					Medium fragments			
(21)	1	0.46	750	-	1.31	0.055	0.043	--
(22)	2	0.46	750	-	1.3	0.05	0.04	--
(23)	2	0.46	711	-	1.84	--	--	--
(24)	2	0.46	711	+	1.18	--	--	--
					Water			
(25)			750	-	0.43	0.40	--	--

[a] All cuvettes were 10×10 mm except for runs 9 through 14 and run 25, which were 3×3 mm.

[b] IF refers to interference filter. A plus sign (+) indicates a suitable interference filter was placed in front of the photomultiplier; a minus sign (-) indicates the absence of the supplementary filter. The symbols applied to the headings ρ_v and ρ_u have the same significance.

[c] In run (3) the photomultiplier voltage was only 1200 volts instead of the usual 1500 volts. This is the reason for the apparently low values of V_u and H_u.

[d] These values of ρ_u are corrected for scattering caused by the cuvette walls (see text for explanation).

[e] In run (14) at 710 mμ the fluorescence and scattering peaks were merging, hence the unusually high value for H_u.

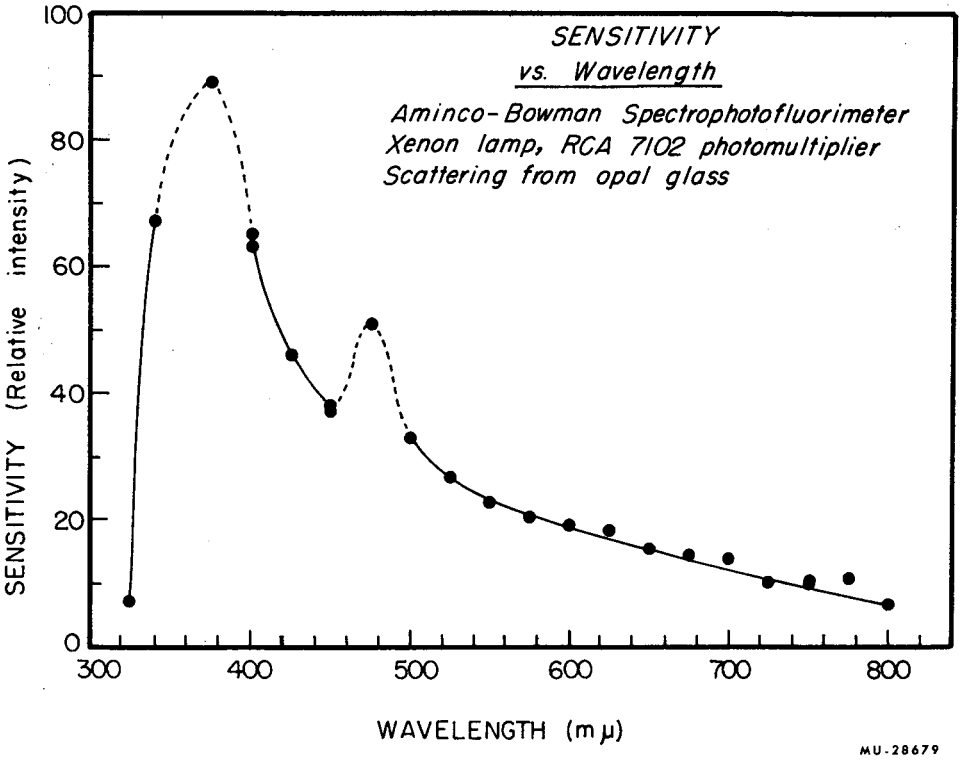

Fig. 3-3. Sensitivity of Aminco-Bowman spectrophotofluorimeter as a function of wavelength.

is dominant in the values for the apparent scattering of water in row (25)–values that are twentyfold greater than the scattering (H_u) from some of the quantasome suspensions placed in 10×10 mm cuvettes. The same effect is observed from comparison of the values of H_u between the otherwise identical runs (8) and (9). Consequently, for all experiments using 3×3 mm cuvettes, a negative correction of 0.40 has been applied to both V_u and H_u in order to calculate the values for ρ_u, which are then given in parentheses.

The results show generally that the light scattered from spinach quantasomes is relatively highly polarized. Values of ρ_u range from 0.02 to 0.1. The most reliable values are undoubtedly those (a) at the longest wavelengths, (b) at the lowest concentrations, (c) for the freshest preparations, and (d) for materials measured in 10×10 mm cuvettes. Each of these factors can be seen, from the table, to have a significant effect on the scattered intensities and/or the depolarization ratios. The principal wavelength effect comes about because at values approaching the absorption maximum at 678 mμ increasing amounts of fluorescence are present along with the light scattering. The peaks of light scattering and fluorescence activation merge together if the emission monochromator wavelength is set at 710 mμ or below. The effect of high concentrations is in the production of multiple scattering, which has the consequence of increasing the depolarization. Comparison of runs (8) and (16) illustrates this point. (The difference in sample age, for example, would be expected to operate in the opposite direction.) It is known from previous studies that aging of the samples produces a steady increase in the overall intensity of light scattering.[9] One is not surprised to find an associated increase in depolarization–e.g., run (9) vs run (10). For this reason the measurements of the depolarization ratio for the two-week-old "monomer" preparation–runs (3) through (6)–must be taken as an upper limit. The measurements of the two-day-old preparation, where the maximum of the V_v curve was off scale and was unfortunately not determined, suggest values of ρ_v severalfold less than 0.04. With this in view, the "best" runs indicate that ρ_u for the fresh monomer quantasomes is less than that for small aggregates (21). This result–which is consistent with observations from electron microscopy, that the lamellar fragments are more asymmetric than monomer quantasomes[8] and hence will depolarize the scattered light more strongly–needs confirmation from further experimentation.

Refractive Index

One of the parameters of Eq. (11) is the refractive index of the pure quantasome material at the wavelength used for the light-scattering measurements. As this wavelength was generally 750 mμ, beyond the region of visual sensitivity, a conventional measurement of refractive index with a Pulfrich or Abbe refractometer could not be made. Values of refractive index measured at shorter wavelengths are likely to be highly misleading, owing to refractive dispersion of the strongly absorbing quantasomes.

Two years ago measurements of the refractive increment of quantasome suspensions were made over the wavelength range 350 to 780 mμ. These measurements have not been reported previously, although a description of the liquid light-pipe refractometer used to make them has been written.[13] The technique suffered from the effect that the measured curve of refractive

dispersion included distortions resulting from absorption by the highly pigmented suspension. At 750 mμ, however, the absorption of quantasomes is exceedingly low; consequently, the measurements at this wavelength should be valid.

The quantasome material studied consisted of medium-sized aggregates resuspended in distilled water. This material contained a negligible amount amount of colorless stroma substances. The particular suspension studied had an absorbance of 45 at 678 mμ, and in the light pipe refractometer gave at 750 mμ a photomultiplier signal of 4.0 mV above that of distilled water. The liquid light pipe itself in this case consisted of a solution of 10% ethanol in water and produced a sensitivity in refractive index of 0.00018/mV at 589 mμ. The calibration was carried out by using a series of ethanol-water solutions of known concentration, as described previously.[13] The principal source of uncertainty in the measurements of the refractive index of quantasomes comes from the difference in wavelengths at which the measurement and the calibration were made. At the present time all we can do is combine the two components, keeping in mind that we are incorporating a source of error whose magnitude is unknown. On this basis, then, the quantasome suspension studied gives a refractive index increment of 0.00072. To calculate the bulk refractive index of pure quantasomes, we use the following data: The molar absorption coefficient of chlorophyll a in quantasomes is 9×10^4 liter/M-cm at 678 mμ;[9] hence, a solution having an absorbance of 45 at that wavelength contains 5.0×10^{-4} M/liter of chlorophyll a. This corresponds to a concentration of 0.45 grams per liter of chlorophyll a. A value of 1.5 has been determined experimentally for the weight ratio of chlorophyll to nitrogen from protein in quantasomes.[14] Furthermore, protein has been determined to constitute 50% by weight of the quantasomes. Assuming that nitrogen is 15% of the weight of the protein, we can readily calculate that the suspension under consideration contains 4.0 grams of quantasomes per liter. The refractive-index increment of quantasomes at 750 mμ is, therefore, 0.18 mliter per gram, which is in very good agreement with values found for proteins generally.[2] The increment in refractive index of pure quantasome material can be calculated by using the measured density of 1.17 grams per mliter, as determined in a sucrose gradient in the ultracentrifuge.[15] Adding this to the published value of 1.329 for the refractive index of water at 750 mμ,[16] we obtain a value of $1.329+(0.18)(1.17) = 1.54$ for the refractive index of quantasomes at 750 mμ. Owing to the number of approximations in the calculation, this value must be held as provisional.

Depolarization of Fluorescence

The study of the depolarization of quantasome fluorescence was undertaken with the twofold object of learning something about the extent of electronic energy migration in quantasomes and of attempting to confirm the

13. K. Sauer, in Bio-Organic Chemistry Quarterly Report, UCRL-9652, April 1961, p.1.

14. R. B. Park and N. G. Pon, J. Mol. Biol., (in press).

15. J. Biggins and R. B. Park, in Bio-Organic Chemistry Quarterly Report (this report).

16. International Critical Tables (McGraw-Hill, New York, N. Y., 1930), Vol. VII p. 13.

existence of oriented chlorophyll molecules in the quantasomes. Rapid and efficient transfer of electronic excitation energy among randomly oriented chlorophyll a and other pigment molecules in the quantasomes would be expected to result in strong depolarization of chlorophyll a fluorescence, as is the case for living algae.[17] If there exists in the quantasomes, in addition, a small number of oriented chlorophyll molecules absorbing and fluorescing at somewhat longer wavelengths than the majority of chlorophyll a, then selective activation of these molecules with monochromatic light might be expected to yield fluorescence which is more strongly polarized than is the major component of fluorescence.[18,19,20]

The results of this study are summarized in Table 3-II. The conclusion made apparent by the study is that the fluorescence from quantasomes is strongly depolarized, as is the case in living algae. It is also clear that the effects of light scattering tend to predominate when the activation and fluorescence wavelengths are 20 mμ or less from one another, even when supplementary interference filters are placed in series with the activation and fluorescence monochromators. The effect can be seen in the three series of runs (15) to (17), (18) to (23), and (24) to (31), where the depolarization ratios decrease sharply as the activating wavelength is brought closer to the fluorescence wavelength. That the effect is truly due to scattering and is not a change in fluorescence polarization is shown by the fact that the decrease in ρ_u with increasing activating wavelength comes about solely from an increase in V_u. The fluorescence activation and emission spectra, Figs. 3-1(b) and 3-2(b), show clearly that no increase in fluorescence intensity is observed at wavelengths increasing from 700 mμ. The scattering interference is less pronounced when an interference filter is placed in series with the activation monochromator, as is to be expected. Figure 3-2(b) illustrates the fact that the scattered component V_u gives a peak with a broad base on the wavelength scale.

When the activating and emission wavelengths are sufficiently far from one another, Table 3-II shows that the values of ρ_u or ρ_v fall generally in the range 1.3 to 1.4. The fact that these values are greater than unity is attributed principally to the elliptical polarization inherent in the fluorimeter. As was mentioned above, fluorescence from rhodamine B solutions gave a depolarization ratio of 1.21. The difference in the numerical values may result from the difference in wavelengths at which the two sets of measurements were made.

The depolarization ratio was not observed to be influenced by (1) whether the sample contained monomer quantasomes, small aggregates, or medium aggregates; (2) concentration (optical density), other than those

17. W. Arnold and E. S. Meek, Arch. Biochem. Biophys. 60, 82 (1956).

18. R. A. Olson, W. L. Butler, and W. H. Jennings, Biochim. Biophys. Acta 54, 615 (1961).

19. R. A. Olson, W. L. Butler, and W. H. Jennings, Biochim. Biophys. Acta 58, 144 (1962).

20. K. Sauer and M. Calvin, J. Mol. Bio. 4, 451 (1962).

Table 3-II. Polarized components of fluorescence from spinach quantasomes.[a]

	Sample age (days)	Concentration (absorbance at 678 mμ)	λ_A (mμ)	IF_A[b]	λ_F (mμ)	IF_F[b]	V_v	H_v	H_h	V_h	$\rho_v^{(+)}$
					Monomers						
(1)	1-2	0.94	680	-	720	+	0.18	0.23	0.35	0.26	1.28
(2)	1-2	0.94	680	-	711	+	0.23	0.26	0.42	0.30	1.13
					Small fragments						
							V_u	H_u	$\rho_u^{(-)}$	$\rho_u^{(+)}$	
(3)	1	1.75	680	-	750	-	0.55	0.72	1.31	--	
(4)	1	1.75	680	-	730	-	0.55	0.77	1.40	--	
(5)	1	1.75	680	-	720	-	0.60	0.85	1.42	--	
(6)	1	1.75	680	-	710	-	Shoulder	(1.7)	--	--	
(7)	1	1.75	500	-	710	-	1.8	2.3	1.28	--	
(8)	1	1.75	500	-	700	-	0.54	0.70	1.30	--	
(9)	1	0.175	500	-	695	-	0.195	0.25	1.28	--	
(10)	1	0.175	685	-	750	-	0.035	0.050	1.43	--	
(11)	1	0.175	685	-	730	-	0.065	0.06	0.92	--	
(12)	1	0.175	685	-	720	-	0.065	0.07	1.08	--	
(13)	1	0.175	685	-	710	-	Shoulder	(0.11)	--	--	
(14)	2	0.350	685	-	720	+	0.05	0.065	--	1.30	
(15)	2	0.350	679	{-/+}	720	+	0.0305 0.0155	0.040 0.0215	1.31 --	-- 1.38	
(16)	2	0.350	692	{-/+}	720	+	0.014 0.0075	0.016 0.010	1.14 --	-- 1.33	
(17)	2	0.350	703	{-/+}	720	+	0.0135 0.005	0.0045 0.001	0.33 --	-- 0.2	
(18)	2	0.88	679	{-/+}	720	+	0.057 0.028	0.069 0.039	1.21 --	-- 1.39	
(19)	2	0.88	692	{-/+}	720	+	0.032 0.017	0.0375 0.0215	1.17 --	-- 1.27	
(20)	2	0.88	698	-	720	+	0.017	0.0195	1.15	--	
(21)	2	0.88	703	{-/+}	720	+	0.025 0.008	0.009 0.0045	0.36 --	-- 0.56	
(22)	2	0.88	706	-	720	+	0.042	0.0075	0.179	--	
(23)	2	0.88	710	-	720	+	0.156	0.0095	0.061	--	
(24)	2	0.88	680	-	730	+	0.0505	0.0605	1.20	--	
(25)	2	0.88	690	-	730	+	0.041	0.048	1.17	--	
(26)	2	0.88	700	-	730	+	0.0125	0.013	1.04	--	
(27)	2	0.88	703	+	730	+	0.0025	0.003	--	1.2	
(28)	2	0.88	705	-	730	+	0.0085	0.0075	0.88	--	
(29)	2	0.88	710	-	730	+	0.009	0.005	0.56	--	
(30)	2	0.88	715	-	730	+	0.013	0.0045	0.35	--	
(31)	2	0.88	720	-	730	+	0.0285	0.004	0.14	--	
					Medium fragments						
(32)	2	0.46	685	-	750	-	0.072	0.082	1.14	--	10×10
(33)	2	0.46	679	-	720	+	0.015	0.010	0.67	--	10×10
(34)	2	0.46	692	{-/+}	720	+	0.024 0.012	0.025 0.014	1.04 --	-- 1.17	10×10 10×10
(35)	2	0.46	703	{-/+}	720	+	0.0365 0.0125	0.023 0.010	0.63 --	-- 0.80	10×10 10×10

[a] All cuvettes were 10×10 mm except for runs (3) through (7), which were 3×3 mm.

[b] See footnote a in Table I.

attributable to self-absorption; (3) wavelength of the activating light; and (4) wavelength of the fluorescence.

As the measurements to date suggest that the oriented chlorophyll molecules have an absorption maximum at 705 mμ and a fluorescence maximum at 720 mμ,[19] the interference resulting from light scattering did not permit the study of the fluorescence polarization of this component by using the techniques available.

Discussion

The observation that light scattering from quantasome monomers is strongly polarized leads to the conclusion that the polarizability of these particles is nearly isotropic. The quantasomes, as observed in the electron microscope, appear as oblate ellipsoids with dimensions 100 to 200 Å., and an axial ratio of approximately 2.[8] The size of the particles, in comparison with the 7500-Å wavelength of light used for the light scattering, is sufficiently small that Rayleigh scattering alone need be considered. Furthermore, the measuring wavelength is well beyond the region of significant pigment absorption. Thus, the first two assumptions listed in the theoretical section are very likely to be valid. Owing to the complex nature of quantasomes, a priori the third and fourth assumptions listed are considered unlikely to be correct. We have, as yet, virtually no information concerning the particle inhomogeneity or its interactions with the aqueous surroundings.

By using the results of the preceding section it is possible to calculate, with Eq. (10) and (11), the molecular anisotropy of the quantasome polarizability. For a Langevin particle, Eq. (7) reduces to

$$\delta = \frac{\alpha - \beta}{\alpha + 2\beta} \quad . \tag{12}$$

Consequently,

$$\frac{\alpha}{\beta} = \frac{2\delta + 1}{1 - \delta} \quad , \tag{13}$$

where α/β is the axial ratio of the polarizability ellipsoid. The evaluations of this ratio for the best representative runs selected from Table 3-I are given in Table 3-III. The qualitative trends discussed previously in terms of ρ_u appear again in comparison of the values of α/β.

For monomer quantasomes a value of 0.14 or less is estimated for the apparent anisotropy of the polarizability. This value represents the sum of the contributions of form anisotropy–resulting from the nature of the geometrical ellipsoid–and intrinsic anisotropy–resulting from different values of the polarizability along different particle axes. Two extreme cases can be considered. In the case where intrinsic anisotropy only is important, the particle must be a sphere whose mutually orthogonal polarizability components are not all equal. In this case Eq. (11) applies rigorously; a molecular anisotropy δ, and a ratio of polarizabilities for a Langevin particle α/β can be calculated. These are listed in Table 3-III.

Table 3-III. Polarizability anisotropy of quantasomes.

Run[a] No.	Particle size	ρ_u	Δ^2	δ^2[b]	$\frac{\alpha}{\beta}$
(2)	monomers (2 days)	0.02[c]	0.02	0.004	1.20
(5)	monomers (15 days)	0.032	0.028	0.0056	1.245
(16)	small (dilute)	0.025	0.021	0.0042	1.21
(10)	small (conc.)	0.056	0.050	0.0100	1.33
(21)	medium	0.043	0.038	0.0076	1.29

[a] Taken from Table 3-I.

[b] The proportionality factor relating Δ^2 and δ^2 in Eq. 11 is

$$\left(\frac{\eta^2-\eta_0^2}{\eta^2-1}\right)^2 = \left[\frac{(1.54)^2-(1.33)^2}{(1.54)^2-1}\right]^2 = 0.20.$$

[c] An estimate, based on the width of the V_u vs wavelength curve where it went off scale; ρ_u may well be smaller than this value for fresh monomers.

In the present instance, however, this is probably not a true representation of the situation. The evidence from electron microscopy suggests that quantasomes are not geometrical spheres, but ellipsoids with an axial ratio near 2. One would then expect a contribution of form anisotropy to the measured apparent anisotropy. The second extreme case–that of an ellipsoidal particle with a homogeneous polarizability–is not so easily treated. A complete theoretical treatment of the effect of placing an ellipsoid of refractive index η in a solvent of refractive index η_0 has not yet been reported in the literature.[1] That such a treatment is of interest in the case of quantasomes is suggested by the observation that the majority of absorbing pigment molecules do not exhibit strong dichroism.[20] A structure containing component molecules in a large variety of orientations is suggested; such a structure may exhibit a homogeneous polarizability. In this event, one would expect the geometrical axial ratio calculated from the polarizability anisotropy to coincide with that observed with the electron microscope. The result of such a treatment applied to the polarizability data on quantasomes is anticipated.

Summary

Light scattered by spinach quantasomes at wavelengths where absorption is negligible is observed to be strongly polarized. Preliminary measurements of the depolarization ratio for several preparations of quantasomes suggest that the apparent anisotropy of the polarizability ellipsoid varies from about 0.14 for monomer quantasomes to about 0.24 for medium-sized aggregates. The significance of these values is discussed qualitatively in terms of intrinsic anisotropy and/or form anisotropy of the polarizability.

Measurements suggest that, at 750 mμ, quantasomes have a refractive index of 1.54.

Fluorescence from each of the quantasome preparations studied was observed to be strongly depolarized. This phenomenon was independent of activating wavelength, fluorescence wavelength, and particle size. The result signifies that even in monomer quantasomes efficient transfer of electronic excitation energy occurs, and confirms the result from the study of electric dichroism that the majority of the pigment molecules have a large variety of orientations within the particle. An attempt to demonstrate by means of fluorescence polarization the existence of a small component of oriented chlorophyll molecules within the quantasomes was unsuccessful, owing to serious interference from light-scattering by the particles under the requisite conditions.

Acknowledgments

The author wishes to thank Mr. John Biggins of the Bio-Organic Chemistry Group for providing him with the preparation of quantasome monomers, and Dr. Gilbert Weill for helpful discussions related to the theory underlying light-scattering.

4. EFFECT OF α-PYRIDYL-HYDROXYMETHANE-SULFONIC ACID ON ^{14}C FIXATION IN CHLOROPLASTS

Johannes Ullrich

The production of glycolic acid during photosynthesis in various plants and isolated chloroplasts is dependent on several conditions. It has been known for a long time that the concentration of glycolic acid shows a sudden rise and a subsequent fall when algae, engaged in strong photosynthetic activity, run out of CO_2.[1] Oxygen deficiency also has an effect on glycolic acid formation, cutting its rate down to lower values.[2] Whittingham and co-workers[3] recently furnished more detailed information on the effects of CO_2 concentration and light intensity, together with the use of isonicotinic hydrazide as an inhibitor, and found a maximum rate of glycolic acid production at very low (not zero) CO_2 concentrations.

For exploration of the pathway that leads to the formation of glycolic acid, the application of specific inhibitors, preventing the further metabolism of glycolic acid, appeared to be of value. At present there are two inhibitors known which strongly influence the build-up of glycolic acid: Zelitch,[4] several years ago, found that α-hydroxysulfonic acids specifically inhibit glycolic acid oxidase–an enzyme previously isolated from tobacco leaves.[5] This enzyme is able to oxidize glycolic acid to glyoxylic acid and, at a lower rate, lactic to pyruvic acid. The inhibition between α-hydroxysulfonic and α-hydroxy-carboxylic acids is competitive, similar to the well-known example of competition between sulfonamides and p-aminobenzoic acid. Whittingham and co-workers[3,6] investigated the effect of isonicotinic hydrazide on glycolic acid production by Chlorella and found it to block the further metabolism of this substance in a later reaction–namely, the last step (glycine → serine) in the sequence glycolic acid → glyoxylic acid → glycine → serine.

To prevent glycolic acid from being further converted, the first inhibitor seemed to be more useful than the second, since it blocks the step immediately following glycolic acid itself. Under appropriate conditions, Zelitch observed a considerable accumulation of glycolic acid in spinach chloroplasts[7] as well as in several plant leaves. Despite Zelitch's description of this type of inhibitor as "very specific," it appeared to be useful to search for additional effects on the label distribution in photosynthesis experiments. In the general formula R-CHOH-SO_3H of α-hydroxy-sulfonic acids, R can vary considerably, and almost all compounds of this type are more or less effective in blocking the oxidation of α-hydroxy-carboxylic acids to keto-acids. However, there is a great difference in their ability to permeate through biological membranes, α-pyridyl-hydroxymethane-sulfonic acid

---

1. A. T. Wilson and M. Calvin, J. Am. Chem. Soc. 77, 5948 (1955).
2. J. A. Bassham and M. Kirk, Biochem. Biophys. Res. Comm. (in press).
3. G. G. Pritchard, W. J. Griffin, and C. P. Whittingham, J. Exp. Botany 38, 176 (1962).
4. I. Zelitch, J. Biol. Chem. 224, 251 (1957).
5. I. Zelitch and S. Ochoa, J. Biol. Chem. 201, 707 (1953).
6. G. G. Pritchard, C. P. Whittingham, W. J. Griffin, Nature 190, 553 (1961).
7. I. Zelitch, Prox. Biochem. Soc., Biochem. J., 77, 11 P (1960).

usually being the most permeable of all the ones tested so far. Therefore this compound was applied exclusively in the experiments described in this paper.

Experimental

Preparation of Chloroplasts

Spinach chloroplasts were isolated and sonicated as previously described by Park et al.[8] The chlorophyll content of the resulting suspension subsequently used for the incubation experiments was 2.1 mg/mliter, its pH being 7.0 at zero time.

Incubation

Each of two light incubation vessels 3.5 cm in diameter was fitted with a short syringe for the addition of $NaH^{14}CO_3$ at zero time, a long syringe for taking samples, and a capillary for pressure exchange. Each vessel was provided with an identical mixture of 1.35 mliter of the above chloroplast fragment suspension and of the following substances (measured in μM) contained in a total of 0.30 mliter of solution: $MgSO_4$, 8; $MnCl_2$, 3.2; adenosine triphosphate, 2; nicotinamide-adenine dinucleotide phosphate, 0.04; thiamine pyrophosphate, 2.8; L-ascorbic acid, 5; glutathione, 2.6; K_2HPO_4, 2.0. To one of the vessels was added 0.1 mliter of 0.2M Na-α-pyridyl-hydroxymethanesulfonate; to the other, 0.1 mliter of 0.1M Na_2SO_4. The vessels were put on a shaker in a water bath that was kept at 18 to 20° throughout the experiment, and illuminated from the bottom with a set of fluorescent lamps which provided a light intensity of approximately 20 000 lux at the bottom of the vessels. Five minutes after the illumination had started, 0.25 mliter of 0.06M $NaH^{14}CO_3$ (0.5 mC) was added (zero time) to each vessel with a few seconds' time difference between them. The total volume of each incubation mixture was then 2.0 mliter. After certain intervals, 0.1-mliter samples were taken out by the long syringe and poured into small screw-cap vials containing about 1 mliter of boiling methanol; then the vials were closed and heated for about 3 min in a boiling-water bath. After collection of all the samples, each of them was spotted on the origin of a two-dimensional paper chromatogram (Whatman No. 4 paper) which was run with "semistench" solvent[9] for 14 h in the first dimension and with butanol-propionic acid-water for 10 h in the second dimension. After the paper was dried, the area that was expected to contain glycolic acid was carefully sprayed with saturated $NaHCO_3$ solution to prevent the acid from volatilizing, and the spots were located on the chromatogram by autoradiography. After being excised from the chromatogram, the spots were counted for their relative radioactivity on a 2-tube automatic counting machine developed in this laboratory;[10] with ^{14}C this machine counts about 10.7% of the total disintegrations on Whatman No. 4 paper. Table 4-I shows the results of this counting procedure; Tables 4-II and 4-III show further mathematical evaluation of the data.

---

8. R. B. Park, N. G. Pon, K. P. Louwrier, and M. Calvin, Biochim. Biophys. Acta 42, 27 (1960).

9. G. J. Crowley, V. Moses, and J. Ullrich, J. Chromatog. (in preparation).

10. V. Moses and K. K. Lonberg-Holm, UCRL-10112 (March, 1962).

Table 4-I. Relative radioactivity of spots in counts/min, as a function of incubation time, with and without inhibitor.

	Spot No.	Inhibitor	Incubation time (min)														
Total activity per chromatogram		-	160	800	2500	7995	15690	33000	64400	105715	193240	312175	440325	516540	580175	620245	709490
		+	150	795	2495	8235	14950	32990	65260	115665	192050	319520	430285	512095	565235	590415	600040
Origin	0	-	45	45	95	390	685	3630	5070	4930	9410	15080	12910	19700	23800	32700	31800
		+	0	10	60	180	340	1300	1780	2330	(blank)	4870	9380	8630	6450	8540	5460
Phosphoglyceric	1	-	115	755	2310	7130	13150	21130	38500	57700	101500	180300	212000	259300	261500	(blank)	248000
		+	150	785	2350	7450	12350	25100	45000	77000	129700	222100	287700	316000	343000	345500	337300
Sugar diphosphates	2	-	--	--	55	120	710	2130	3100	3110	5620	15660	58200	70100	91000	96700	114170
		+	--	--	35	140	415	1230	2270	2440	2710	3000	4670	4280	5460	4450	4320
Succinic acid	3	-	--	--	--	--	240	290	1365	3700	7540	14330	26400	21200	21500	15440	15570
		+	--	--	--	30	105	590	2190	6200	11920	19000	26200	32000	37200	37600	38300
Sugar monophosphates	4	-	--	--	40	355	905	4000	11570	21900	44800	61900	61900	64100	89800	91200	101200
		+	--	--	50	370	1520	4130	11880	21750	33300	42200	41300	55600	39600	38000	47800
Phosphoenolpyruvic acid	5	-	--	--	--	--	--	--	485	615	915	1900	2650	2970	3650	3930	4920
		+	--	--	--	25	85	120	250	625	985	1670	3250	4120	4820	5310	5280
Unidentified compound	6	-	--	--	--	--	--	--	--	440	1160	1600	1445	1960	1890	1550	2350
		+	--	--	--	40	135	100	270	715	995	1590	1980	1960	2090	2200	2370
Glycine + serine + glutamine	7	-	--	--	--	--	--	--	--	720	1930	6720	19300	24500	21250	45900	62200
		+	--	--	--	--	--	105	115	445	1025	1900	2440	3760	6240	4880	6220
Alanine	8	-	--	--	--	--	--	--	270	795	1540	2450	4350	3900	4060	4560	5080
		+	--	--	--	--	--	120	480	915	1660	2910	5530	7280	11300	16100	18430
Sucrose	9	-	--	--	--	--	--	--	--	240	370	650	1480	3750	5990	6720	8770
		+	--	--	--	--	--	--	--	170	355	960	2470	4280	6350	7180	9100
Aspartic acid	10	-	--	--	--	--	--	--	--	745	1850	5040	11700	14200	17730	23440	40200
		+	--	--	--	--	--	90	--	995	2010	4900	9600	16400	28800	37900	47000
Glutathione (oxidized)	11	-	--	--	--	--	--	--	--	130	630	1110	1090	985	1355	1735	2090
		+	--	--	--	--	--	105	210	155	200	190	290	165	130	100	130
Pyruvate	12	-	--	--	--	--	--	--	--	--	--	265	685	570	680	655	780
		+	--	--	--	--	--	--	160	525	880	1070	1430	1850	2800	3480	3360
Pentose monophosphate	13	-	--	--	--	--	--	--	--	460	430	880	905	1055	1230	1525	1635
		+	--	--	--	--	--	--	285	485	585	790	1000	1360	1200	1255	1740
Glutamic acid	14	-	--	--	--	--	--	--	--	--	585	1110	2620	3220	4360	5320	5430
		+	--	--	--	--	--	--	--	195	495	915	1670	2290	3630	4750	5320
Glycolate	15	-	--	--	--	--	--	--	--	--	480	1120	2200	2930	5180	5000	6800
		+	--	--	--	--	--	--	--	--	365	1110	3980	6550	11500	14240	12670
α-Ketoglutarate	16	-	--	--	--	--	--	--	--	135	280	950	1925	2010	2270	2590	3280
		+	--	--	--	--	--	--	--	--	450	640	1300	1090	1330	1260	1310
Unidentified compound	17	-	--	--	--	--	--	--	--	115	100	195	245	285	330	445	800
		+	--	--	--	--	--	--	--	--	105	325	295	550	1040	1255	2660
Uridinediphospho-glucose	18	-	--	--	--	--	--	1820	3880	9560	12860	12190	13820	13100	12900	14040	37600
		+	--	--	--	--	--	--	270	720	1630	8650	24600	41200	48600	50750	42700
Unidentified compound	19	+	--	--	--	--	--	--	--	--	--	50	170	195	215	185	215
Glycerate	20	-	--	--	--	--	--	--	--	120	170	225	395	520	445	675	1580
		+	--	--	--	--	--	--	--	--	--	640	700	1780	2520	4230	6260
Malate	21	-	--	--	--	--	--	--	--	--	140	525	1660	3160	4570	5850	8990
		+	--	--	--	--	--	--	--	--	--	40	205	310	430	550	890
Citrate	22	-	--	--	--	--	--	--	--	--	230	340	390	605	850	850	1065
		+	--	--	--	--	--	--	--	--	--	--	125	235	270	340	280
Unidentified compound	23	+	--	--	--	--	--	--	--	--	--	--	--	210	260	360	355
	24	+	--	--	--	--	--	--	--	--	--	--	--	--	--	--	570
	25	-	--	--	--	--	--	--	--	--	--	--	380	530	840	595	540
Fumarate	26	-	--	--	--	--	--	--	--	--	--	65	175	295	720	900	1255
Unidentified compound	27	-	--	--	--	--	--	--	--	--	--	235	635	580	665	645	855
	28	-	--	--	--	--	--	--	--	--	--	--	--	--	380	510	895
	29	-	--	--	--	--	--	--	160	420	700	835	865	1015	1230	1470	1635

Table 4-II. Ratio of counts/min with inhibitor vs counts/min without inhibitor for important spots in Table 4-I.

		Incubation time (min.)											
	Spot No.	4	6	10	15	20	30	45	60	75	90	105	120
Total activity	Σ	1.03	0.95	1.00	1.01	1.09	0.99	1.03	0.98	0.99	0.97	0.95	0.85
Origin	0	0.46	0.50	0.36	0.35	0.47	0.29	0.32	0.80	0.44	0.54	0.26	0.17
Phosphoglyceric acid	1	1.04	0.94	1.19	1.17	1.33	1.28	1.23	1.36	1.22	1.31	1.35	1.36
Sugar diphosphates	2	1.17	0.58	0.58	0.76	0.78	0.48	0.19	0.08	0.06	0.06	0.05	0.04
Succinate	3	--	0.44	2.03	1.61	1.67	1.60	1.33	0.99	1.51	1.73	2.44	2.46
Sugar monophosphates	4	1.04	1.68	1.03	1.01	0.99	0.74	0.68	0.67	0.87	0.44	0.42	0.47
Phosphoenolpyruvic acid	5	--	--	--	0.52	1.02	1.08	0.88	1.23	1.39	1.32	1.35	1.07
Unidentified compound	6	--	--	--	--	1.63	0.86	0.99	1.28	1.00	1.11	1.42	1.01
Glycine + serine + glutamine	7	--	--	--	--	0.62	0.53	0.28	1.13	0.15	0.29	0.11	0.10
Alanine	8	--	--	--	1.78	1.15	1.08	1.19	1.27	1.87	2.79	3.53	3.63
Sucrose	9	--	--	--	--	0.71	0.96	1.48	1.67	1.14	1.06	1.07	1.04
Aspartic acid	10	--	--	--	--	1.33	1.09	0.97	0.82	1.16	1.63	1.62	1.17
Glutathione (oxidized)	11	--	--	--	--	1.19	0.32	0.16	0.27	0.17	0.10	0.06	0.06
Pyruvate	12	--	--	--	--	--	--	4.04	2.09	3.25	4.12	5.32	4.32
Pentose monophosphate	13	--	--	--	--	1.05	1.36	0.90	1.11	1.29	0.98	0.82	1.06
Glutamic acid	14	--	--	--	--	--	0.85	0.82	0.64	0.71	0.83	0.89	0.98
Glycolate	15	--	--	--	--	--	0.76	0.99	1.81	2.23	2.22	2.85	1.86
α-Ketoglutarate	16	--	--	--	--	--	1.61	0.67	0.68	0.54	0.59	0.49	0.40
Unidentified compound	17	--	--	--	--	--	1.05	1.66	1.20	1.93	3.15	2.82	3.32
Uridine diphosphoglucose	18	--	--	--	0.07	0.08	0.13	0.71	1.78	3.46	3.77	4.10	1.14
Glycerate	20	--	--	--	--	--	--	2.84	1.77	3.43	5.89	6.25	3.96
Malate	21	--	--	--	--	--	--	0.08	0.12	0.10	0.09	0.09	0.10
Citrate	22	--	--	--	--	--	--	--	0.32	0.39	0.32	0.40	0.26
Fumarate	26	--	--	--	--	--	--	0	0	0	0	0	0

Table 4-III. Average ratios for the spots in Table 4-II from 60 to 120 min.

Compound	Spot No.	Counts/min with inhibitor / Counts/min without inhibitor	Compound	Spot No.	Counts/min with inhibitor / Counts/min without inhibitor
	Σ	0.95	Origin	0	0.44
Phosphoglyceric acid	1	1.32	α-ketoglutarate	16	0.54
Sugar diphosphates	2	0.06	Succinate	3	1.83
Sugar monophosphates	4	0.57	Fumarate	26	0.00
Pentose mono-phosphates	13	1.05	Malate	21	0.10
Phosphoenolpyruvic acid	5	1.27	Citrate	22	0.34
Uridinediphospho-glucose	18	2.85	Pyruvate	12	3.82
Aspartic acid	10	1.28	Glycolate	15	2.19
Glutamic acid	14	0.81	Glycerate	20	4.26
Glycine + serine+ glutamine	7	0.16	--	--	--
Glutathione (oxidized)	11	0.13	--	--	--
Alanine	8	2.62	?	6	1.16
Sucrose	9	1.20	?	17	2.48

Discussion

In addition to the expected preservation of glycolic acid, the results of the experiment show a strong blocking effect of the inhibitor on succinic dehydrogenase. This explains the accumulation of ^{14}C succinate, the lack (in decreasing order) of ^{14}C in fumarate, malate, and citrate (Fig. 4-1), and as a consequence of this, the accumulation of pyruvate which is prevented from entering the Krebs cycle and therefore gives rise to a greatly increased formation of alanine. As a result of this increased alanine formation, less nitrogen is available for the synthesis of glycine and serine.

The numbers in the Tables also demonstrate a considerable effect on the pool size of metabolic phosphates. However, these results cannot be regarded as unequivocal because of the poor resolution on the chromatograms in the phosphate area.

An attempt to reproduce the experiment and to extend it to a reliable phosphate analysis, by chromatographing half of each sample for a long time in both dimensions, failed because of a still-unexplained breakdown of the chloroplast preparation. There was not sufficient time for me to repeat this experiment before I left the laboratory, and I shall attempt to do this in Freiburg.

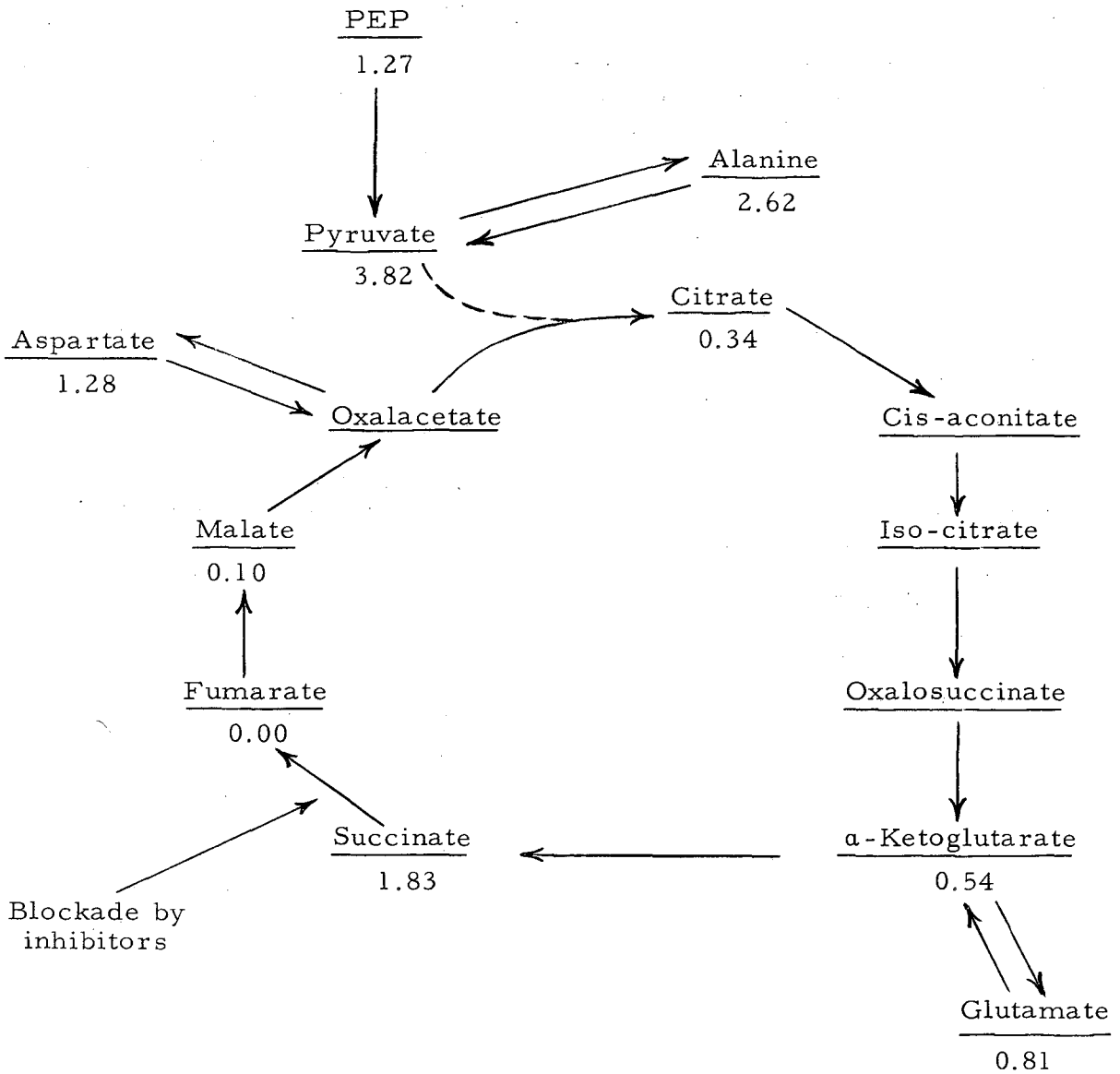

Fig. 4-1. Krebs cycle, showing the effect of the inhibitor on the involved acids by the ratios of Table 4-III and the apparent blockade of succinate-dehydrogenation. The numbers refer to the ratio of counts/min with inhibitor to counts/min without inhibitor (see Table 4-III).

5. ON THE USE OF THE NUCLEAR ACTIVATION REACTION $^{18}O(\alpha,\eta)\,^{21}Ne$ FOR ^{18}O ANALYSIS

Elie A. Shneour

Since 1957 there has accumulated a rapidly growing body of evidence to underscore the ubiquitous role of molecular oxygen and of oxygen atoms in biological systems.[1] Unfortunately, no suitable radioactive isotope of this element is known. Oxygen-15 and ^{19}O have half-lives of 126 (β^+) and 27 (β^-) sec, respectively. Other radioactive nuclides are not likely to have better properties in this respect. Next to ^{16}O, stable ^{18}O is the most abundant natural isotope (0.204 atom %) and is the logical choice for oxygen tracer work. Mass spectrographic analyses have been greatly improved, but still suffer from elaborate experimental requirements. Activation analysis remains the only known avenue for a potentially simple and sensitive method of assay. The basic requirements for an effective activation procedure are:

1. Specificity of bombarding particle. That is to say, ^{18}O must have a significantly larger reaction cross section than other common elements found in biological systems, such as: H, C, N, O, Na, Mg, P, S, K, Fe, and Mn.

2. High yield of the desired reaction product to be analyzed.

3. Ready availability of the bombarding particle within the desired energy range.

4. Homogeneous flux of particles bombarding the assay target.

The nuclear activation reaction $^{18}O\,(p,n)\,^{18}F$ was the object of a study in this laboratory[2] but the routine use of that method has been discouraging for the following reasons:

1. A cyclotron is required to develop protons with an energy spectrum of 2.6 to 6.0 MeV.

2. The proton beams lack homogeneity.

3. The samples are destroyed under bombardment, primarily due to thermal effects.

A specific example of these problems, applied to the assay of photosynthetic pigments is discussed in an earlier report.[3] It is clear, however, that reasons 2 and 3 enumerated above are susceptible of solution and present primarily a substantial engineering problem.

---

1. J. B. Neilands, Ann. Rev. Biochem. 27, 455 (1958).

2. I. Fogelstrom-Fineman, O. Holm-Hansen, B. M. Tolbert, and M. Calvin Intern. J. Appl. Radiation Isotopes 2, 280 (1957).

3. E. A. Shneour, in Bio-Organic Chemistry Quarterly Report, UCRL-9900, October, 1961, p. 21.

Theoretical Considerations

A report from a Soviet Union team[4] suggested the following reaction for ^{18}O assay, $^{18}O\ (\alpha, \eta)\ ^{21}Ne$:

$$_{8}^{18}O + _{2}^{4}He \rightarrow [_{10}^{22}Ne]^{*} \rightarrow _{10}^{21}Ne + _{0}^{1}n;\ Qm + -0.705.$$

The probability of $[_{10}^{22}Ne]^{*}$ going to the ground state by γ emission is very low compared with that of the reaction written above. This is shown by the fact that at E_{α} = 5.3 MeV, a 360 ± 10-keV γ is observed. This occurs in 70% of the transitions, with a direct ground-state reaction taking place in 30%.[5]

No specific cross-section data are available, but it has been shown that there is a tenfold increase when the E_{α} is increased from 3 to 5 MeV. This has been confirmed by our own preliminary studies with a ^{210}Po source with and without a gold window, when ^{18}O-malonic acid was the target.

Sources

The sources studied for suitability are shown in Table 5-I. The nominal neutron yield for a thick target of ^{18}O is only 3.0×10^{-5} per α particle.[6] Thus a high flux density is required and a significant neutron yield is obtained only with ^{210}Po and ^{242}Cm sources. Under these conditions 5×10^{3} neutrons/sec can be expected from a 1 mC/cm^2 deposited ^{210}Po source protected with a gold-flashing window of 30 to 50 μg/cm^2. (^{210}Po has a high vapor pressure and is a serious health hazard.) Since ^{210}Po has the highest α-specific activity and was more readily available than ^{242}Cm, it was chosen for these studies. The specifications for this source (prepared by Monsanto Chemical Company, Mound Laboratory, Miamisburg, Ohio) were as follows:

Source number: MF 5445806 AP-137

Source strength: 107.7 mC ($2.39 \times 10^{11}\ \alpha \rightarrow$ d/min) deposited over 11.6 cm^2 or 9.28 mC/cm^2

Form of ^{210}Po: plated metal

Window material: gold plated over polonium (35 μg/cm^2)

Maximum E_{α}: 3.28 MeV (equals a range in air of 2.80 cm)

Backing support: copper, 3×3×1/16-in. thickness.

As $t_{1/2}$ = 138 days, and as the source was used for a period from t = 9 days to t = 80 days, the α-activity range was 0.998 to 0.670 of the initial specification.

---

4. V. V. Ivanova, A. I. Nazarov, E. V. Polunskaya, A. G. Khabakhpashev, and E. M. Tsenter, At. Energ. (USSR) 7, 166 (1959).

5. F. Ajzenberg-Selove and T. Lauritsen, Nucl. Phys. 11, 292 (1959).

6. A. Nir, Isotope Division, The Weitzman Institute of Science, Rehovoth, Israel, personal communication.

Table 5-I. Characteristics of α sources for activation analysis.

Source	α-specific activity	$t_{1/2}$	Decay sequence
${}_{84}^{210}Po$	4.5×10^{3} C/g	138 d	$\xrightarrow[100\%]{\alpha}$ ${}_{82}^{206}Pb$ (stable)
${}_{94}^{239}Pu$	6.0×10^{-2} C/g	2.4×10^{4} y	$\xrightarrow{\alpha}$ ${}_{92}^{235}U$ $\xrightarrow[7.1\times10^{8}\ y]{\alpha}$ ${}_{90}^{231}Th$ $\xrightarrow[25\ y]{\beta^-}$ ${}_{91}^{231}Pa$
${}_{95}^{241}Am$	3.00 C/g	4.75×10^{2} y	$\xrightarrow{\alpha}$ ${}_{93}^{237}Np$ $\xrightarrow[2.2\times10^{6}\ y]{\alpha}$ ${}_{91}^{233}Pa$ $\xrightarrow[27.4\ d]{B^-}$ ${}_{92}^{233}U$
${}_{96}^{242}Cm$	3.00×10^{3} C/g	162 d	$\xrightarrow{\alpha}$ ${}_{94}^{238}Pu$ $\xrightarrow[92\ y]{\alpha}$ ${}_{92}^{234}U$ (stable)

Target Support

The target material containing ^{18}O must be deposited on a support with a very low cross section for low-energy neutrons. Three suitable metals are magnesium, aluminum, and zirconium. Reactor-purity material is essential and could best be obtained in zirconium sheets of 30-mils thickness.

Neutron Detection

Two types of neutron detectors are available: solid-state and gaseous. Solid-state detection is based on the very large capture cross section of thermalized neutrons by boron or lithium:

$$_{5}^{10}B + _{0}^{1}n \longrightarrow _{3}^{7}Li + _{2}^{4}He$$

$$_{3}^{6}Li + _{0}^{1}n \longrightarrow _{1}^{3}H + _{2}^{4}He.$$

The α particles produced activate a zinc sulfide-sliver matrix that produces scintillations in the visible spectrum. A suitable photomultiplier in close proximity to this scintillator collects light pulses which are then amplified, discriminated, and counted on an integrating digital device. The geometry and specifications of this system were as follows:

In a 3×3×20-in. (i.d.) grooved lucite box:

3×3-in. copper support, 1/16-in. thickness

Deposited ^{210}Po

Deposited gold window

0.5 mm interval

Material containing ^{18}O (thick target)

3×3-in. Reactor-grade zirconium support, 30 mils thickness

3-in. diameter slow neutron boron polyester detector

(Nuclear Enterprises, Winnipeg, Canada, Model NE 400, or NE 402)

Silicone oil

Photocathode surface of photomultiplier (Dumont 6292 or equivalent

Preamplifier for photomultiplier

Shielded leads to amplifier, discriminator, and counters.

This solid-state type of detector provides an excellent neutron-to-gamma response ratio (about 100 to 1 for Po-Be neutrons to ^{60}Co gammas is easily attained). The NE 400 detector depends on the $^{10}B(\eta, \alpha)^{7}Li$ reaction with a cross section of about 750 b and has an absolute detection efficiency of 20% for thermal neutrons, and 0.1% for $^{18}O(\alpha,\eta)^{21}Ne$ neutrons without thermalization.

The NE 402 detector has a much higher enrichment in ^{10}B, which permits absolute detection efficiencies of 35% for thermal neutrons and 0.2% for $^{18}O(\alpha, \eta)^{21}Ne$ neutrons without thermalization.

Results obtained with this system and an infinitely thick target of malonic acid (20 atom % ^{18}O) compared to identical malonic acid (^{16}O) targets showed results indistinguishable from background counts after counting periods upward of 100 h. When a 10-cm-thick paraffin moderator was inserted between the zirconium support and the face of the solid-state detector, no difference could be observed.

Therefore, the equipment was redesigned to enhance sensitivity. This was attempted by using a second method of neutron assay, the boron trifluoride gaseous detector in a 4π geometry. This device consisted of a 6-in.-i.d. 1/8-in. brass cylinder 15 in. long, open at one end. It was lined internally with a 30-mil cadmium neutron shield and completely filled with paraffin. Around the inner periphery and equidistant from each other, three type RSN-7A Reuter-Stokes BF_3 neutron detectors were embedded in the paraffin and connected in parallel (see Fig. 5-1). These tubes are 1×12 in., of which a length of 8-1/8 in. is active. They have a BF_3 fill pressure of 20 to 120 cm mercury. Those made available by the Livermore Laboratory for the ^{18}O device had a fill pressure of 20 cm. These three tubes provided a total sensitivity of 10 counts/min per neutron per cm^2/sec, and by using a maximum of twelve tubes with a fill pressure of 120 cm, a total sensitivity in excess of 100 counts/min per neutron per cm^2/sec could have been obtained. These sensitivity measurements were made with a Po-Be standard neutron source. Into a 3×3-in. ^{210}Po source, a malonic acid-zirconium 40 sand-which was inserted. The detector was connected to a maximum-sensitivity low-noise preamplifier counter electronic system. The best results obtained are tabulated below:

Photomultiplier B+ voltage: 2000 V

(1) Relative discriminator position (%)	(2) Malonic acid ^{18}O 0.2% (counts/min)	(3) Malonic acid ^{18}O 20% (counts/min)	(4) Δ [(3) minus (2)] (counts/min)	(5) Δ% [100×(4) divided by (3)]
50	9 504	10 717	1 213	11.3
60	4 836	4 975	139	2.8
70	2 553	2 775	222	8.0
80	1 450	1 559	109	7.0
90	690	760	70	9.2
100	394	431	37	8.6

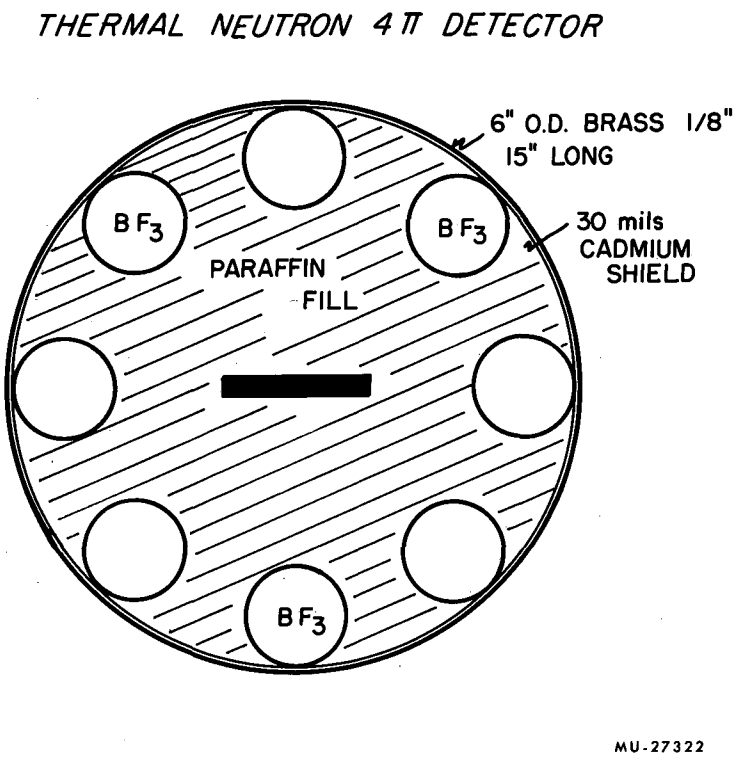

Fig. 5-1. Schematic diagram of the BF_3 thermal-neutron detector.

The results in the last column show that this method is not reliable within a range required for a sensitive ^{18}O assay, except where differences in ^{18}O content between controls and experimental samples are extremely large. Even with a tenfold improvement in sensitivity (with 10 to 12 BF_3 tubes as the detector) this system falls short of minimum requirements for ^{18}O assay.

In conclusion, assay of ^{18}O in biological material by the $^{18}O(\alpha,\eta)^{21}Ne$ nuclear activation reaction offers some promise, but in order to achieve desired results it will be necessary to improve the neutron detector sensitivity to give a signal-to-noise ratio of the order of 10^4 or better. This could be achieved by one or more of the following:

1. Increase in E_α from 2.8 to 5 MeV or better. This presents a very serious health hazard because both ^{210}Po and ^{242}Cm have high vapor pressures.

2. A rigorous purification of the α-source to remove the relatively high β and γ emissions caused by impurities.

3. Improved geometry of neutron detection.

4. Improved geometry of the activation system.

Acknowledgments

The author is indebted to many members of the University of California Lawrence Radiation Laboratory staff for valuable assistance, and in particular to the following:

Mr. Frank Upham, IRE, Electronics Engineer
Dr. Homer E. Conzett
Mr. Robert Walker, Health Chemistry
Mr. Charles Curry, Livermore Laboratory (for the loan of BF_3 tubes)

This work was done during the tenure of an Advanced Fellowship from the American Heart Association.

6. PHOTO-INDUCED ABSORPTION CHANGES. I. INSTRUMENTATION

Irwin D. Kuntz, Jr.

Introduction

The primary energy conversion process in photosynthesis has been of considerable interest to workers in this laboratory.[1,2] This paper is concerned with investigations of the early steps in the conversion of light energy into chemical energy. These investigations study changes in the absorption spectra of photosynthetic materials when samples are exposed to light. These "photo-induced absorption changes" are linked to the primary processes by a large amount of indirect evidence.[3] This evidence includes:

1. All photosynthetically active materials studied to date show photo-induced absorption changes.

2. Some of the readily identifiable bands are assigned to molecules such as chlorophylls, cytochromes, and carotenoids–pigments independently implicated in quantum conversion activity.

3. The rapid reversible nature of many of these absorption changes points to processes occurring before the enzymatic reactions of the Calvin cycle.

In this first paper we shall concentrate on the instrumentation developed to study these absorption changes. Our desire to follow the wavelength dependence (spectrum) and the kinetic behavior (rise and decay times) of the absorption changes presented three problems. First, we needed a means of taking the spectrum of an illuminated sample. This requires two light sources. The first, the analyzing beam, measures the absorption of the sample; the second, the actinic beam, causes excitation of the sample. The second problem was that the changes in absorption are quite small–large ones being of the order of 0.1 to 1%. We wished to investigate changes of 0.05 to 5×10^{-6} optical density units. Much of this range is well within the noise level on a conventional spectrophotometer. Third, the reversible transients cover a wide range of rise and decay times. Some have been reported of microsecond duration, others persist for some minutes. Time constants of less than a second are inaccessible on many commercial instruments. In summary, then, we required a spectrophotometer that had both high sensitivity and a wide range of response times. It also had to have a suitable physical layout to permit an auxiliary light source to illuminate the sample while the spectrum was being run.

---

1. M. Calvin, J. Theoret. Biol. 1, 258 (1961).
2. K. Sauer, UNESCO Symposium on Amplification Techniques in Cell Biology, Buffalo, N. Y., 1962.
3. A partial list of references would include:
   a. W. Arnold and R. K. Clayton, Proc. Nat. Acad. Sci. U.S. 46, 769 (1960).
   b. L. N. M. Duysens and J. Amesz, Biochim. Biophys. Acta 64, 243 (1962).
   c. B. Kok and G. Hoch, Light and Life (Interscience, 1961), p. 397.
   d. H. T. Witt et al., Nature 194, 854 (1962).

Clearly the high-sensitivity and fast-response requirements were the major source of difficulty. Devices described previously have, in general, emphasized one or the other of these characteristics. Early spectrometers constructed by Duysens,[4] Lundegardh,[5] and Chance[6] were designed primarily for sensitivity. They are much like the commercial instruments available today from Cary or Beckman in that they have a chopper-stabilized double-beam arrangement, permitting one compartment to be exposed to an actinic light while the other (reference) chamber remains darkened (i.e., with only the weak analyzing beam illuminating it).[7] The difference signal is modulated at the chopping frequency and is amplified by means of a tuned circuit. The bandpass of the amplifiers and/or the response time of the recording system determine the minimum noise level. Typical values of the noise level in the best systems approach 0.01% for response times of one second.[6] It is easily appreciated that decreasing the response time of this type of instrument can only lead to a loss in sensitivity. Further, the use of a low-frequency light-chopper places a practical restriction on the upper limit of the frequency response.

Witt has developed an instrument with much faster transient response.[8] The time resolution of his spectrometer approaches a few microseconds. This is accomplished by excitation of the sample with a flash lamp and presentation of the optical density changes directly on an oscilloscope. The sensitivity of this instrument is perhaps 10 to 50 times less than that of those described above.

The apparatus we finally settled upon was designed to meet three objectives: First, it had to have a sensitivity that was approximately independent of its response time. Second, it should be flexible enough to use both extremes of excitation sources: flash lamps and steady light. Third, it should have automatic data presentation.

These objectives have been met in most respects by the instrument described below. Repetitive changes in absorption as small as 0.01% can be detected. With this sensitivity it has provided 10-μsec time resolution. An automatic recorder readout of changes in optical density as a function of wavelength or time is available. These specifications are routine. Optimum conditions can provide a tenfold improvement.

The major shortcoming is that we have not yet developed suitable modifications for the use of a steady actinic source; our excitation must be modulated, although this modulation can be as slow as 0.1 cps. Experiments using steady excitation were performed on a slightly modified Cary 14M using

---

4. L. N. M. Duysens, Ph.D. Thesis, Utrecht, 1952.
5. H. Lundgardh, Biochim. Biophys. Acta 27, 653 (1958); 35, 340 (1959).
6. B. Chance, Rev. Sci. Instr. 22, 619 (1951).
7. Chance uses a reference wavelength, comparing the light minus dark effects at other wavelengths to the changes at the selected wavelengths. This enables him to use a single sample
8. H. T. Witt, Nature 42, 72 (1955); Z. Elektrochem. 59, 10, 981 (1955).

an available accessory, the scattered transmission apparatus. Work on the Cary will be discussed in a later paper. (These experiments were performed in collaboration with Dr. P. Loach.)

Experimental

General Considerations

A block diagram of the spectrometer is given in Fig. 6-1. The present physical layout is shown schematically in Fig. 6-2. In brief, the spectrometer operates as follows: The light from the monochromator passes through the sample and then falls on a photomultiplier. A modulated actinic beam also illuminates the sample. Changes in the absorption of light by the sample thus appear as a modulation on the transmitted intensity. The photomultiplier output, then, consists of a dc signal (transmitted intensity) and a small ac signal (repetitive absorption change). The ac signal is amplified further while the dc level is stripped off by ac coupling or dc suppression. The amplified signal now consists of a pulse train whose voltages represent the periodic fluctuations in the absorbance of the sample. The pulses are fed into a sampling circuit–the so-called "boxcar integrator." The boxcar integrator is turned on for a very short time at the pulse repetition frequency. It is held in a fixed (but adjustable) phase relation to the incoming signal and acts as a rectifier. Thus a dc signal related to the average input voltage is available to charge an RC circuit. The noise level on the output depends on the value of the integrating time of this filter circuit. However, the time resolution depends only on the small time interval that the boxcar circuitry is on. Thus we have achieved our goal of the independence of sensitivity and transient response time. The filtered output drives the Y axis of an X-Y recorder. Appropriate motor drives permit an automatic readout proportional to the changes induced in the sample by the actinic light. Figure 6-1 shows the waveforms in various parts of the spectrometer.

Detailed Analysis of the Spectrometer

Monochromator. A commercial Bausch and Lomb grating monochromator is used. The source is either a 500-W tungsten bulb or a 150-W Hydrogen Lamp. The tungsten source is run from a highly stable low-ripple Mid-Eastern power supply (Model ST 100-10). Typical slits are 1 to 3 mm (1.5 to 5 mμ half-band width). Although this is rather poor resolution for visible spectroscopy, the broad absorption bands and the equally broad photo-induced bands do not generally warrant better resolution. Some care must be taken to keep the intensity of the analyzing beam fairly low (less than 10^{14} quanta/sec-cm^2). A fast monochromator with a bright source can provide sufficient light to produce measurable excitation of the sample. The stray light transmitted by the Bausch and Lomb offers two potential difficulties. In an intense absorption band, much of the transmitted light can be the 1% of stray white light which leaks through the monochromator. Second, a considerable amount of the first-order wavelengths are passed through the second order of the grating. The first difficulty has not been a problem to date. The second can be easily removed by use of a Corning color glass.

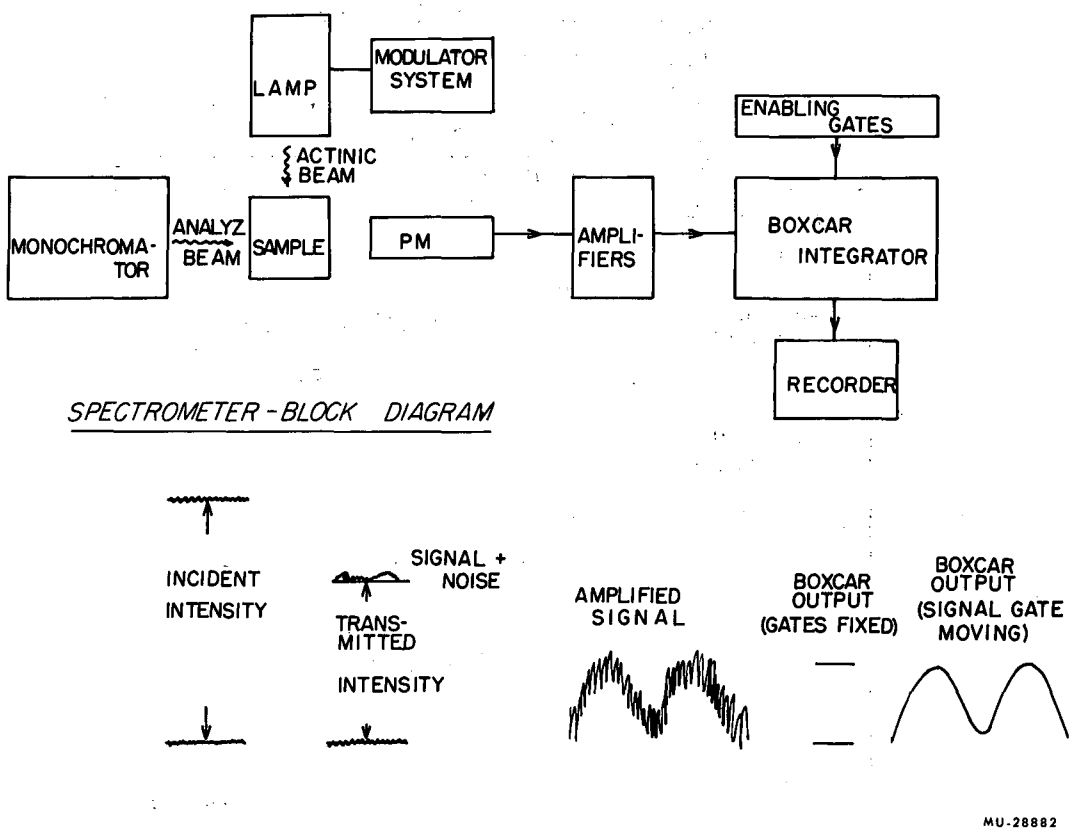

Fig. 6-1. Block Diagram of spectrometer and signals present.

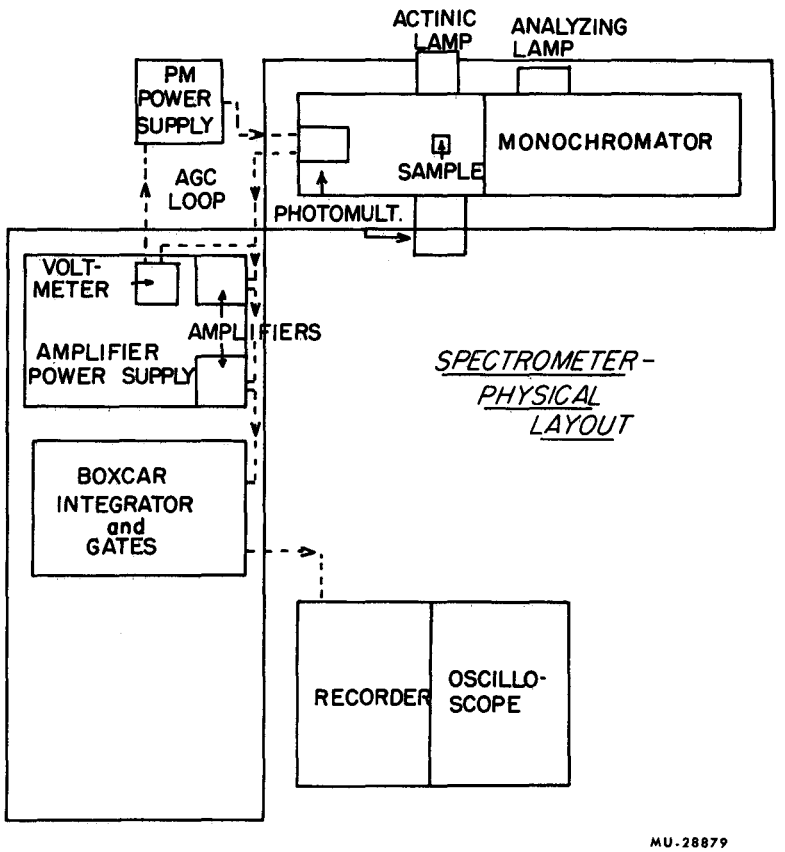

Fig. 6-2. Physical Layout of spectrometer (schematic).

Sample Compartment. The sample compartment is shown in Fig. 6-3. It has been designed for either single- or double-beam operation and can accommodate a variety of cell shapes and sizes. It is currently used as a single-beam unit. In this mode of operation the spectrometer only measures the reversible differences in absorption caused by the modulated actinic lamp. The actinic and analyzing beams are at right angles to reduce scattering. Provisions have also been made to place filters in both light beams, to help with the scattering problem. The proximity of the sample to the photomultiplier face permits highly scattering materials such as whole algae or bacteria to be studied without loss of sensitivity.

Actinic Lamps. Three different light sources have been used: a neon glow-discharge bulb which can be modulated electronically; a commercial 500-W tungsten projection bulb modulated with a rotating sector wheel; and a commercial flash lamp triggered repetitively.

The neon lamp was kindly made available for our use by Dr. L. Piette of Varian Associates.* Its ease of modulation, rapid rise and decay times (about 5 μsec), and convenient spectral lines make it an almost ideal source. Its one disadvantage is a relatively low intensity—about 10^{16} quanta/sec-cm^2 output. The tungsten bulb was used to test for saturation of the photoeffects. We have employed a commercial flash lamp (Edgerton Microflash Model 549) on a few occasions. The lamp delivers 7 watt-seconds in a 5-μsec flash.

The Detector. The detection of the abosrption changes is, of course, the heart of the problem. The detection circuits can be considered as three units: the photomultiplier, the amplifiers, and the boxcar integrator.

We have employed four commercial photomultipliers: Dumont 7664 (uv), Dumont 6292, and RCA 6217 (visible), and Dumont 6911 (Near ir). They are all of the 2-in. end-window variety. The photomultipliers have conventional base circuitry with approximately microsecond response time. They are run at 500 to 1000 V from a well-regulated NJE power supply. The photocurrent drawn is kept small—well down in the linear range of operation. Since the limiting noise in the spectrometer is the shot noise in the analyzing beam, no significant improvement is to be gained by cooling the phototubes. Some care has been taken to shield the photomultipliers from sources of electrical pickup. In particular, the sample compartment is enclosed in a wire-mesh electrostatic shield and the tubes themselves are enclosed in mumetal shields to reduce magnetic pickup. One unexpected difficulty developed when the flash lamp and the neon lamp were run off the same power line as the photomultipliers. The lamps draw sufficient power to cause detectable line fluctuations. Simply plugging them into a different outlet removed this problem.

Voltage amplification of 100 to 10 000 is used to boost the initial signal above the internal noise in the detection circuit. We have employed Tektronix plug-in preamplifiers with limited success. Since these units were designed for oscilloscope use, they do not have long-term stability of very low noise levels. For various applications we have used the Type D, Z,

* Although the lamp is not commercially available, some details of its circuitry are in the literature: W. E. Bell, A. C. Bloom, J. Lynch, Rev. Sci. Instr. 32, 688 (1961).

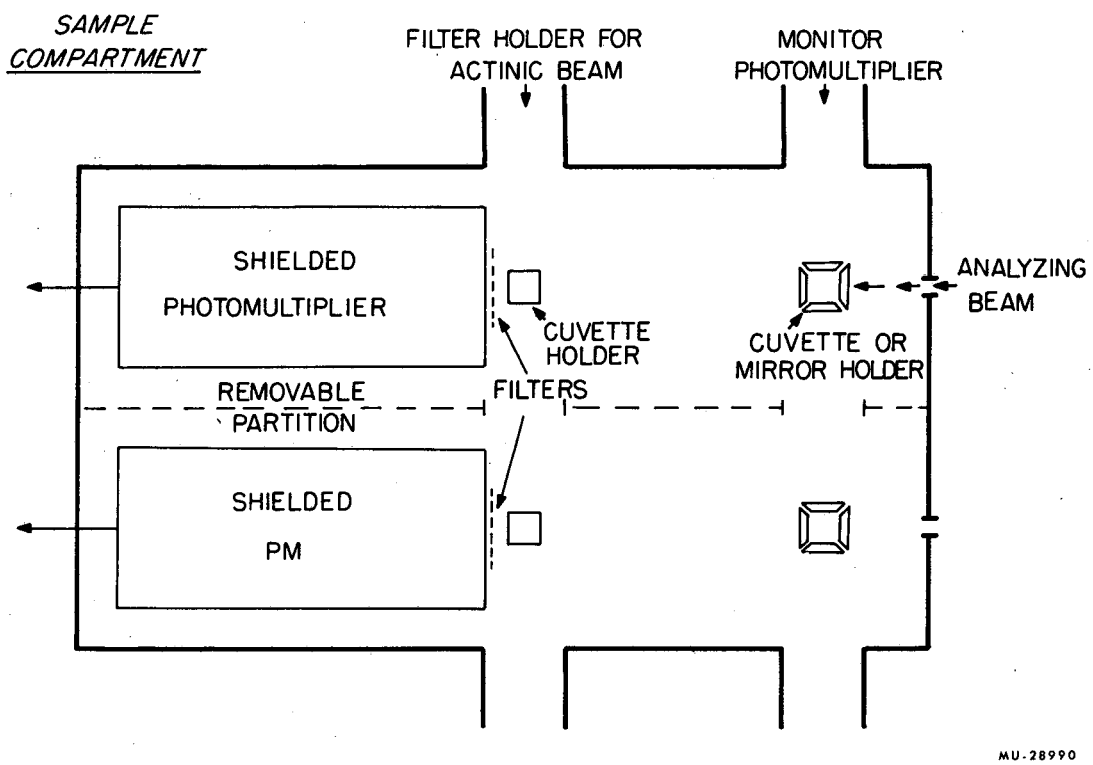

Fig. 6-3. Sample compartment.

and E plug-ins, powered from a Type 127 power supply. More suitable amplifiers will be available in the near future.

The boxcar integrator was constructed locally from a circuit due to Blume.[9] Figure 6-4 shows the circuit we used. It differs only in minor details from that described by Blume. The unit can be thought of as an electronic switch and a storage circuit. The four diodes (Vi-4) are normally back-biased and nonconducting until an enabling gate is supplied. The average incoming potential during the gate interval is impressed across the capacitance (Cl). If the RC charging time (often called the "learning time") is short compared to the gate duration, the voltage across Cl is equal to the average input voltage. After the enabling gate is turned off, this potential remains unchanged except for leakage paths to ground. Since the back resistance through the ceramic diodes (V3, 4) is about 10^{13} ohms, the discharge time (or "holding time") is very long, on the order of thousands of seconds. Note that if one gate interval is not of sufficient length to charge the capacitance to the full input voltage, successive pulses will also contribute to the potential across the condensor. Thus one can average many samples of the same signal, allowing signal-to-noise improvement.

The proper phasing of the enabling gates with the incoming signal is essential. We use a four-trace preamplifier in conjunction with a Tektronix 531 oscilloscope. Also, we use two separate boxcar channels, one to give us a reference signal. The two enabling gates, the amplifier output, and the signal from a photomultiplier which monitors the flash lamp are all presented simultaneously. Figure 6-5 shows a block diagram of the required trigger circuits. Figure 6-6 presents the phase relationship of the spectrometer waveforms. Figure 6-7 shows the boxcar output obtained by slowly changing the phase of the "signal gate," allowing the boxcar to trace out a signal. The boxcar output is compared to that obtained when a low-pass filter is used to reduce the noise in a conventional circuit. For comparable noise levels the latter would greatly distort the transient shape.

For construction details, the reader is referred to Blume's paper. Considerable care must be taken because of the very high resistances required for successful operation. For instance, ordinary shielded cables represent virtual short circuits. Teflon-insulated wire is required in the vicinity of the storage circuit and the diodes. The high resistances also require the use of the electrometer tube. Trying to read the potential on the condensor with an oscilloscope or an ordinary vacuum tube voltmeter rapidly discharges the circuit.

The performance of the boxcar integrator has been quite satisfactory. Typical operating conditions are 10-μsec to 10-msec gate durations, 1 to 10 cps repetition rates, and storage times of 0.01 to 1 sec. Internal noise under these conditions is less than 1 mV. The peak-to-peak noise level from the incoming signal is 5 to 50 mV (with amplifier gains of 200) and corresponds to a change in absorbance of 5 to 50 ppm. The center of the noise (the signal detectability) can be read as closely as 1 ppm under optimum conditions.

---

9. R. J. Blume, Rev. Sci. Instr. 32, 1016 (1961).

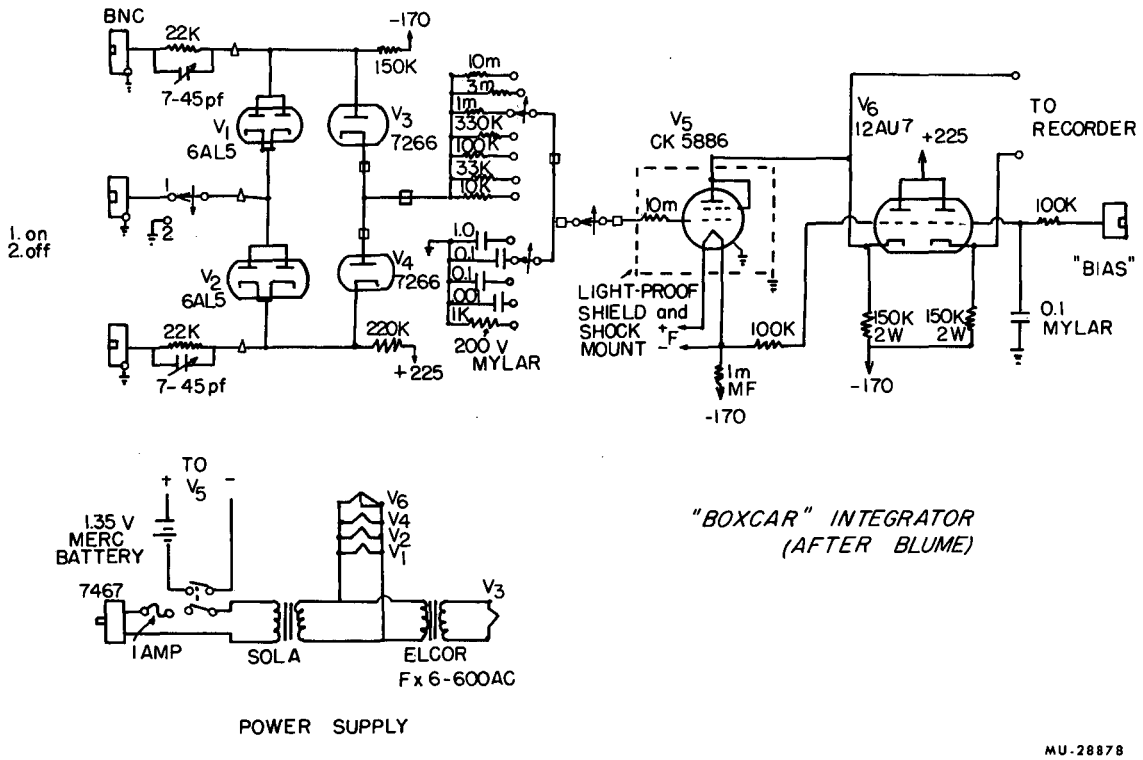

Fig. 6-4. Boxcar-integrator circuitry.

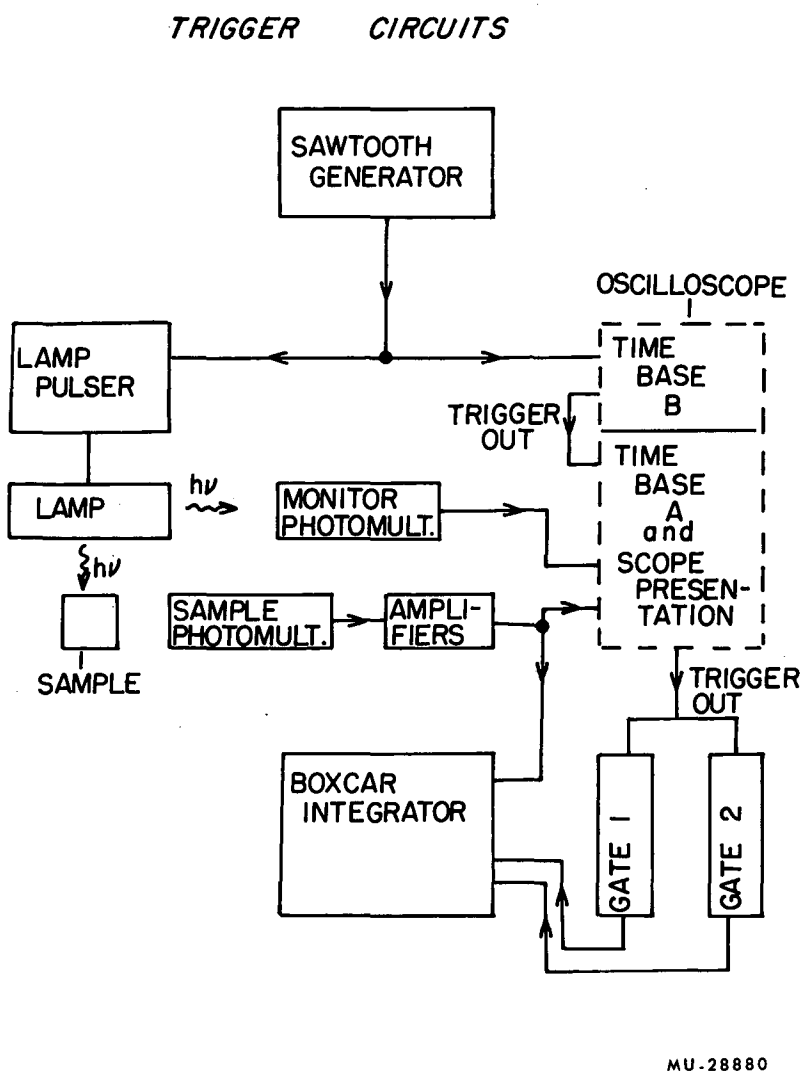

Fig. 6-5. Boxcar trigger circuits.

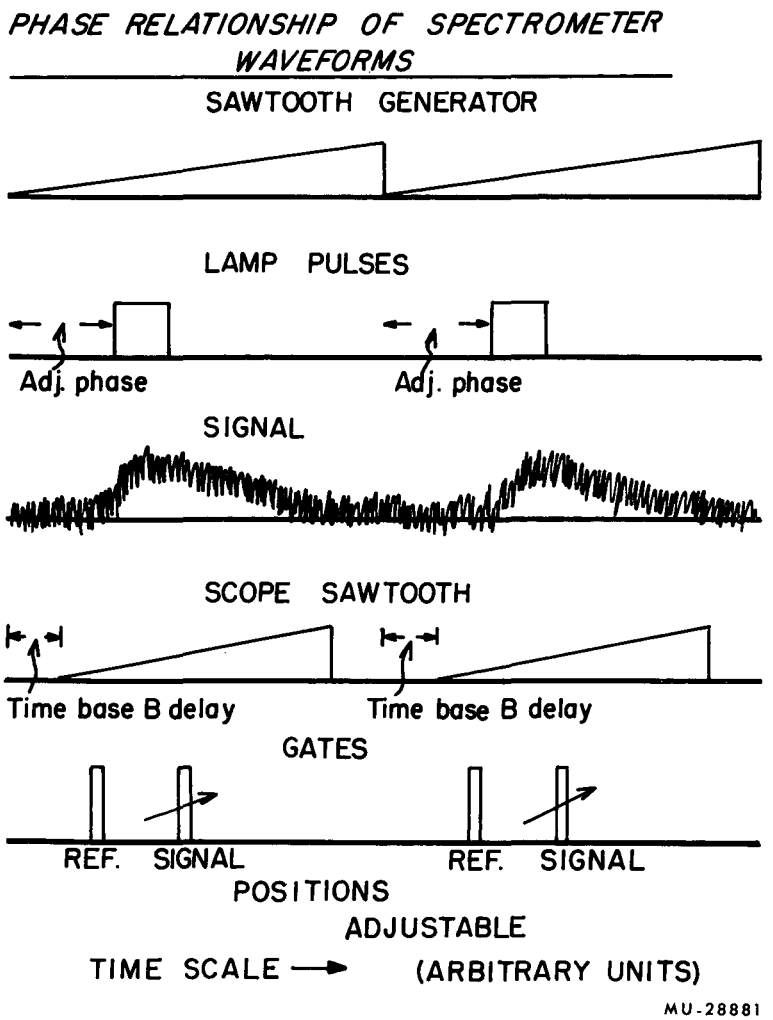

Fig. 6-6. Phase relationship of spectrometer waveforms.

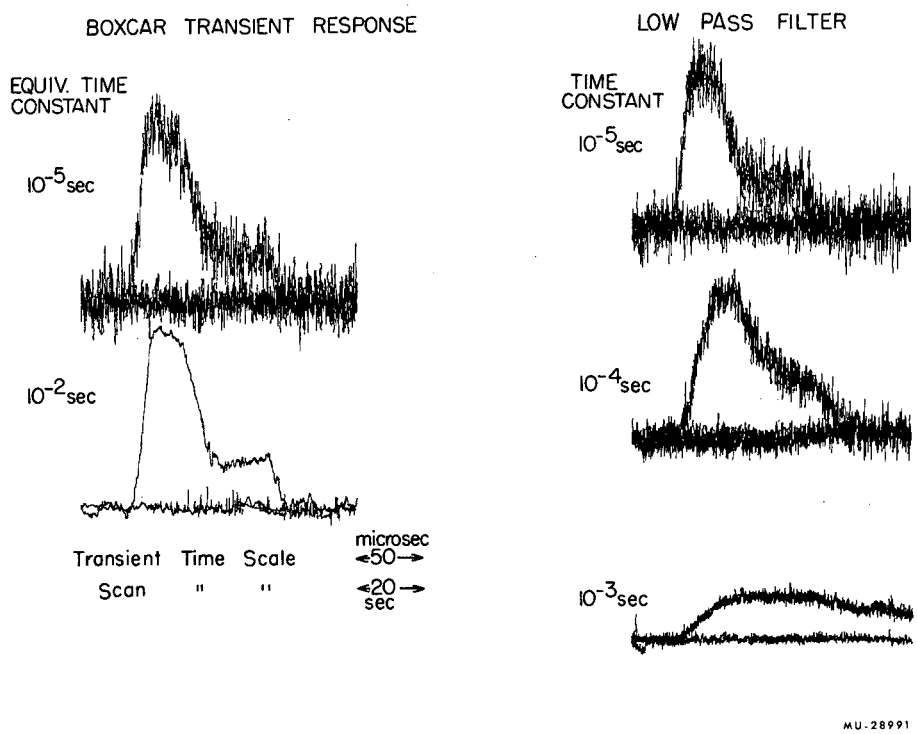

Fig. 6-7. Boxcar transient response compared to low-pass filter circuit.

Transient response has not been fully tested. In Fig. 6-7 we have employed a 10-μsec gate to display a 50-μsec transient. No difficulty is envisaged in using 1-μsec gates.

Readout Devices. The signal from the boxcar is fed into the Y axis of an Electro Instruments Model 500 X-Y recorder. The X axis has been used with a time base for transient presentation or driven from a battery-potentiometer circuit connected to the monochromator wavelength drive for spectral presentation.

Summary

This paper has given a preliminary discussion of a high-sensitivity rapid-response spectrophotometer. Sampling techniques are used to allow the presentation of microsecond transients. These techniques allow the use of long-time constant filters to improve instrument sensitivity without distortion of the transient waveform. An obvious limitation of this approach is the requirement for a repetitive signal.

A more detailed discussion of the noise-reduction properties of this type of circuitry is in preparation.

Acknowledgments

The author gratefully acknowledges the expert electronic assistance rendered by R. Thompson and F. Upham in the construction of the spectrometer.

7. MICROSPECTROPHOTOMETRIC STUDIES OF SOME ORGANIC SOLIDS

David Ilten and Kenneth Sauer

A useful method for studying the optical spectra of single crystals is the microspectrophotometer. Nakamoto[1] used the microscopic method of Tsuchida and Kobayashi[2,3] to obtain the spectra of organic solids and to demonstrate the dichroism of the transitions. He first studied benzene and other pure compounds and then applied the technique to small crystals of charge-transfer solids.[4] Crystals were prepared by mixing solutions of the donor and the acceptor compounds and allowing the resulting mixture to evaporate so that crystallization would take place. More recently, Lower, Hochstrasser, an Reid[5] have used the microscopic method to study the dichroism of the intermolecular charge-transfer spectrum of crystalline anthracene-trinitrobenzene complex. Their samples were prepared by fusing crystals of the complex between quartz discs and then allowing the melt to recrystallize under pressure.

The spectra in Fig. 7-1, 7-2, 7-3, and 7-4 were recorded by using a microspectrophotometer, a prototype instrument designed and constructed by the Applied Physics Corporation, Monrovia, California, as an attachment for their Cary Model 11 spectrophotometer. A block diagram of the instrument is shown in Fig. 7-5. The device can be used either as a microscope or as a recording spectrophotometer.

Light from a microscope lamp is focused by a condensing lens onto the sample on a glass slide, from which it passes through an objective lens. When a mirror is inserted at this point, the beam is deflected to an eyepiece. The numerical aperture of the condensing lens is 0.56 and the total magnification obtained from the lenses and eyepiece is 300 diameters.

Crystals are placed on the slide and a specimen of suitable transparency for spectral work is selected visually. When the microscope lamp is turned off and the deflecting mirror is moved out of position, the instrument can function as a spectrophotometer. For this work the tungsten lamp normally provided with the spectrophotometer was replaced with a General Electric 1958 lamp operated at 28 V and 150 W. The lamp is a small source that is operated at a high temperature. It is enclosed in a quartz sheath and employs a tungsten-iodine cycle to reduce deposits on the sheath. The beam from this source passes through the monochromator and is then split into a reference beam and a sample beam.

---

1. K. Nakamoto, J. Am. Chem. Soc. 74, 390 and 392 (1952).
2. R. Tsuchida and M. Kobayashi, Bull. Chem. Soc. Japan 13, 619 (1938); ibid. 60, 769 (1939).
3. R. Tsuchida, M. Kobayashi, and K. Nakamoto, Nature 167, 726 (1951).
4. K. Nakamoto, J. Am. Chem. Soc. 74, 1739 (1952).
5. S. K. Lower, R. M. Hochstrasser, and C. Reid, Molecular Physics 4, 161 (1961).

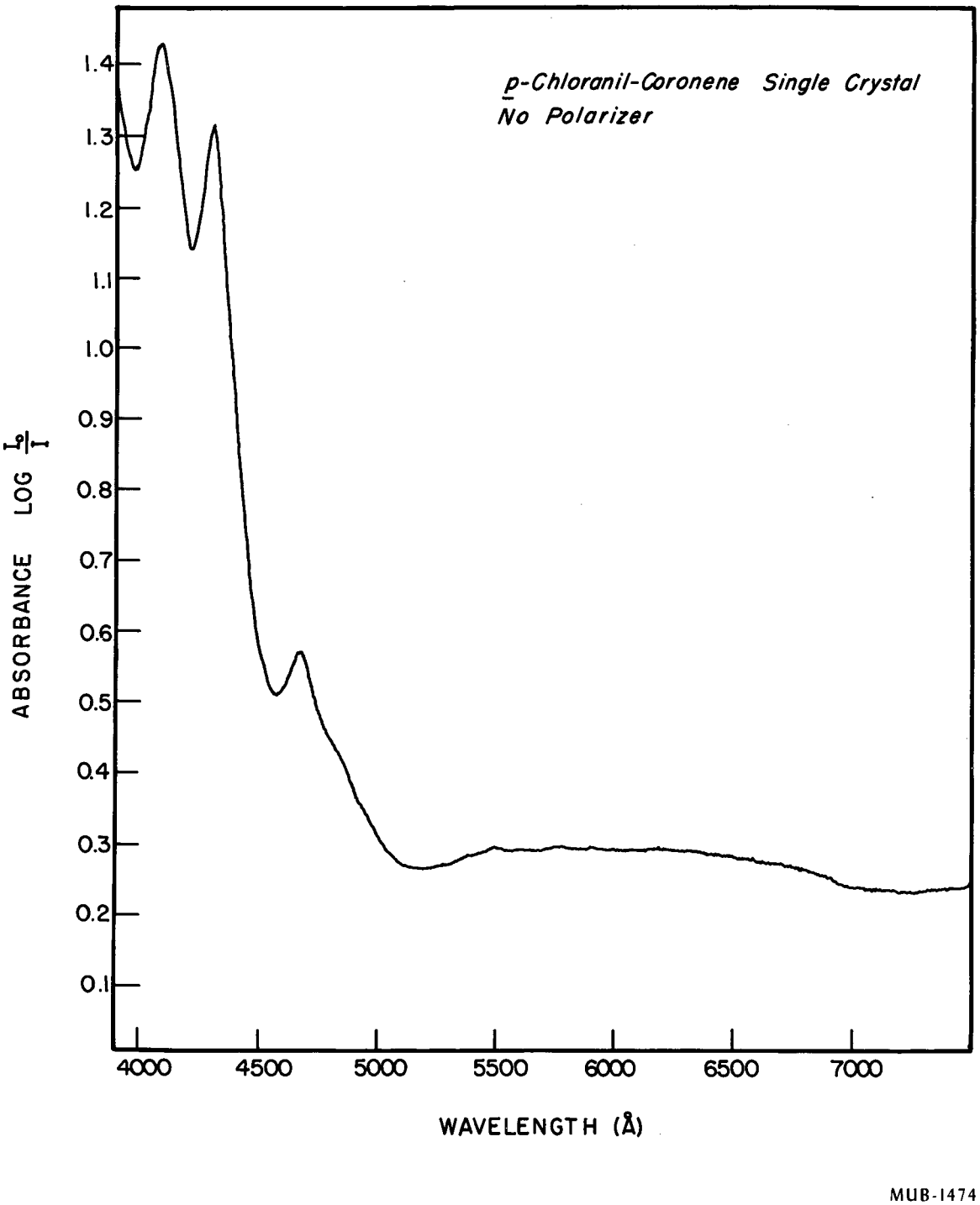

Fig. 7-1. Optical spectrum of p-chloranil-coronene complex taken with Cary Model 11 spectrophotometer with microscope attachment. (Base line subtracted.)

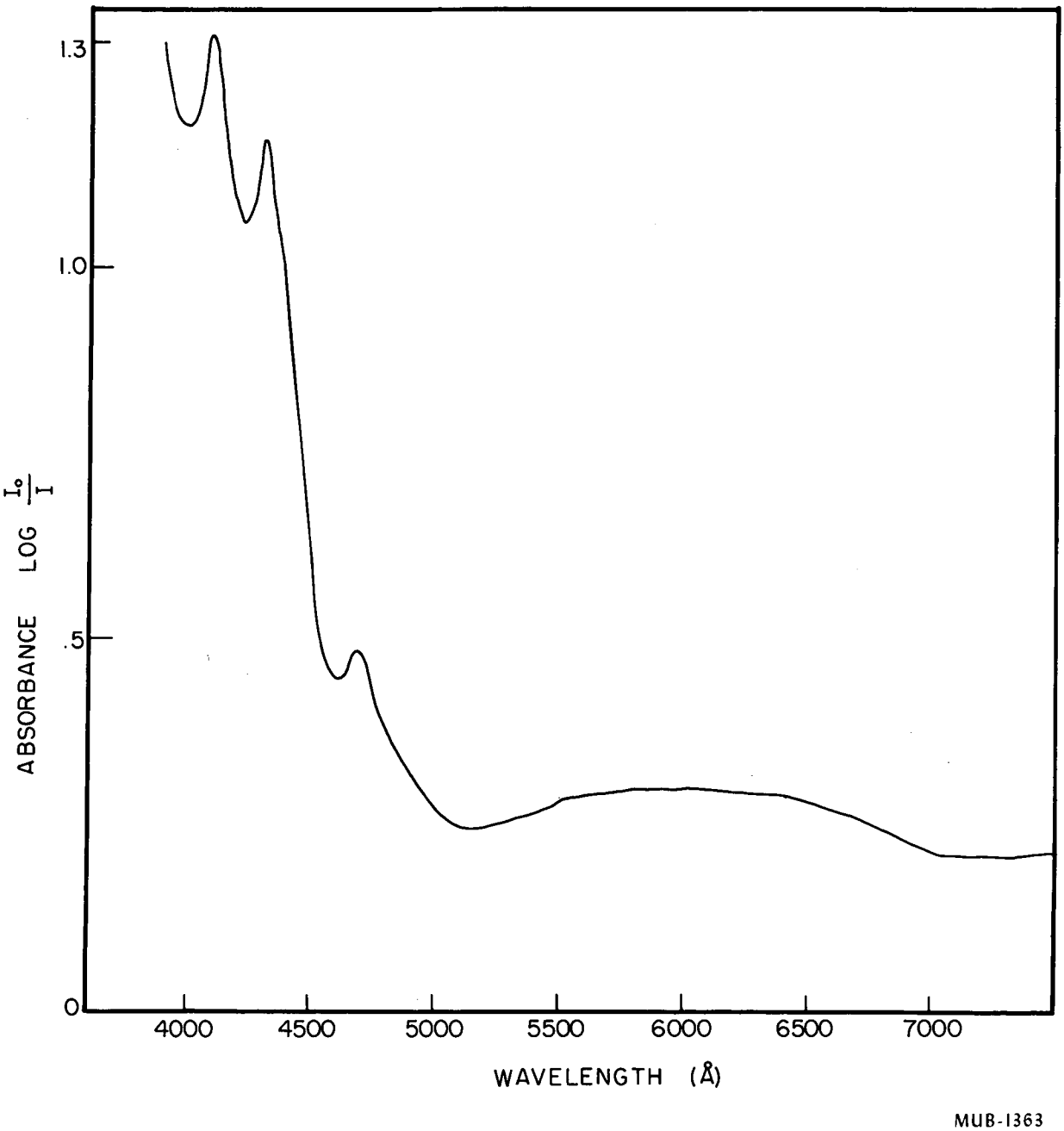

Fig. 7-2. p-Chloranil-coronene complex with polarizer parallel to needle axis of crystal.

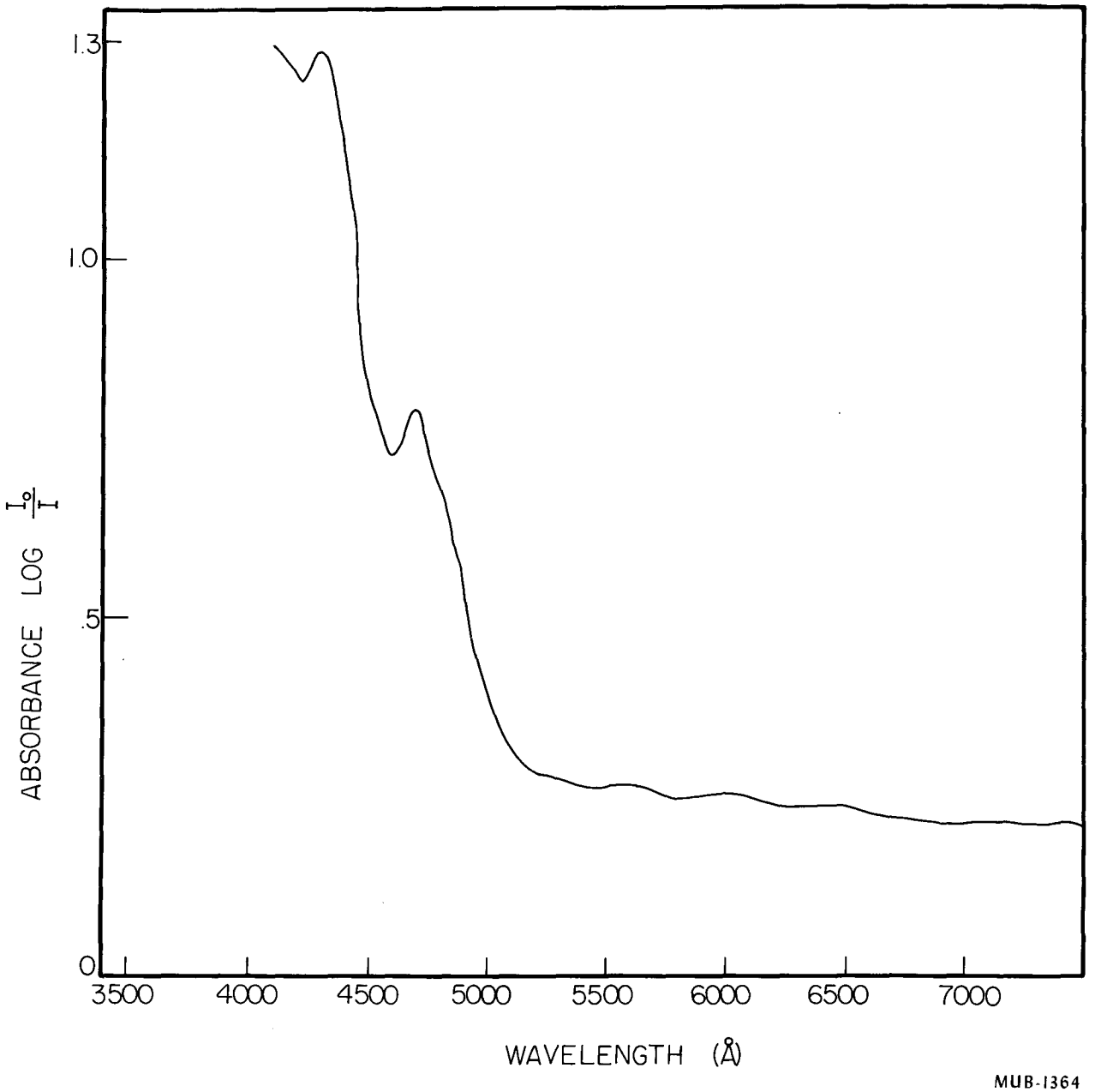

Fig. 7-3. p-Chloronil-coronene complex with polarizer perpendicular to needle axis of crystal.

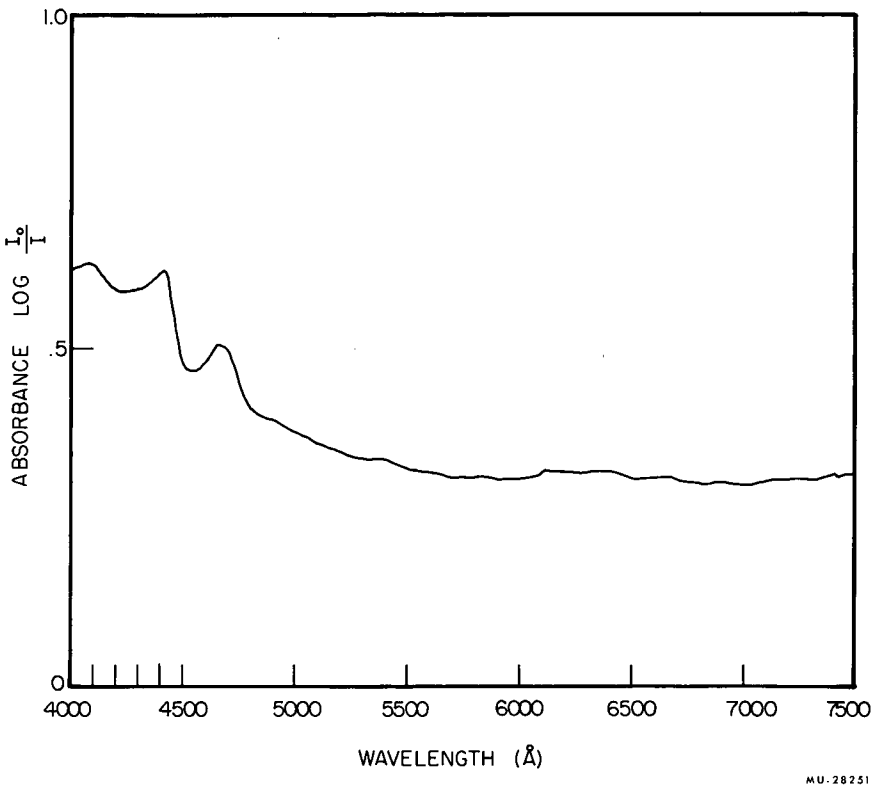

Fig. 7-4. Coronene with polarizer perpendicular to needle axis of crystal.

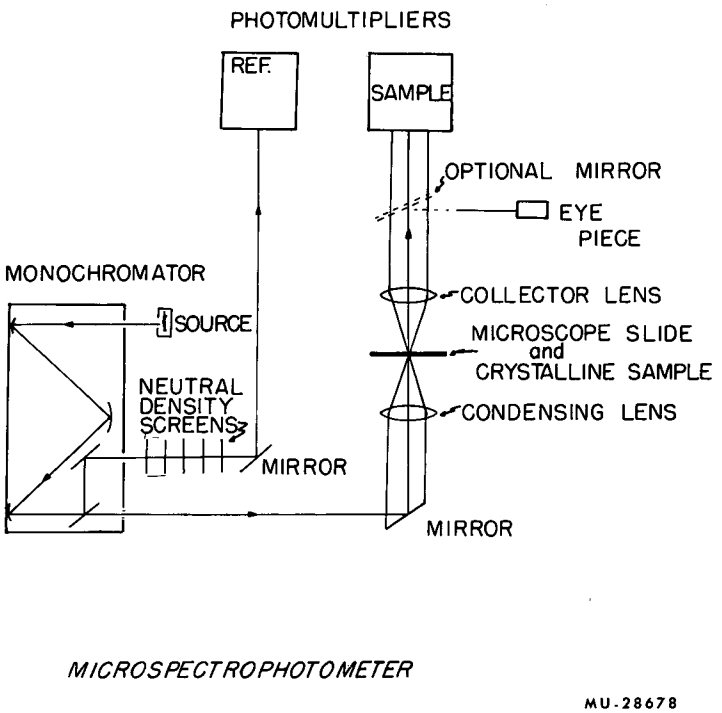

Fig. 7-5. Block diagram of the microscpetrophotometer.

The spectrophotometer is a double-beam type which uses two photomultipliers to determine the ratio of the intensities of the reference and the sample beams. The sample beam passes from the monochromator through one of a set of apertures such that the field illuminated on the microscope slide has a diameter of 12, 20, or 80μ. The sample beam is then reflected from a front face mirror and focused by the condensing lens onto the crystal on the microscope slide. An objective lens collimates the sample beam, the intensity of which is measured by one photomultiplier. Before the reference beam passes to the second photomultiplier for detection, its intensity can be matched approximately to the intensity coming from the aperture by using any combination of five neutral density screens provided with the instrument. The 1P28 photomultipliers originally supplied with the spectrophotometer were replaced with HTV-R136 photomultipliers (Applied Physics Corporation, Monrovia, California), which have a high sensitivity at wavelengths in the red. Because reflecting optics are used throughout, the microscope is completely achromatic. It has been possible to obtain solid-state spectra over the range from 3500 to 7500 Å for a sample somewhat larger than 20 μ in diameter.

p-Chloranil-coronene complex

Figures 7-1, 7-2, and 7-3 are spectra of crystals of p-chloranil-coronene complex. In each case the base line has been subtracted and the spectrum replotted. The samples were prepared by mixing the pure components in the solid state, dissolving the mixture in boiling 1, 2-dichloroethane, and then allowing the complex to recrystallize upon cooling. Crystals which appeared reasonably smooth and transparent when viewed through the microscope eyepiece were selected for spectroscopic work. The dichroism of the charge-transfer transition can be demonstrated by inserting a polarizer (Polaroid Type HN38) in the sample beam and orienting it either parallel or perpendicular to the long needle axis of the crystalline complex. For the cases investigated, the charge-transfer band appears much more intense with the polarizer axis parallel to the needle axis than it does with the polarizer axis perpendicular to the needle axis of the crystal. This can be seen by comparing Figs. 7-2 and 7-3. The charge-transfer band is clearly visible in Fig. 7-2 (polarizer axis parallel to needle axis of crystal) as a broad almost structureless band extending from 5000 to 6500 Å, and having a maximum at about 6100 Å. This band does not appear in Fig. 7-3 (polarizer axis perpendicular to long needle axis of crystal). Figure 7-4 is the spectrum of a single crystal of coronene. Figure 7-6 shows the position of the charge-transfer band for p-chloranil-coronene complex in 1, 2-dichloroethane solution.

The crystal structure of p-chloranil-coronene complex has not been determined. However, fluoranil-perylene[6] and a number of other charge-transfer complexes have been shown to crystallize in alternate layers of donor and acceptor arranged in planes oriented almost perpendicular to the needle axis of the crystal. In these cases the needle axis of the crystal roughly represents the normal to the planes of the aromatic rings of the donor and

6. A. W. Hanson, Division of Pure Physics, National Research Council, Ottawa, Canada, private communication.

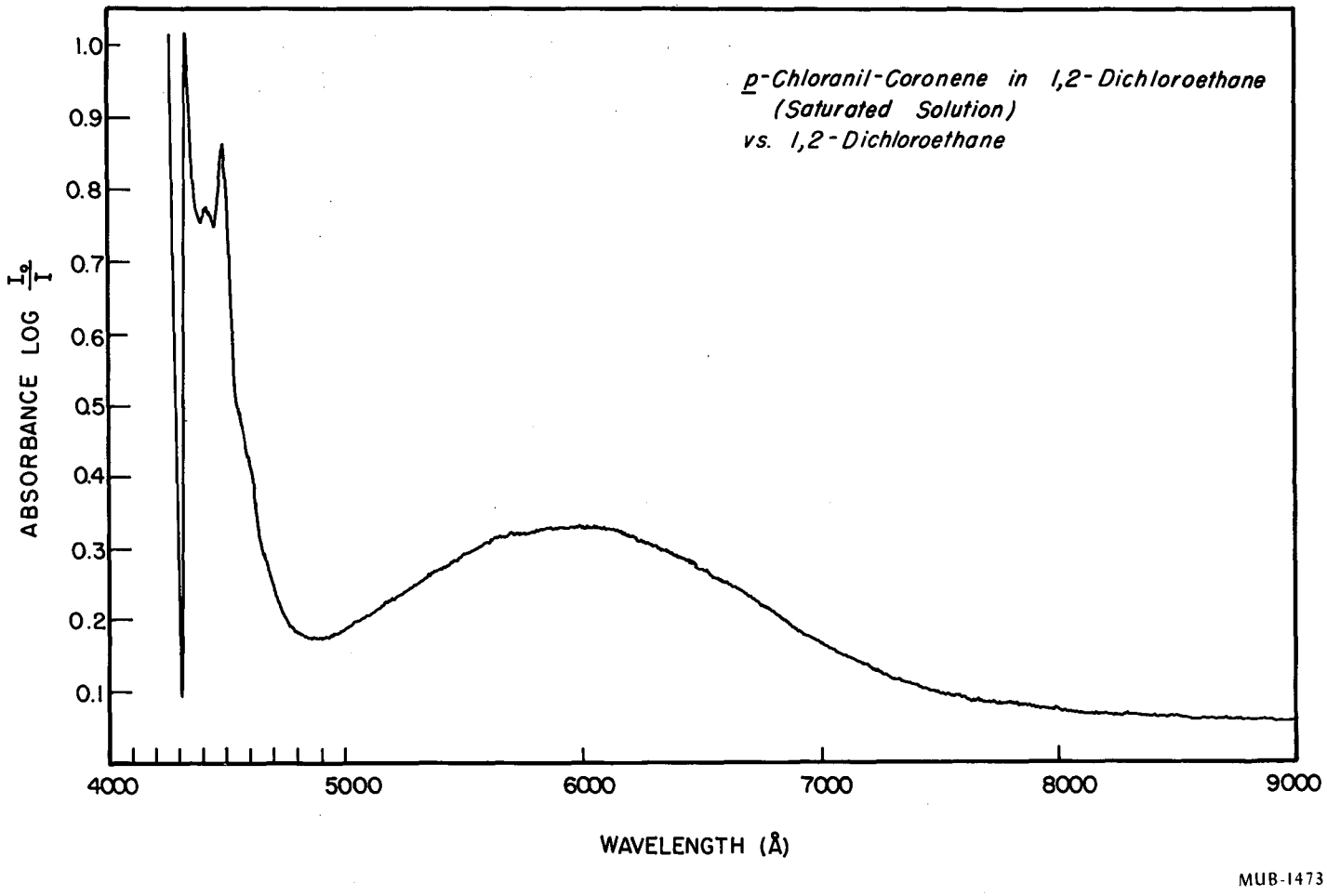

Fig. 7-6. Spectrum of p-chloranil-coronene complex in 1,2-dichloroethane, showing the charge-transfer band.

the acceptor. The work of Nakamoto[4] on chloranil-hexamethylbenzene and of Lower[5] on anthracene-trinitrobenzene demonstrates that the charge-transfer absorption for these complexes is polarized perpendicular to the planes of the benzene rings of the donor and acceptor—i. e., the transition is polarized in the direction of the intermolecular bond. This is what one would expect theoretically. If the structure of p-chloranil-coronene is similar to that of the other complexes which have been determined, then the needle axis of the crystal roughly represents the direction of the intermolecular bond. Since the charge-transfer transition is polarized along the direction of the needle axis, it would then be polarized along the intermolecular bond as well.

o-Chloranil-perylene

Crystals of o-chloranil-perylene complex grown under several sets of conditions were studied. Crystals grown slowly were too thick to give good spectra. Some of those that were crystallized rapidly, however, were thin enough to yield spectra. All of the crystals appeared black by reflected light, but when viewed under the microscope various crystals were violet, blue, green, or orange by transmitted light. For some crystals the color varied from one end of the crystal to the other. This undoubtedly results from differences in thickness. All of the crystals observed were strongly dichroic. With the axis of the polarizer parallel to the long needle axis of the o-chloranil-perylene crystal, the color was orange. When the polarizer was shifted to a perpendicular orientation, the color changed to an intense green. As was the case for the p-chloranil-coronene complex, the charge-transfer band is strongly polarized along the needle axis for the o-chloranil-perylene complex.

The work of Macintyre and Singh[7] demonstrates that the structure of o-chloranil-perylene is almost certainly the same as that for fluoranil-perylene, so that the needle axis does, in fact, represent the direction of the intermolecular bond. Again, this is in agreement with the findings of Nakamoto and Lower. The charge-transfer band extends from 6000 to 7750 Å and has a maximum at approximately 6800 Å.

One advantage of the microspectrophotometer is that it can be used to study a single crystal without requiring a foreign embedding medium. Also, polarized spectra can be obtained readily. The operating noise level of the instrument is inherently high for single-crystal measurements. It is frequently difficult to obtain crystals of suitable thickness and smoothness for measurements.

Acknowledgment

The authors wish to thank the Applied Physics Corporation, Monrovia, California, for the use of their prototype microspectrophotometer attachment.

---

7. W. M. Macintyre, University of Colorado, Boulder, Colorado, private communication.

8. ISOTOPIC STUDIES ON THE RADIATION DECOMPOSITION OF CRYSTALLINE CHOLINE CHLORIDE

Margaret A. Smith and Richard M. Lemmon

A previous report[1] summarized our initial efforts to establish the movements of hydrogen atoms during the radiolysis of crystalline choline chloride. The interest in these investigations stems from the extraordinary radiation sensitivity of this compound.[2] We have now completed our investigations of the hydrogen shifts in various deuterium-labeled cholines, and the results are reported here.

Experimental Procedures

Preparation of Deuterated Choline Chlorides

The $[(CD_3)_3NCH_2CH_2OH]^+Cl^-$ and $[(CH_3)_3NCD_2CH_2OH]^+Cl^-$ used were samples of the compounds whose preparation and properties were previously reported.[2,3] Our preparations of $[(CH_3)_3NCH_2CD_2OH]^+Cl^-$ and $[(CH_3)_3NCH_2CH_2OD]^+Cl^-$ were described in our previous report.[1] The trideuterated choline, $[(CH_3)_3NCH_2CD_2OD]^+Cl^-$, also used in this work, was prepared by dissolving the O-methylene deuterated compound in a 100-fold excess of 99% D_2O. The solution was evaporated to dryness and the deuterated compound recrystallized from N, N-dimethylformamide, a solvent whose carbonyl-bound hydrogen does not exchange with D_2O. The identities of the deuterated compound were established by satisfactory elemental analyses and, except for the hydroxyl-deuterated compounds, by NMR spectra. (No suitable aprotic solvent could be found for the NMR spectroscopy of the hydroxyl-deuterated compounds.)

Irradiations

The deuterium-labeled cholines were irradiated with Co^{60} γ-rays in a 1000-curie source.[4] In all experiments the radiation dose (2 to 6×10^6 rads) was sufficient to cause approximately 10% decomposition. Direct determinations of the amounts of decomposition were not made.

Purification of the Evolved Acetaldehyde and Trimethylamine

The irradiated choline chloride sample tube was cooled in liquid nitrogen and opened. It was then attached to a vacuum line and volatile components vacuum-distilled into a trap suitable for introducing the sample into a

1. Margaret A. Smith and Richard M. Lemmon, in Bio-Organic Chemistry Quarterly Report, UCRL-9900, October 1961, p. 72.
2. R. O. Lindblom, R. M. Lemmon, and M. Calvin, J. Am. Chem. Soc. 83, 2484 (1961).
3. R. O. Lindblom, in Bio-Organic Chemistry Quarterly Report, UCRL-8910 October 1959, pp. 24-32.
4. B. M. Tolbert et al., in Chemistry Division Quarterly Report, UCRL-3710, March 1957, p. 72.

gas chromatograph (Wilkens, Model A-350, 10-ft by 1/4-in. dimethylsulfolane-on-firebrick column). By using helium as the carrier gas, with a flow rate of 90 cc/min, at room temperature, the acetaldehyde is cleanly separated (retention time: 11 min) from all other volatile materials (very small amounts of methyl chloride and ethyl ether).

Trimethylamine was recovered, after the acetaldehyde was removed, by making the solution of the irradiated choline alkaline. The volatile trimethylamine was also swept over into a cold (-196°) trap from which it was introduced into a gas chromatograph. By using the same chromatographic conditions as described above for acetaldehyde (with the exception only of a flow rate of 60 cc/min) the trimethylamine is also cleanly separated (retention time: 3.5 min) from other volatile compounds (traces of dimethylamine and acetaldehyde).

Deuterium Contents of Evolved Acetaldehyde and Trimethylamine

The amounts of deuterium in the chromatographically-purified gases were determined by observations of the enhancement, or lack of it, of such mass peaks at 46 (CH_2DCDO), 45 (CH_2DCHO), and 30 (CDO) for acetaldehyde. Appearance of deuterium in trimethylamine would result in enhancement of mass peak 59 (58 is the major peak for ordinary trimethylamine). An additional check of the deuterium in the methyl group of acetaldehyde was made by photolyzing part of the acetaldehyde, in the presence of iodine vapor, following the procedure of Blacet and Heldman.[5] The resultant methyl iodide contains the methyl group of the acetaldehyde, and the presence of deuterium is reflected in the appearance of peaks at mass 143 and above. The methyl iodide was also purified by gas chromatography (on dimethylsulfolane and Apiezon columns).

Results

Acetaldehyde from $[(CD_3)_3NCH_2CH_2OH]^+Cl^-$

The mass spectral data are presented in Table 8-I.

Table 8-I. Mass spectral data[a] for CH_3CHO (A. P. I. catalog and our data) and for acetaldehyde from $[(CD_3)_3NCH_2CH_2OH]^+Cl^-$.

Mass	CH_3CHO		Deuterated acetaldehyde		
(m/e)	A. P. I.	Ours[b]	Expt. 1	Expt. 2	Expt. 3
29	100.0	100.0	100.0	100.0	100.0
30	1.1	1.1	1.4	1.4	1.4
43	26.7	30.1	28.3	28.0	27.8
44	45.7	54.0	50.2	49.7	49.5
45	1.2	1.3	2.6	2.4	2.5
46	0.1	0.1	v. small	v. small	v. small

[a] Relative peak heights.

[b] Reagent grade, after GLC purification on dimethylsulfolane.

5. F. E. Blacet and J. D. Heldman, J. Am. Chem. Soc. 64, 889 (1942).

The data of Table 8-I clearly indicate that there is little, if any, involvement of the methyl protons in the radiolysis of crystalline choline chloride. The mass spectrum of the acetaldehyde is almost identical to that of the acetaldehyde from ordinary choline. There is a slight enhancement of the mass 45 peak, but this increase is so small as to be of dubious significance.

Acetaldehyde from $[(CH_3)_3NCD_2CH_2OH]^+Cl^-$

The mass spectral data are presented in Table 8-II.

Table 8-II. Mass spectral data[a] for CH_3CHO (A. P. I. catalog) and for acetaldehyde from $[(CH_3)_3NCD_2CH_2OH]^+Cl^-$.

Mass (m/e)	CH_3CHO	Deuterated acetaldehyde Expt. 1	Expt. 2	Expt. 3
29	100.0	100.0	100.0	100.0
30	1.1	4.8	4.8	5.7
43	26.7	11.6	11.9	9.4
44	45.7	28.4	28.5	22.9
45	1.2	30.2	29.9	32.4
46	0.1	14.8	14.4	23.9
47	--	2.8	2.5	2.2

[a] Relative peak heights.

The data of Table 8-II show: (1) There is a small fraction at mass 30; thus some CDO is formed. (2) The major peak is at mass 45, not 46. Therefore, there is more CH_2DCHO than CHD_2CHO formed (by a factor of nearly 2). (3) The appearance of a small peak at mass 47 indicates the formation of acetaldehyde with three deuterium atoms. This is evidence of intermolecular hydrogen transfers during the radiolysis.

Acetaldehyde from $[(CH_3)_3NCH_2CD_2OH]^+Cl^-$

Consistent mass spectral data on the acetaldehyde from the O-methylene deuterated choline chloride proved difficult to obtain. The acetaldehyde mass spectrum was taken after 13 different radiolysis experiments, including those from three different preparations of the deuterated compound. Mass 30 was always the largest peak; however, the mass 45/mass 46 ratio varied all the way from 2.75 to 0.40; the average was 0.99. That this was not due to varying amount of water present in the crystals was shown by our obtaining similar mass spectra regardless of whether the crystals were handled with rigorous exclusion of water or in the presence of atmospheric moisture.

The major products, occurring in about equal amounts, appear to be CH_3CDO and CH_2DCDO. The mass 47 peak is no greater than is the mass 45 peak for ordinary acetaldehyde; therefore, there is no evidence of CD_3CHO or CD_2HCDO.

Typical mass spectral data follow:

Table 8-III. Mass spectral data[a] for CH_3CHO (A. P. I. catalog) and for acetaldehyde from $[(CH_3)_3NCH_2CD_2OH]^+Cl^-$.

Mass (m/e)	CH_3CHO	Deuterated acetaldehyde[b] Expt. 1	Expt. 2	Expt. 3
29	100.0	11.6	9.6	9.3
30	1.1	100.0	100.0	100.0
43	26.7	14.7	8.5	9.6
44	45.7	10.9	15.4	13.6
45	1.2	33.8	16.4	19.9
46	0.1	16.8	33.9	30.8
47	--	--	1.5	1.4

[a] Relative peak heights.

[b] Representative data from a total of 13 experiments.

Acetaldehyde from $[(CH_3)_3NCH_2CH_2OD]^+Cl^-$

The mass spectral data are presented in Table 8-IV.

Table 8-IV. Mass spectral data[a] for CH_3CHO (A. P. I. catalog) and for acetaldehyde from $[(CH_3)_3NCH_2CH_2OD]^+Cl^-$.

Mass (m/e)	CH_3CHO	Deuterated acetaldehyde Expt. 1	Expt. 2	Expt. 3
29	100.0	100.0	100.0	100.0
30	1.1	2.5	3.5	3.4
43	26.7	22.3	25.0	18.7
44	45.7	43.0	49.4	40.4
45	1.2	20.7	23.8	26.6
46	0.1	3.3	5.8	7.1

[a] Relative peak heights.

There are three conclusions to be drawn from the data of Table 8-IV: (1) There is a small, but definite, fraction of deuterium appearing in the aldehyde group (mass 30)—that is, a small amount of CDO is formed; (2) a considerably greater fraction appears in the methyl group (mass 45 = CH_2DCHO); and (3) the increase of mass 46 (= CHD_2CHO) shows that intermolecular hydrogen transfer occurs during the radiolysis.

Acetaldehyde from $[(CH_3)_3NCH_2CD_2OD]^+Cl^-$

The mass spectral data for the acetaldehyde from this triply-deuterated choline is presented below.

Table 8-V. Mass spectral data[a] for CH_3CHO (A. P. I. catalog) and for acetaldehyde from $[(CH_3)_3NCH_2CD_2OD]^+Cl^-$.

Mass (m/e)	CH_3CHO	Deuterated acetaldehyde
29	100.0	7.1
30	1.1	100.0
43	26.7	6.2
44	45.7	10.5
45	1.2	17.1
46	0.1	24.5
47	--	15.5
48	--	4.9

[a] Relative peak heights.

The peak at mass 48 shows that some perdeutero-acetaldehyde is formed. This is further evidence (added to that presented in Tables 8-II and 8-IV) that intermolecular hydrogen transfers take place during the radiation decomposition process.

Trimethylamine from Deuterated Cholines

The data of Table 8-VI establish the failure of hydrogens to transfer from the ethanol moiety to the triemthylamine during the raiolysis.

Table 8-VI. Mass spectral data[a] for $(CH_3)_3N$ (A. P. I. catalog and our data) and for trimethylamine from deuterated choline chloride.

Mass (m/e)	$(CH_3)_3N$ A. P. I.	$(CH_3)_3N$ Ours[b]	Trimethylamine from deuterated choline chlorides[c] $\geqq NCD_2CH_2OH$	$\geqq NCH_2CD_2OH$	$\geqq NCH_2CH_2OD$
14	6.3	5.4	6.8	4.9	5.4
15	33.7	45.5	43.0	37.1	35.0
16	0.5	0.6	1.1	0.6	0.7
57	7.4	8.5	7.5	7.5	6.5
58	100.0	100.0	100.0	100.0	100.0
59	38.7	44.3	43.7	46.9	45.0
60	1.3	1.5	1.6	1.8	1.3

[a] Relative peak heights.
[b] Trimethylamine, from the radiolysis of ordinary choline chloride, after GLC purification on dimethylsulfolane.
[c] Representative data only—either two or three experiments were done on each deuterated choline. For each compound, the separate determinations of trimethylamine mass spectra were in good agreement.

Deuterium Contents of CH_3I from CH_3CHO

The deuterium contents in the methyl group of acetaldehyde products were checked by measurements of the mass spectra of the CH_3I obtained from aliquots of the different acetaldehydes. This was done in seven different experiments. In all cases when there was little or no deuterium in the aldehyde group, the deuterium found in the CH_3I (ratios of masses 142:143:144:145) followed closely that found in CH_3CHO (ratios of masses 44:45:46:47). When the aldehyde group was essentially all CDO (as in the acetaldehyde from O-methylene deuterated choline), the ratio of masses 142:143:144 in the CH_3I closely matched the ratio of masses 45:46:47 in the acetaldehyde. The finding of significant mass 145 (= CD_3I) from the acetaldehyde from N-methylene deuterated choline is further substantiation of our conclusion that intermolecular hydrogen transfer is occurring.

Summary and Conclusions

The results presented here have increased our understanding of the mechanism of the unique radiation decomposition of crystalline choline chloride. Unfortunately, however, we still have no understanding of why choline chloride is so sensitive to ionizing radiation. What we now further know about the mechanism, as a result of the present work, is the following:

1. None of the hydrogen atoms of the three methyl groups of choline chloride appear in the radiolytically produced acetaldehyde.

2. The five hydrogen atoms of the ethanol moiety show considerable mobility during the radiolysis. It is difficult to give quantitative values for these hydrogen transfers, but the following intramolecular processes do occur:

   a. Unexpectedly, protons are often lost from the N-methylene group during its transition to the methyl group of the acetaldehyde. Sometimes N-CH_2 hydrogens appear in the CHO group of the acetaldehyde. More often, a detached N-CH_2 hydrogen is simply eliminated (to appear as HCl).

   b. O-methylene hydrogens appear to have about equal probabilities of elimination and of appearance in the acetaldehyde methyl group.

   c. Hydroxyl hydrogens usually are eliminated, but their elimination probability is only about twice that of their appearance in the acetaldehyde methyl group. This latter appearance is, in turn, about ten times as probable as appearance in the acetaldehyde CHO group.

3. Although they are only minor processes, intermolecular hydrogen transfers do take place. Transfers to another molecule occur in the cases of the N-methylene and hydroxyl hydrogens, but do not involve O-methylene hydrogens.

9. SYNTHESIS OF ORGANIC COMPOUNDS BY ELECTRIC DISCHARGES

John Oró

Introduction

The use of electric discharges for the synthesis of organic compounds under possible primitive earth conditions was initiated by Miller.[1-4] Miller obtained some amino acids, hydroxy acids, and a few other organic compounds by the prolonged action of spark discharges on mixtures consisting essentially of methane, ammonia, and water. These results have been confirmed by other investigators under identical or slightly different conditions.[5-10]

Further studies on this synthesis were carried out in this laboratory with the hope of obtaining additional amino acids and perhaps also some uv-absorbing compounds.

In order to increase the probability of formation of new compounds, ethane was also included in the reaction mixtures (the use of methane in these experiments is justifiable since the C_2 species has been detected spectroscopically in star atmospheres, comets, and interstellar space.[11,12] In order to determine the overall pattern of the compounds formed, ^{14}C hydrocarbons, mainly ^{14}C methane, were used as tracers. Furthermore, it was thought that the patterns obtained by autoradiography of two-dimensional chromatograms of the products may help in establishing a correlation between these and other experiments.[13,14,15]

---

1. S. L. Miller, Science 117, 2351 (1953).
2. S. L. Miller, J. Am. Chem. Soc. 77, 2351 (1955).
3. S. L. Miller, Biochim. Biophys. Acta 23, 480 (1957).
4. S. L. Miller, Ann. N. Y. Acad. Sci. 68, 260 (1957).
5. L. Hough and A. F. Rogers, J. Physiol. (London) 132, 289 (1956).
6. P. H. Abelson, Science 124, 935 (1956).
7. P. H. Abelson, Ann. N. Y. Acad. Sci. 69, 274 (1957).
8. K. Heyns, W. Walter, and A. E. Meyer, Naturwissenschaften 44, 385 (1957).
9. T. B. Pavlovskaya and A. G. Pasynskii, in The Origin of Life on the Earth, I. U. B. Symposium Series, A. I. Oparin et al. eds. (Pergamon Press, New York, 1959), Vol. 1, p. 151.
10. B. Franck, Ber. 93, 446 (1960).
11. J. Oró, Nature 190, 389 (1961).
12. J. Oró, Ann. N. Y. Acad. Sci. (in press).
13. C. Palm and M. Calvin, J. Am. Chem. Soc. 84, 2115 (1962).
14. C. Palm and M. Calvin, in Bio-Organic Chemistry Quarterly Report UCRL-9900, October 1961, p. 51.
15. J. Oró, in following section of this report.

The results obtained show that an appreciable number of organic compounds are formed by the action of electric discharges on the above mixtures. The products obtained, in addition to some of those identified by Miller, include isoleucine, asparagine, possible glycinamide, a yellowish oil, a highly insoluble polymer, and several uv-absorbing compounds. The formation of products that give brown and green-colored derivatives with ninhydrin has also been observed. These compounds are presumably amines, amino amides, and amino nitriles. The ^{14}C patterns produced by autoradiography of two-dimensional chromatograms of the products are reasonably simple. They are not much more complex than the patterns produced by spraying the same chromatograms with ninhydrin.

Experimental Procedure and Results

Conditions of the Reaction

Figure 9-1 shows the design of the apparatus used, which consists of a three-liter flask provided with removable tungsten electrodes, and with inlets and outlets for reactants and products. Temperature and pressure of the system were measured by means of a thermometer and a vacuum gauge, respectively. The liquid phase was agitated by means of a magnetic stirrer. The spark gap of the electrodes was usually 1.5 cm, but in later experiments it was increased to 3 cm.

The current was supplied by a transformer (Rhordarson Electric Manufacturing Co: V.P. 110, Sec. 25 000, V×A 1000, cycle 50-60) from an x-ray apparatus connected to a 100-V line through a "variac" that was used to regulate the voltage. The discharge voltage was approximately 10 000 volts when the spark gap was 1.5 cm, and 15 000 volts when the electrodes were separated 3 cm.

After complete evacuation of the apparatus, 300 mliter of boiled distilled water was admitted to it. Then, methane, ethane, and concentrated ammonium hydroxide (15M) were allowed into the system. Pressure readings were obtained after the introduction of each component. Whenever ^{14}C hydrocarbons (1 mC or less) were used, they were admitted into the evacuated apparatus before anything else (water, nonradioactive hydrocarbons, and ammonium hydroxide). All the reactants used were C.P. reagents. Care was exercised to prevent any infiltration of air into the system. Aside from this, no special treatment was followed to eliminate traces of air possibly present in the reagents. Table 9-I gives the data for each experiment.

Course of the Reaction

The reaction time was only 7 h or less, instead of the usual one week. This was done, in part, in order to detect some of the presumed amino acid intermediates such as amino nitriles and amino amides, and, in part, in order to have reaction times comparable to those of other experiments carried out in this laboratory with high-energy electrons.[13,14,15]

The course of the reaction in the gas phase was followed by measuring the increase with time of the pressure of the system (Fig. 9-2). It can be seen that under the conditions used, the increase in pressure levels off after about 4 to 7 h, depending on the concentration of reactants.

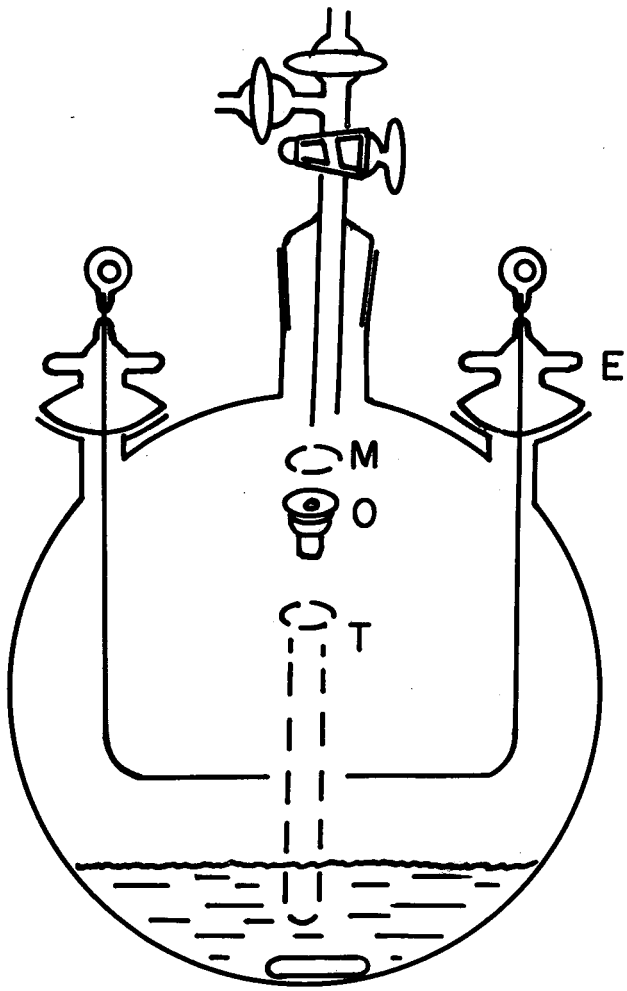

MU-27954

Fig. 9-1. Diagram of apparatus for the synthesis of organic compounds in an electric discharge: E, removable electrodes; M, manometer connection; O, gas-sampling orifice; T, thermometer well. Dotted lines are used to represent parts on the back of the reaction vessel.

Table 9-I. Composition of gas mixtures and other data of the experiments with electric discharges.

	Experiment No.						
	S-1	S-2	S-3	S-4	S-5	S-6	S-7
CH_4 pressure (cm Hg)	12.7	7.6	10.1	10.1	7.6	10.6	22.8
CH_4 activity (μC)	-	-	-	-	960	660	-
C_2H_6 pressure (cm Hg)	12.7	7.6	10.1	10.6	7.6	(31.2)[a]	-
H_2O (ml liquid)	310	300	346	346	300	346	392
NH_4OH (moles per liter)	0.16	1.1	2.0	2.0	2.2	2.0	3.3
Average temperature (°C)	30	30	30	28	28	28	28
Duration of discharge (h)	1	6	5	5	7	5	5
Spark gap (cm)	1.5	1.5	1.5	1.5	1.5-3	3	3
Weight of residue (mg)	7	40	77	73	50	78	130
Activity of residue (μC)	--	--	--	--	36	22	--
Activity of distillate (μC)	--	--	--	--	260	100	--
Conversion of ^{14}C methane to nonvolatile products (%)	--	--	--	--	3.7	3.0	--
Conversion of ^{14}C methane to volatile water-soluble products (%)	--	--	--	--	28	15	--

[a] Residual gaseous products from S-5, containing probably a large amount of hydrogen.

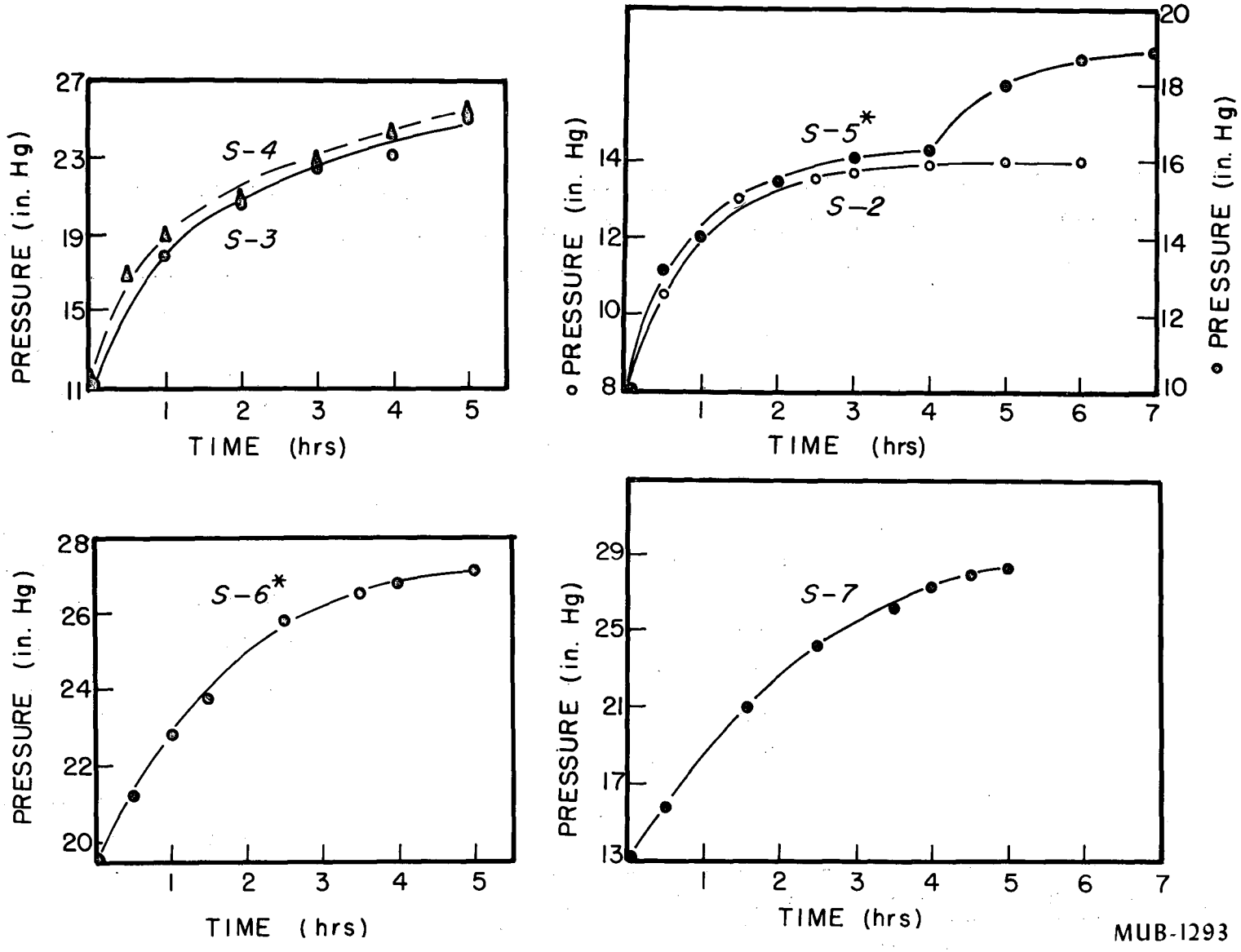

Fig. 9-2. Course of the reaction in the gas phase of the experiments with electrical discharges. The increase in pressure is supposed to be due mainly to the hydrogen formed by dehydrogenation reactions. The experiments marked with an asterisk were carried out with ^{14}C reactants. At the fourth hour of experiment S-5, the spark gap was increased from 1.5 to 3 cm.

The temperature oscillation between the start and end of the experiment was only 2 or 3 degrees, usually from 27 to 30°C, and the pressure values were not corrected for the resulting small variations in pressure.

By comparison of different experiments it can be seen that the curves are quite reproducible, and their shape is mainly determined, as might have been expected, by the initial reactant concentration in the gas phase and by the energy put into the system (spark gap). Analyses of the gas phase were not made and therefore the nature of the gases responsible for the increased pressure was not determined. However, on the basis of previous results and knowing that dehydrogenation takes place with electric discharges, hydrogen probably was one of the main gases formed. Thus, the leveling off would simply indicate that equilibrium of the dehydrogenation reaction in the gas phase at a given discharge voltage had been reached. By increasing this voltage the equilibrium would be displaced to higher hydrogen pressures. Such a change of equilibrium can be seen in curve S-5* of Fig. 9-2. (In the fourth hour of experiment S-5 the spark gap was increased from 1.5 to 3 cm.)

The curves of Fig. 9-2 should not only give an indication of the formation of hydrogen but also of the resulting dehydrogenation products; i.e., alkenes, alkynes, aldehydes, hydrogen cyanide, nitriles, hydrazine, etc., which are supposed to be precursors of organic and biochemical compounds. These curves, however, do not give any information on the processes that go on in the liquid phase. It is obvious that condensations, and mainly hydrolytic and ammonolytic reactions, will continue in the liquid phase even after the gas phase appears to have reached equilibrium. The electric discharge was stopped at the time indicated for each experiment.

Analysis of Products

The gas phase was not analyzed. The total volume of the liquid phase (about 350 mliter) was filtered and then concentrated in a vacuum rotating evaporator at 40 to 45°C. When the volume had been reduced to less than 20 mliter it was transferred to a weighed 50-mliter flask and the evaporation was continued until dryness. The distillate was collected in a very large trap immersed in liquid nitrogen. The distillates were set aside. The flasks with the dry residues were first weighed (Table 9-I) and the residues were then dissolved in 5 mliter of 0.1N hydrochloric acid. The solutions thus obtained were used in the subsequent analyses, which were carried out by two-dimensional paper chromatography, ion-exchange chromotography, autoradiography, and spectrophotometry.

Ultraviolet-Absorbing Compounds

The solutions from the first three experiments, after appropriate dilution with 0.1N hydrochloric acid, were directly examined for uv-absorbing compounds. They gave somewhat similar spectra. An aliquot of S-1 diluted 25 times showed a sharp absorption band at about 236 mμ (O.D.=0.85). An aliquot of S-2 diluted 100 times, and also an aliquot of S-3 diluted 200 times, showed a shoulder at about 236 mμ (O.D. = 0.6) and a broad absorption band between 250 and 300 mμ.

Aliquots of the same solutions were then analyzed by two-dimensional chromatography by the ascending technique, using Whatman No. 1 paper and n-propanol-1N ammonium hydroxide, 3:1, (PA) and n-butanol-acetic acid-water, 4:1:1, (BAW) as solvents. The dry chromatograms were scanned with a short-wavelength (2537 Å) uv-light lamp. Two major uv-absorbing compounds were detected in the three chromatograms. One of these two compounds (A) had Rf 0.80 in PA and 0.40 in BAW. The other (B) had Rf 0.42 in PA and 0.17 in BAW. By the intensity of the spots the formation of these compounds followed this order: S-3 > S-2 > S-1.

The areas corresponding to A and B from experiment S-3 were cut from the paper and the compounds were eluted with hydrochloric acid. Their uv spectra are shown in Fig. 9-3. As can be seen, compound A shows a maximum at 257 mμ and a minimum at 232 mμ. For comparison, isocytosine shows a maximum at 257 mμ and minimum at 234 mμ in 0.1N hydrochloric acid. This maximum shifts to 267 mμ in 0.12N sodium hydroxide. For comparison, under the same conditions, adenine shifts from 262 to 269 mμ and purine from 261 to 273 mμ.

Although a certain similarity of compounds A and B with purines and pyrimidines is apparent, no definite statements in this respect can be made until these compounds are isolated and characterized more fully. The formation of uv-absorbing compounds in experiments with electrical discharges has also been observed recently by Knight.[16]

Amino Acids and Other Ninhydrin-Positive Compounds

The reaction product was next analyzed for amino acids by paper chromatography and by ion-exchange chromatography. Figure 9-4 shows the reproduction of two-dimensional chromatograms (Whatman No. 3 MM, ascending) of experiments S-1, S-2, and S-3, sprayed with ninhydrin. There are three chromatograms for each reaction product. The first corresponds to the reaction product before ion-exchange treatment, the second to the water eluate (W) from Dowex 2, and the third to the acid eluate (A) from the same resin. Several ninhydrin-positive compounds—which are likely amino acids, peptides, or other derivatives of amino acids—can be observed in the chromatograms of the acid eluates. At least 8 spots were obtained in S-1-A, 16 in S-2-A, and 20 in S-3-A. The ninhydrin-positive compounds of the water eluates are presumed to be amines, amino amides, and amino nitriles. Some of the compounds in the acid or water eluates gave a green (G) or a yellow (Y) coloration with ninhydrin. Other compounds gave first a tan or yellow-brown coloration which eventually changed into purple. Some of the amides of amino acids are known to give the above colors with ninhydrin.[17]

The amino acids present in the acid eluate from experiment S-3 were identified by ion-exchange chromatography with a Beckman-Spinco automatic analyzer.[18] The results are given in Fig. 9-5. The amino acids—which were

16. C. A. Knight, Virus Laboratory, University of California, Berkeley, private communication.

17. R. W. Chambers and F. H. Carpenter, J. Am. Chem. Soc. 77, 1522 (1955).

18. These analyses were carried out by B. L. Martin in Dr. F. H. Carpenter's laboratory (Virus Laboratory, University of California, Berkeley).

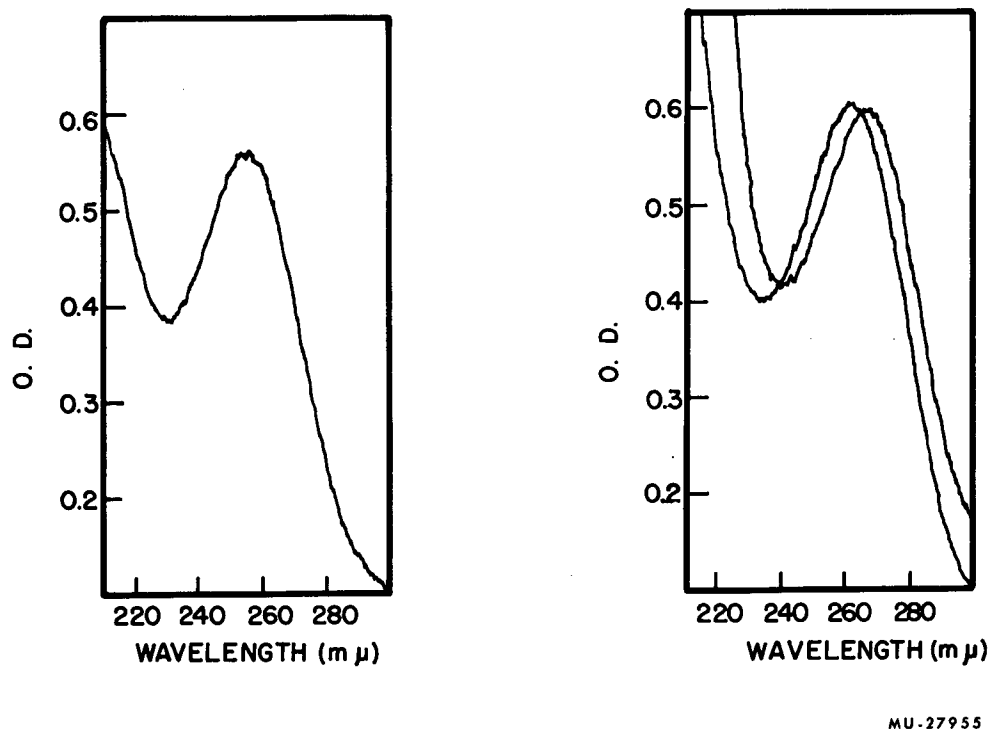

Fig. 9-3. Ultraviolet spectra of two compounds eluted from two-dimensional paper chromatograms of experiment S-3. The spectrum of A (left) was obtained in 1N HCl; the spectra of B (right) in 0.1N HCl and in 0.12N NaOH.

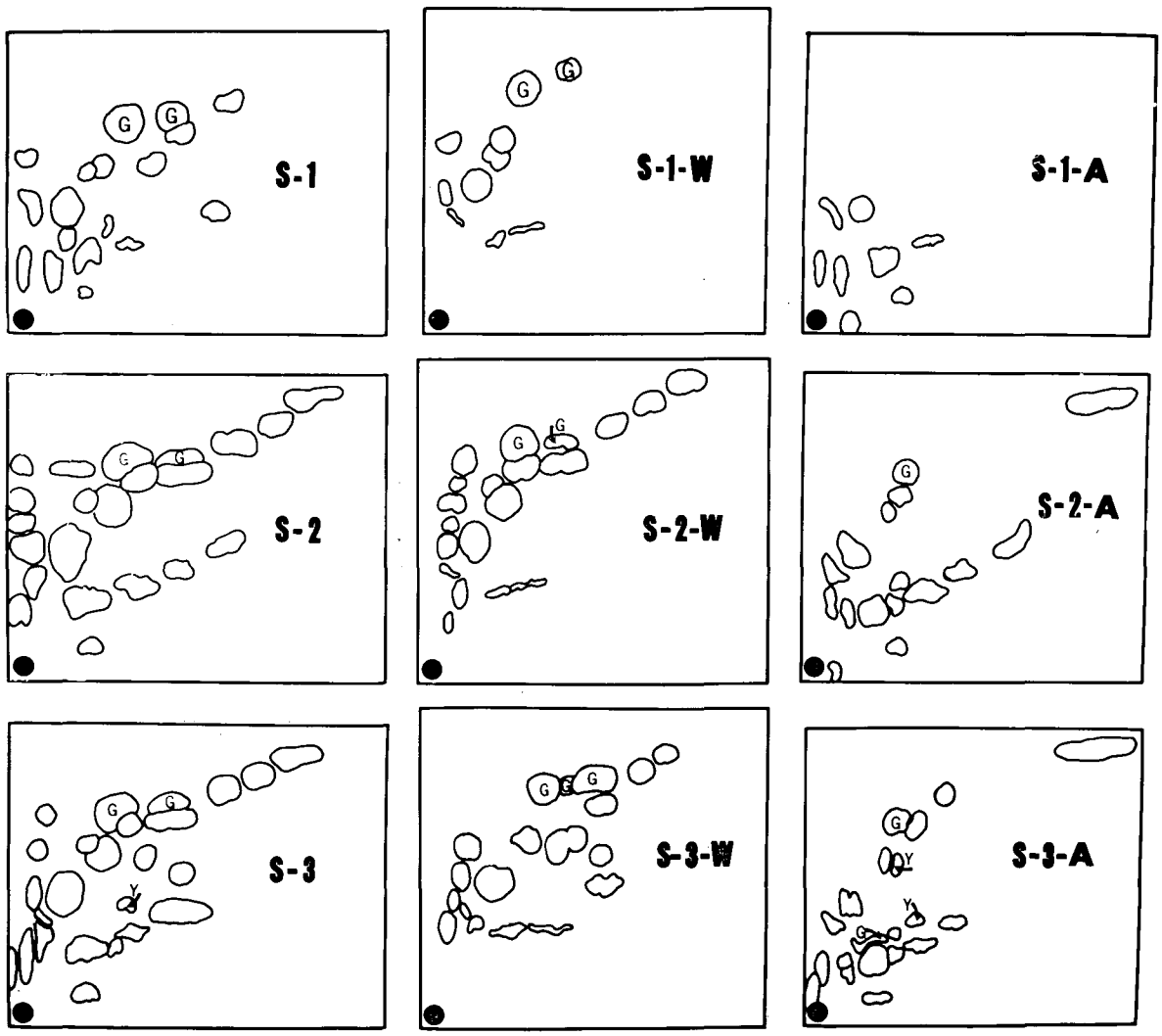

MUB-1592

Fig. 9-4. Two-dimensional chromatograms (ascending) of experiments S-1, S-2, and S-3, sprayed with ninhydrin. The dark spot represents the origin. The development was first in n-propanol-1N ammonium hydroxide, 3:1 (ordinate) and then in n-butanol-acetic acid-water, 4:1:1 (abscissa). The unlettered spots were purple or brown-purple in color. The spots labeled G are green, labeled Y are yellow. The W series are water eluates from Dowex-2; the A series are acid eluates from the same resin. To make chromatograms less complex, the uv-absorbing spots are not shown here.

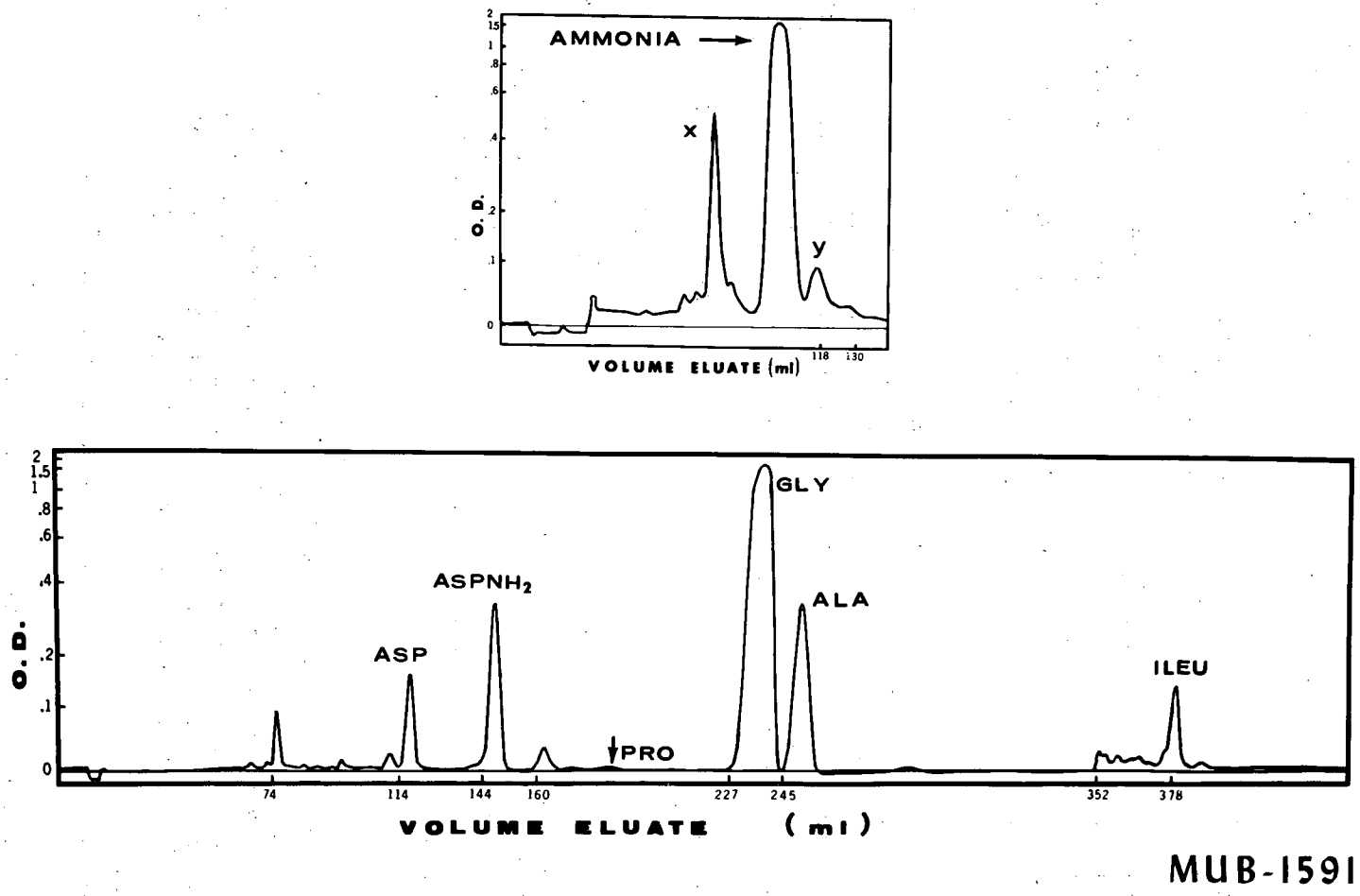

Fig. 9-5. Elution diagrams of the amino acids of S-3-A separated by two ion-exchange columns. A short column (top) was used for basic amino acids, and a long one (bottom) for acidic and neutral animo acids (Beckman-Spinco Model 120 analyzer).

identified by their positions in the eluate from a long column–include aspartic acid, asparagine, glycine, alanine, and isoleucine. Traces of other amino acids can also be observed. One of these corresponds to proline by its position in the eluate and the color given with ninhydrin.

Several unidentified peaks (X, Y, etc.) can also be observed in the eluate from the short column, which is usually run for basic amino acids. The large ammonia peak shown here is no doubt the result of hydrolysis of amino acid amides such as asparagine.

Evidence for the formation of asparagine was also obtained in experiment S-7, as shown by comparing a two-dimensional chromatogram of the reaction product of this experiment (Fig. 9-6) with that of a standard mixture of amino acids containing asparagine (Fig. 9-7). These chromatograms were obtained by descending development, using oxalic acid-washed Whatman No.4 paper and n-propanol-15M ammonium hydroxide-water, 6:3:1 (PAW) and n-butanol-propionic acid-water, 14:9:10 (BPW), as the first and second solvents, respectively. After the chromatograms were dried they were sprayed with ninhydrin.

A spot with Rf 0.49 in PAW and 0.36 in BPW can be observed in Fig. 9-6. This spot showed a change in color from brown to purple (Br → P). Authentic asparagine has Rf 0.53 in PAW and 0.39 in BPW (Fig. 9-7) and also showed an identical change in color (Br → P). The smaller differences in Rf were probably caused by the higher ionic strength of the concentrated product of S-7 as compared with that of the standard mixture of amino acids.

To the right of asparagine (Fig. 9-6) a more intense spot which underwent the same color change (Br → P) can be observed. By its Rf in the two solvents this compound corresponds to glycinamide. The characterization of this amide and other possible amino amides, which are suggested by the spots with similar color changes (Br → P) in the upper right corner of the chromatogram (Fig. 9-6), could not be carried out further because ion-exchange-column chromatographic methods have not yet been developed for amino amides. No identification of the green spots (G) of S-7 was attempted at this time. Tentatively these spots are presumed to be amino amides and amino nitriles since aspartic acid diamide[17] and β-amino propionitrile form green derivatives with ninhydrin.

The formation of asparagine and glycinamide in these experiments is significant in two respects. First, it confirms earlier observations,[19] made in similar experiments, that the amides of amino acids are the immediate precursors of the latter compounds. Secondly, it adds experimental support to the hypothesis that amino amides may have played a role in the synthesis of polypeptides under possible primitive earth conditions,[20] since it has been shown that polypeptides can be obtained from asparagine in aqueous systems.[21]

---

19. J. Oró, A. Kimball, R. Fritz, and F. Master, Arch. Biochem. Biophys. 85, 115 (1959).

20. J. Oró and C. L. Guidry, Nature 186, 156 (1960).

21. J. Kovacs and H. Hagy (Kovacs). Nature 190, 531 (1961).

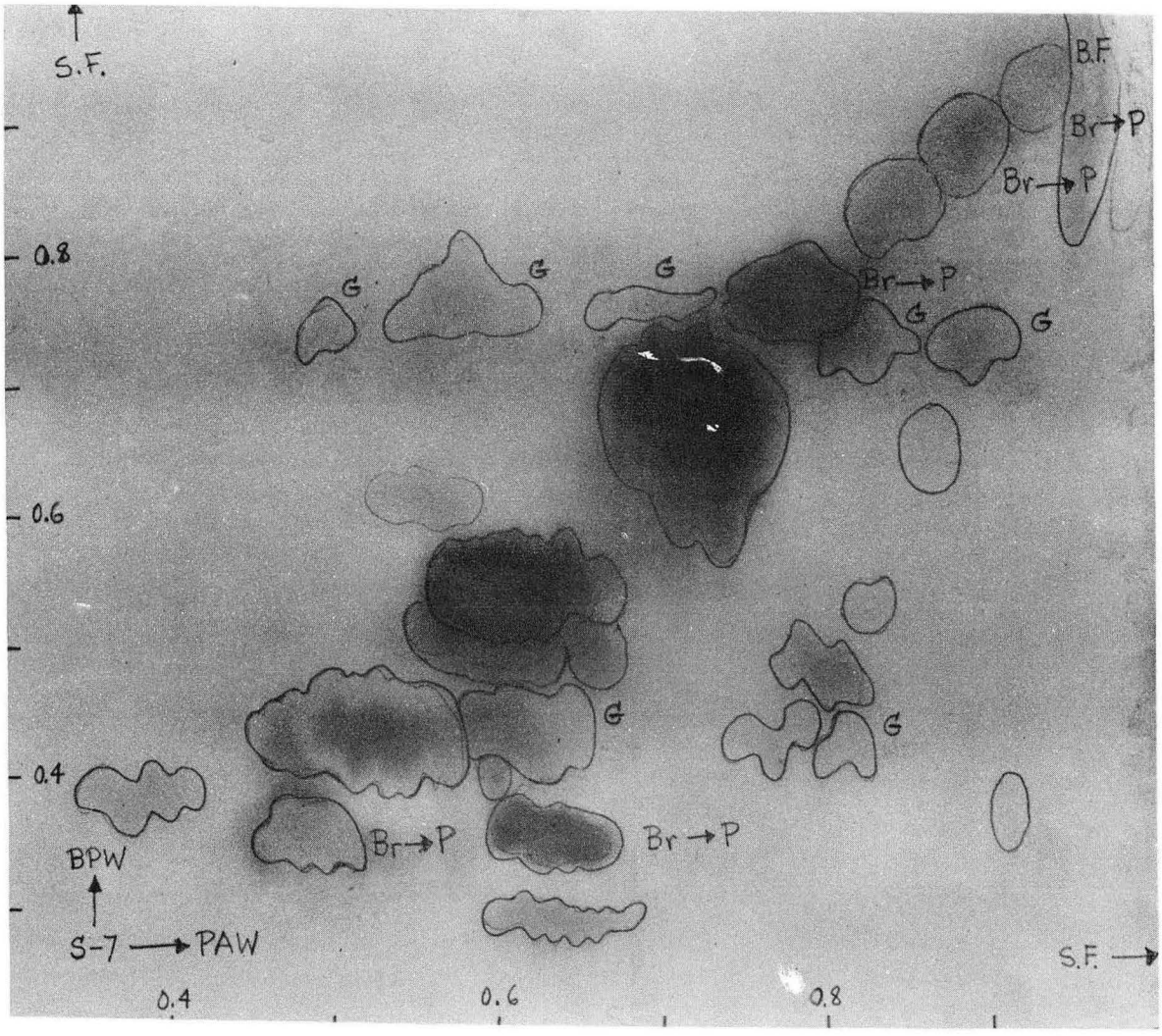

ZN-3558

Fig. 9-6. Photograph of a two-dimensional paper chromatogram of S-7, sprayed with ninhydrin. Descending development in the BPW and PAW solvents (see text). Letters to the right or above the spots indicate color or color changes; i. e., G: green Br → P: color first brown, then turned into purple. Unlettered spots are purple.

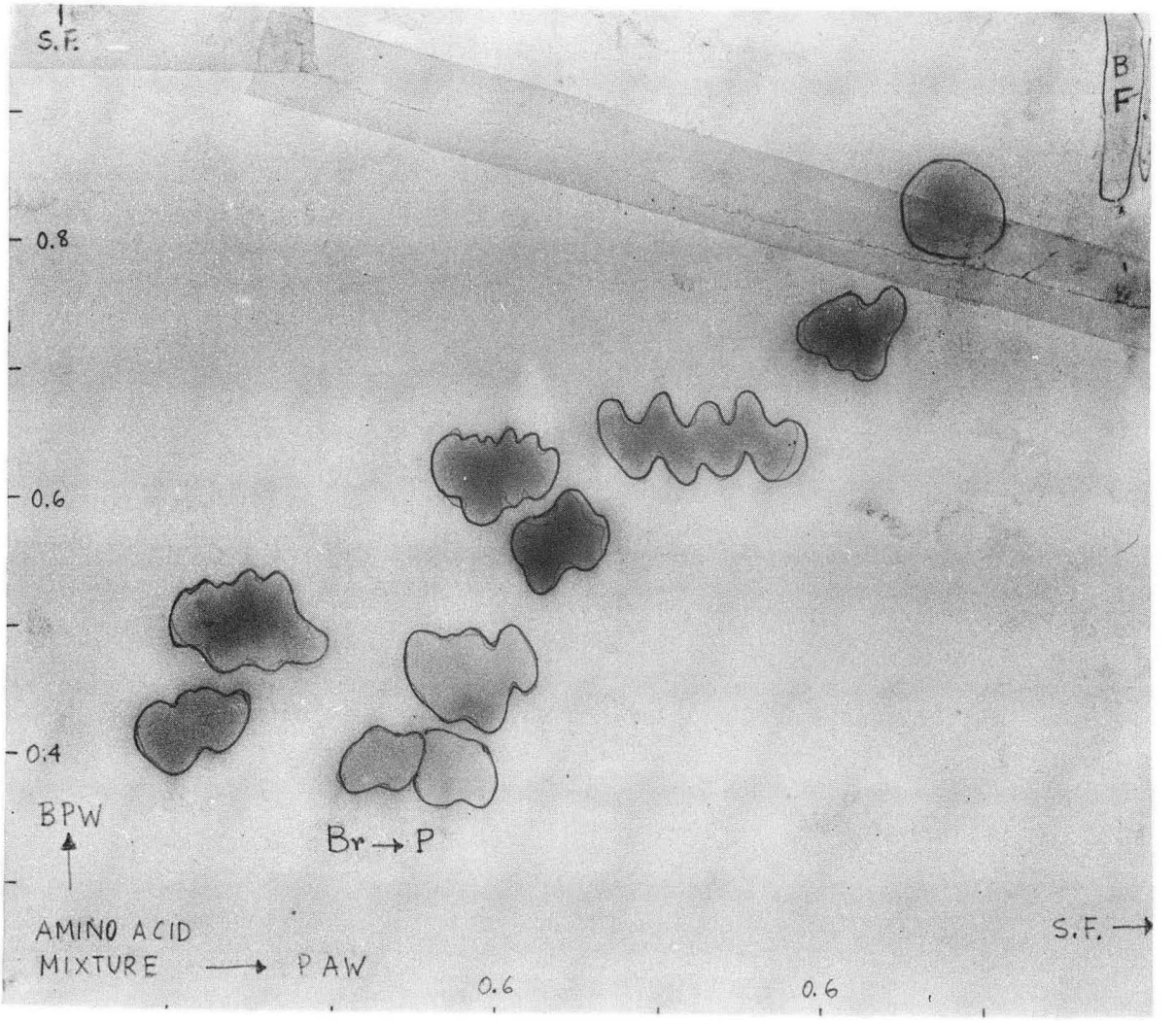

ZN-3559

Fig. 9-7. Photograph of a two-dimensional chromatogram of a standard amino acid mixture. From top to bottom following approximately the diagonal line the spots correspond to: Leu + ileu, val, α-n-but, β-ala, gly + ser, asp-NH_2 (Br→P), and lys. The two spots on the left, close to 0.4 and 0.5 (BPW) correspond to asp and glu, respectively.

The identification of isoleucine (Fig. 9-5) provides indirect information concerning the formation of the aliphatic aldehydes, which are supposed to be the early precursors of the amino acids in these experiments. By the addition of ethane to the methane-ammonia-water reaction mixture, the probability of formation of aldehydes with hydrocarbon chains of four or five carbon atoms increases significantly, assuming that they are formed by processes of methyl radical recombination.[10] Valine has also been detected in similar experiments with electrical discharges by using ethane-methane-ammonia-water reaction mixtures.[22] However, it is not clear why valine was not also formed in experiment S-3 and why only traces of leucine (if any) were formed. An extension of these studies would probably reveal details of the mechanism of aldehyde formation.

Little can be said with regard to the formation of proline except to state that a very small peak was obtained at the corresponding elution place (Fig. 9-5) and that the O. D. for this elution peak at 440 mμ was almost 100% higher than that at 570 mμ. If this peak corresponds to proline the small peak in front of proline would correspond to glutamic acid.

^{14}C compounds

Two experiments were carried out with ^{14}C reactants. In the first of these experiments (S-5), 1mC of ^{14}C methane (8 mg) was used. The unreacted ^{14}C methane and other gaseous ^{14}C components from S-5 were recovered and used in a subsequent experiment (S-6). This was done as follows: At the end of the first experiment, the gases of the reaction product were trapped into two cold traps, immersed in liquid nitrogen, which were connected in series. The trap farther away from the flask contained 50 g of molecular sieve (Linde Type 4A 1/16-in. pellets) for the absorption of methane. In less than 1 h the pressure in the reaction flask fell to about 1 in. Hg, which is approximately the vapor pressure of water at 27°C. This indicated that essentially all the gases and volatiles had been condensed in the cold traps. After removing the main reaction product (yellowish solution) from the flask, the flask was evacuated and connected again to the traps, which were allowed to warm to room temperature. In this manner the bulk of the gases from the traps diffused back into the reaction flask. These gases—together with additional nonradioactive methane, ammonia, and water—were used as reactants for the second experiment (S-6).

The concentrated reaction products from S-5 and S-6 were then individually chromatographed in the PAW-BPW solvent system described previously. Autoradiographs of these chromatograms are shown in Figs. 9-8 and 9-9, respectively. By comparing the autoradiograms of S-5 and S-6 with the ninhydrin-sprayed chromatogram of S-7, a general resemblance of distribution of spots in the three chromatograms can be observed, even though different methods of detection were used and the three chromatograms correspond to three different experiments.

The first three spots on the diagonal line of S-6 (Fig. 9-9) correspond, very likely, to asparagine, glycine, and alanine. This is shown by comparing

22. J. Oró and L. Enberg (University of Houston), unpublished experiments.

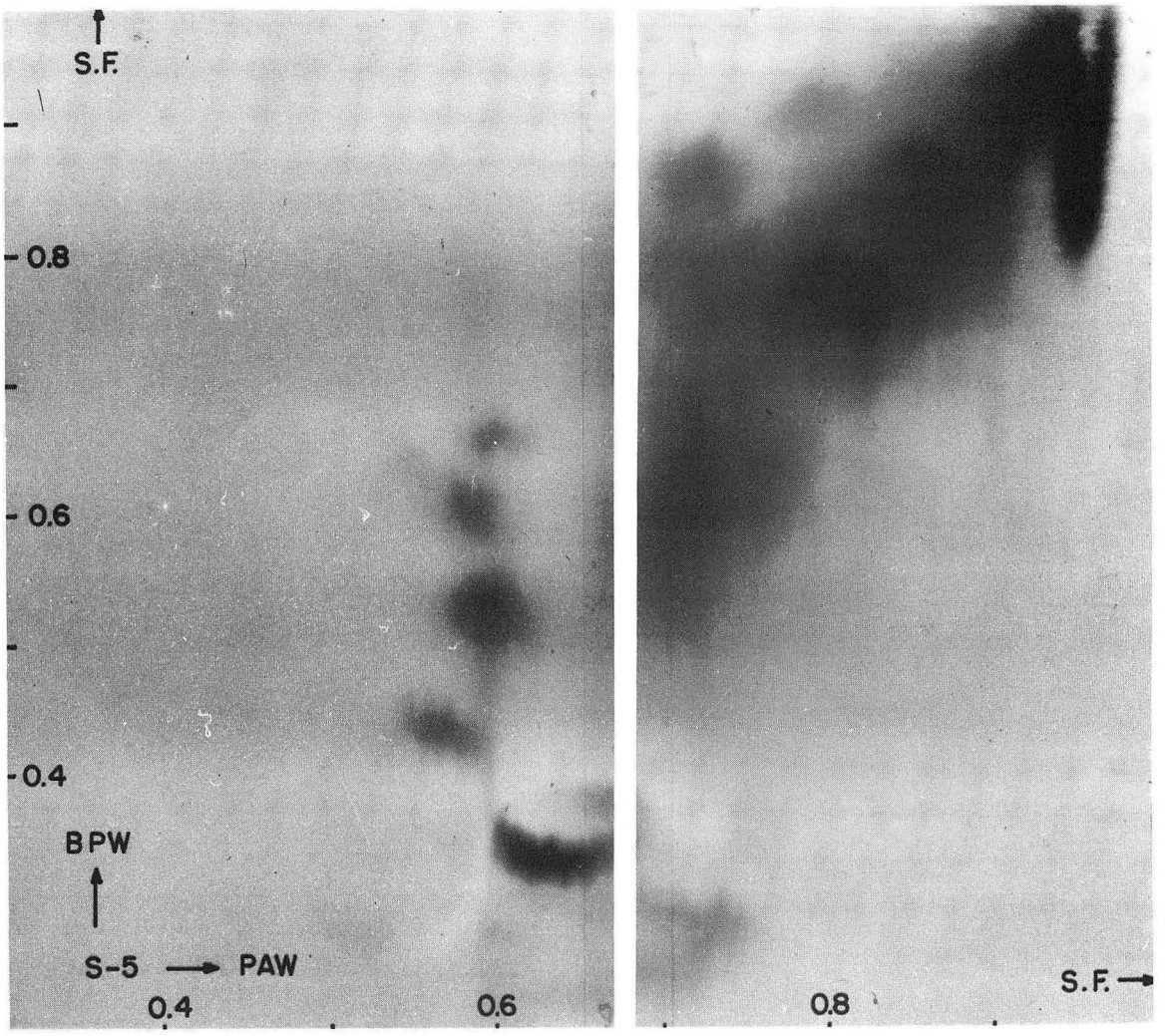

ZN-3561

Fig. 9-8. Radioautograph of a two-dimensional chromatogram of S-5. Because of their size, this and other chromatograms had to be folded to expose two film plates, which were placed back to back in the same holder. The white band corresponds exactly to the bent portion of the paper chromatogram.

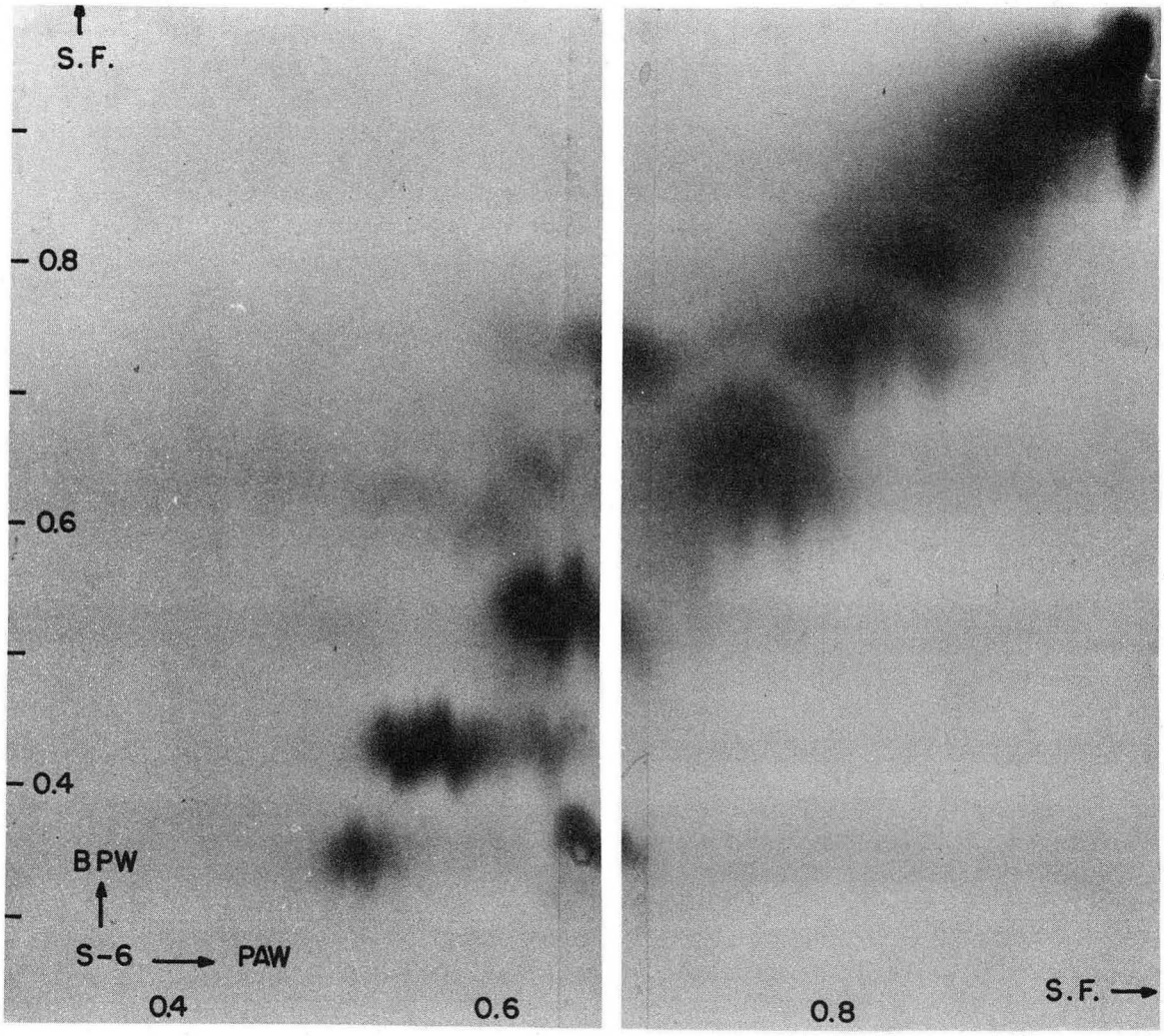

ZN-3560

Fig. 9-9. Radioautograph of a two-dimensional chromatogram of S-6. (See Fig. 9-8 for explanation of white band.)

this chromatogram with that of S-7 (Fig. 9-6) and with the chromatogram of a standard mixture of amino acids (Fig. 9-7). Radioactive and ninhydrin-positive spots can also be detected in the areas corresponding to valine and leucines. However, since no separation of bases from amphoteric substances was carried out before chromatography, some of these spots may correspond to the amides of the above amino acids, instead of the amino acids as such. The ^{14}C spot to the right of asparagine in S-6 corresponds, most likely, to glycinamide.

The largest and most diffused ninhydrin-positive compound of S-7 (Fig. 9-6) is probably caused by an aliphatic amine. (Aliphatic amines are known to produce diffused spots.) A radioactive spot corresponding to this compound can be observed clearly in S-5 (Fig. 9-8).

Aside from amino acids, amino amides, and aliphatic amines, it is of interest that other radioactive spots appear in the area of purines and pyrimidines.[23] It should be possible to identify these compounds by eluting them from the chromatogram and co-chromatographing them individually with the suspected authentic compounds. However, a more systematic approach would be to obtain a sample sufficiently large and submit it to analytical ion-exchange chromatography. The eluate could be automatically scanned with a short-wavelength uv-light lamp and with a scintillation counter. Coincidence of uv-absorption with radioactivity would exclude any possibility of contamination.

Polymers and Other Compounds

In a number of experiments a transparent solid material was observed to be formed on the glass surface of the apparatus close to the electrodes. It extended in the form of a thin layer, around each electrode, to about one-fourth of the total area of the flask.

This product was insoluble in ordinary organic solvents and water, and could not be dissolved, degraded, or hydrolyzed by boiling in 6N hydrochloric acid overnight. It could be separated in the form of thin flakes from the glass surface only after long standing in acid. This material is presumed to be similar to the one obtained by Wilson[24] in analogous experiments with electric discharges. Because of its nature, which is supposed to be a highly cross-linked polyethylene-type polymer with some functional groups, and its peculiar way of formation (surface or interphase electrodic phenomena), it remains uncertain at this moment what role this or similar polymers may have played in prebiochemical evolution.

Preliminary evidence for the formation of small-molecular-weight peptides was given by some of the two-dimensional paper chromatograms of Fig. 9-4. In particular S-3 and S-3-A showed two elongated spots close to the origin, which gave a brown color after being sprayed with ninhydrin. This brown coloration changed very slowly into purple. Because of their low rate

---

23. C. Ponnamperuma, in Bio-Organic Chemistry Quarterly Report, UCRL-9900, October 1961, p.45.

24. A. T. Wilson, Nature 188, 1007 (1960).

of migration and their characteristic way of reacting with ninhydrin, these compounds are most likely peptides or polymers of amino acids. Almost identical spots were observed in the reaction product from hydrogen cyanide-ammonia-water reaction mixtures,[25] and it has been definitely shown by Lowe and associates[26] that polymers of amino acids are formed in these experiments. The above-mentioned ninhydrin-positive spots shown in chromatograms of S-3-A are supposed to correspond to the compounds X and Y which were observed to be eluted from a short ion-exchange column (Fig. 9-5). The product analyzed by column chromatography was also S-3-A.

Finally, it will be recalled that the gaseous and volatile products of experiment S-5 were condensed in two traps immersed in liquid nitrogen. After allowing the gases to diffuse back to the reaction flask, a few milliliters of water–together with a white suspended material and three or four droplets of a transparent pale-yellow oil–were observed in the trap adjacent to the flask. The yellow oil was soluble in carbon tetrachloride. These materials were not analyzed, but they suggest the possibility of formation of lipophilic substances in experiments with electric discharges.

Acknowledgments

The author would like to thank Professor M. Calvin for providing the stimulus and laboratory facilities to carry out these experiments, and Dr. R. Lemmon for continued advice during the course of this investigation. The technical assistance of F. Woeller in some phases of this work is also gratefully acknowledged.

25. J. Oró and S. S. Kamat, Nature 190, 442 (1961).

26. C. U. Lowe, M. Reese, and R. Markham, Nature (in press).

10. SYNTHESIS OF ORGANIC COMPOUNDS BY HIGH-ENERGY ELECTRONS

John Oró

The use of ionizing radiation for the synthesis of organic compounds under possible primitive earth conditions was initiated by Calvin and associates.[1] These investigators obtained formic acid and formaldehylde by irradiating aqueous solutions of carbon dioxide with 40-MeV helium ions. Getoff et al.[2] confirmed these results by using ^{60}Co γ-rays; in addition, they observed the presence of acetaldehyde among the reaction products.

Since the above initial observation was made, a number of experiments have been reported[3-7] which show the formation of a few amino acids and other organic molecules by the action of ionizing radiation on simple compounds, or mixtures of compounds, containing C, N, O, and H.

More recently, Palm and Calvin[8]–using ^{14}C methane in aqueous ammonia mixtures and irradiating with 5-MeV electrons from a linear accelerator–observed the formation of glycine, alanine, aspartic acid, several hydrocarbons, and a relatively large number of other unidentified compounds. Among these compounds, purines and pyrimidines were suggested to be present.[9,10]

Further experiments using ^{14}C methane and 5-MeV electrons have been performed in this laboratory and are discussed here. Some experiments were carried out with the irradiated mixture mainly in the gas phase so that the results obtained here may be compared with those obtained with electrical discharges under similar conditions.[11] An experiment was carried out with a mixture of ^{14}C methane, ammonia, and water in the solid phase. It was thought that such an experiment may give some insight into the possible products formed by electrons ejected from the protosun acting on "ices"[12] or

---

1. W. M. Garrison, D. C. Morrison, J. G. Hamilton, A. A. Benson, and M. Calvin, Science 114, 416 (1951).
2. N. Getoff, G. Scholes, and J. Wiss, Tetrahedron Letters No. 18, 17 (1960).
3. T. Hasselstrom, M. C. Henry, and B. Murr, Science 125, 350 (1957).
4. R. Paschke, R. W. H. Chang, and D. Young, Science 125, 881 (1957).
5. K. Dose and B. Rajewsky, Biochim. Biophys. Acta 25, 225 (1957).
6. K. Dose and K. Ettre, Z. Naturforsch. 13b, 784 (1958).
7. R. Berger, Proc. Natl. Acad. Sci. U. S. 37, 1434 (1961).
8. C. Palm and M. Calvin, J. Am. Chem. Soc. 84, 2115 (1962).
9. M. Calvin, Chemical Evolution, Condon Lectures, Oregon State Board of Higher Education (University of Oregon Press, 1961).
10. C. Palm and M. Calvin, in Bio-Organic Chemistry Quarterly Report UCRL-9900, October 1961, p. 51.
11. J. Oró, in preceding section of this report.
12. F. L. Whipple, Astrophys. J. 111, 375 (1950).

hydrates[13] of simple compounds of carbon and nitrogen assumed to have been present in the primordial solar nebula. (Such interactions may also have occurred in protoplanetary bodies,[14] and may be occurring presently in comets[15] and other cosmic bodies of the solar system.)

The results have shown that the pattern of compounds formed by the irradiation of the above-mentioned mixtures in the gas phase is similar to the pattern of compounds formed by the action of electrical discharges on analogous mixtures. Secondly, it has also been observed that the irradiation in the solid phase of methane-ammonia-water mixtures leads to the formation of a reasonably large number of nonvolatile organic compounds.

Experimental Procedure and Results

Irradiation Technique and Dosimetry

In general, the irradiation technique, particularly that used in the gas-phase experiments, was essentially that of Palm and Calvin.[8] High-energy electrons (5 MeV) were delivered from a linear accelerator.* The absorbed dose was measured by means of a cobalt glass dosimeter. For this purpose a tube similar to the irradiation vessel was built (Fig. 10-1), and small pieces of cobalt glass were located inside the tube every 5 cm along its axis. The tube was partially evacuated, placed in front of the linear accelerator with its axis coinciding with that of the electron beam, and irradiated for a given time. The color change of the cobalt glasses was measured by means of a spectrophotometer. The corresponding number of rads/μC was plotted against the distance of each piece of cobalt glass to the window of the linear accelerator. The results are shown in Fig. 10-2. It can be seen that the dose absorbed at about 25 cm (middle of the tube) is of the order of 1.5×10^4 rads per microcoulomb. In general, each irradiation was carried our for a period of 2 h. The current used during this time was 64 800 microcoulombs. Therefore, considering complete linearity, the dose absorbed was of the order of 10^9 rads (10^{11} ergs per gram).** For individual experiments the approximate values for the absorbed dose are given in Table 10-I.

---

13. S. L. Miller, Proc. Natl. Acad. Sci. U. S. 47, 1798 (1961).

14. W. A. Fowler, Science 135, 1037 (1962).

15. J. Oró, Ann. N. Y. Acad. Sci. (in press); Proc. Lun. Plan. Explor. Colloq. (in press).

* The linear accelerator was operated by W. Everette and D. Pounds, of of the Lawrence Radiation Laboratory, who also carried out the dosimetry. Their help is gratefully acknowledged.

** It is of interest to note that this measured value agrees with the upper value calculated previously by Palm and Calvin.[8]

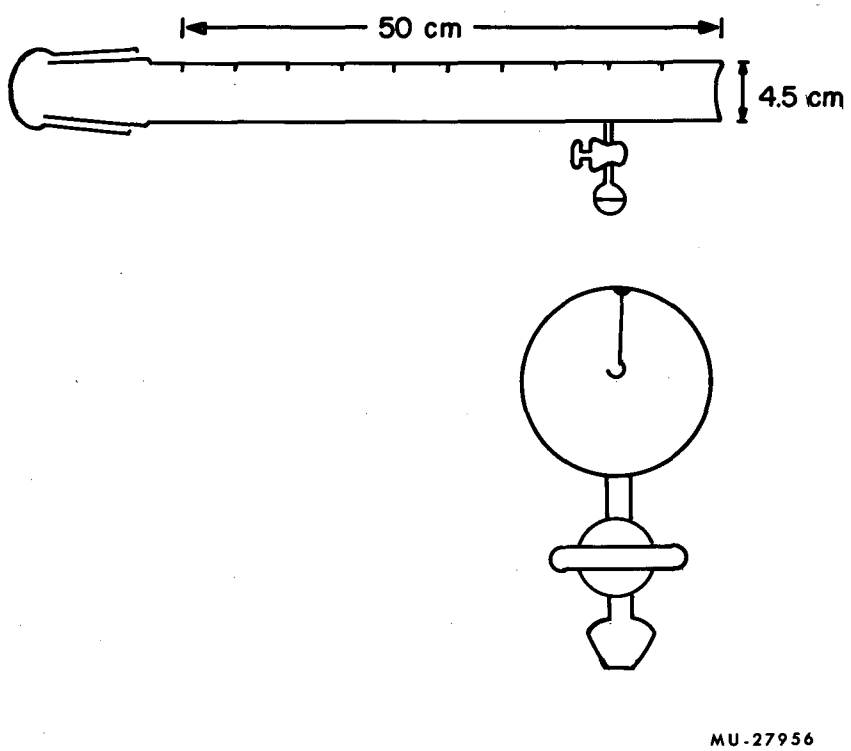

Fig. 10-1. Diagram of a Pyrex glass tube used for dosimetry. Small rectangular pieces of cobalt glass were placed inside the tube at distances of 5 cm along the tube, but in different radial positions.

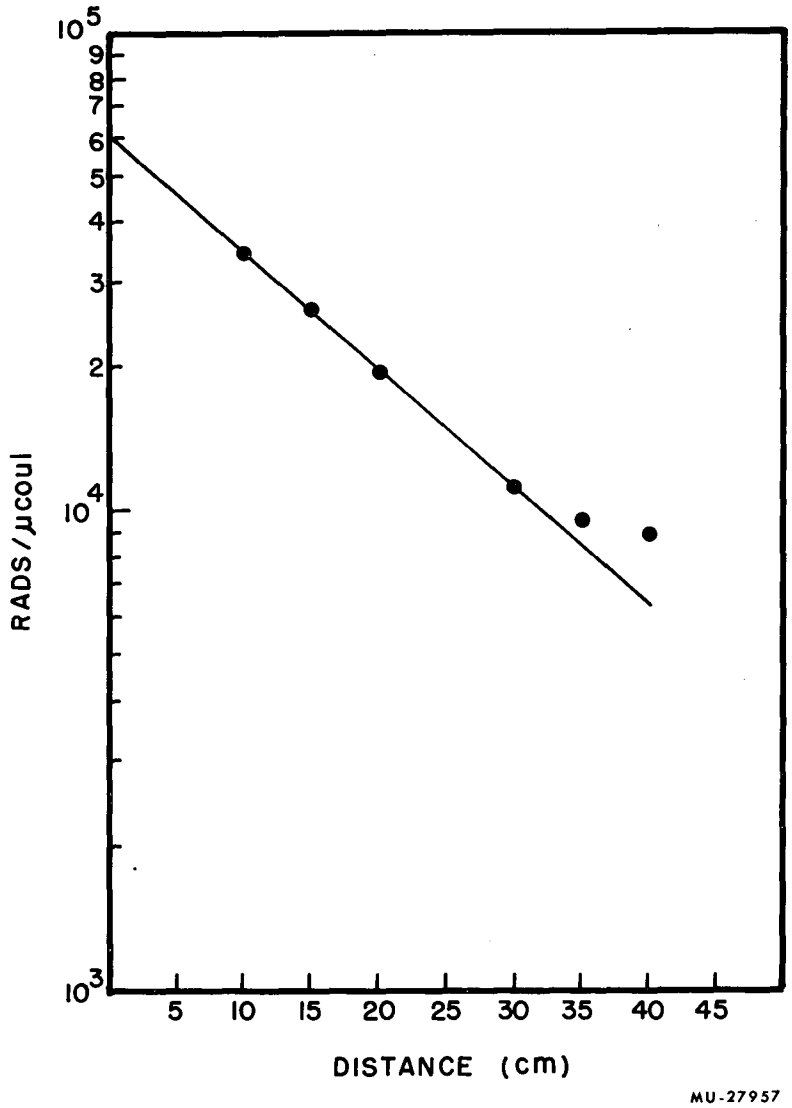

Fig. 10-2. Semilogarithmic plot of rads per microcoulomb vs the distance of each piece of cobalt glass to the window of the linear accelerator.

Gas-Phase Experiments

Not all the experiments were performed under the same conditions. The first and second experiments (RS-1 and RS-2) were carried out with the hydrocarbons in the gas phase under slightly reduced pressure, and water and ammonia in both the liquid and vapor phases. The vessel used in these two experiments was the same tube B described by Palm and Calvin.[8] Only a minor modification was made: two permanent stopcocks were attached to the inlet and outlet of the tube.

After evacuation, the radioactive and nonactive hydrocarbons and a solution of ammonium hydroxide were successively introduced into the vessel. The ammonium hydroxide solution was prepared by using boiled distilled water, and care was exercised to avoid any bubbles of air going into the system. The tube was placed in front of the linear accelerator and irradiated. In experiment RS-2 the bottom well of the tube B was heated during irradiation to reflux the water and thus increase the partial pressure of the water vapor. In experiment RS-1 this was not done.

Solid-Phase Experiment

Experiment RS-4 was carried out in the apparatus described in Fig. 10-3 with the reactants in the solid phase. The reactants were admitted into the horizontal tube at ambient temperature under slightly reduced pressure and then liquid nitrogen was added into the adjacent dewar flask. Immediate condensation of water, ammonia, and methane took place on the inside of the window facing the liquid nitrogen. The resulting layer of white crystals, approximately 2 mm thick, was irradiated for about 2 h as in the case of the gas-phase experiments. The dewar flask was always kept full of liquid nitrogen during the irradiation process, so that no volatilization or liquefaction of the solid layer took place at any time. Visual observation of the integrity of this layer was afforded by a system of mirrors which reflected the image to the outside of the irradiation chamber.

Liquid-Phase Experiment

Experiment RS-3 was performed by using a small tube, of 6.8 cc of volume, filled partially with water. The methane and ammonia were admitted while the tube was immersed in liquid nitrogen. The tube was then sealed and allowed to warm to room temperature. This resulted in a substantial positive pressure. In consequence, an appreciable portion of the methane was dissolved in water. This tube was irradiated for only 25 min; the current used during this time was 8 100 microcoulombs. The pressure measured after irradiation was of the order of 12 atm.

Analysis of Products

The gaseous and highly volatile products present in the gas phase of each experiment were not analyzed. At the end of each run the contents of each tube were diluted with water and transferred quantitatively into a small tared flask. This solution was evaporated to dryness in a vacuum rotating evaporator. The water and other volatile products were trapped in a tube immersed in liquid nitrogen. The flask containing the dry residue was

Table 10-I. Composition of gas mixtures and other data of the experiments with high-energy electrons.

	Experiment No.			
	RS-1	RS-2	RS-3	RS-4
Volume, irradiation tube (cc)	755	755	6.8	260
CH_4 pressure (cm Hg)	25	9	670	40
CH_4 activity (μC)	-	370	100	300
C_2H_6 activity (μC)	680	-	-	-
N_2 pressure (cm Hg)	25	24.5	-	-
H_2O (mliter liquid)	20	5	2	0.2
NH_4OH (m/liter)	0.5	14	6	6
Average temperature (°C)	25	80	30	-196
Time of irradiation (h)	2	2	0.4	2.5
Dose (1×10^9 rads)	1	0.97	0.12	1.3
Weight of residue (mg)	12	4.4	2	3.3
Activity of residue (μC)	28	5.5	0.07	14.0
Activity of distillate (μC)	26	1.3	0.10	3.6
Conversion of ^{14}C reactants to nonvolatile products (%)	4.1	1.5	0.07	4.6
Conversion of ^{14}C reactants to volatile water-soluble products (%)	3.8	0.3	0.10	1.2

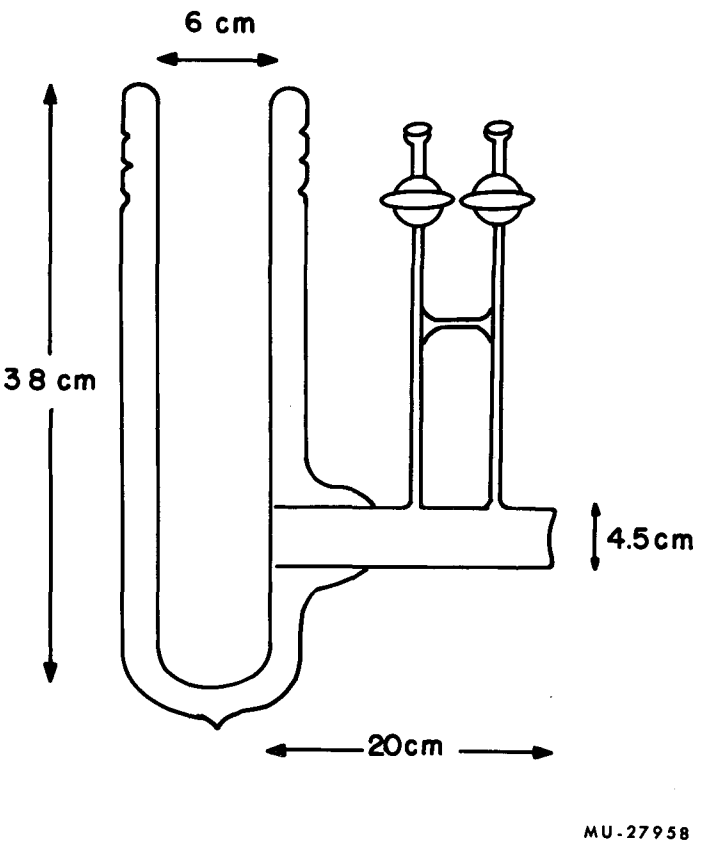

Fig. 10-3. Pyrex glass vessel used in the solid-phase irradiation experiment. The horizontal tube contained the reactants which condensed in a solid layer on the left window as soon as the dewar flask was filled with liquid nitrogen.

weighed and the residue was dissolved in 0.2 to 0.4 mliter of 0.1N hydrochloric acid. A small aliquot of the product from each experiment containing approximately 1×10^6 dpm was analyzed by two-dimensional paper chromatography and autoradiography. The chromatographic procedure followed was identical to that used in the previous experiments with electric discharges.[11]

A radioautograph of a two-dimensional chromatogram of experiment RS-2 (gas-phase irradiation) is shown in Fig. 10-4. By comparison with the radioautograph of experiment S-5 (preceding report, Fig. 9-8) it can be seen that the general distribution of compounds is similar. Since amino acids, hydroxy acids, and their respective amides and nitriles seem to predominate in the experiments with electric discharges, the tentative conclusion is made that analogous compounds are formed by irradiation with electrons.

In particular, on the left side of the RS-2 radioautograph there appear to be at least five compounds that show rates of migration essentially identical to those of five compounds on the left side of the S-5 radioautograph. Of these five compounds, it is suggested that three more intense lower spots correspond to alanine, glycine, and glycinamide. Spots corresponding to the latter compounds can also be observed in the chromatogram of S-7 (preceding report, Fig. 9-6) which was sprayed with ninhydrin.

An analogous correlation can be observed by comparing the right side of RS-2 with the right side of S-5. At least three compounds appear to have identical Rf values in the two chromatograms. This area of the chromatogram corresponds to the area of migration of some of the less polar amino acids, such as the leucines, and also of some purines and pyrimidines.

The radioautograph of the other gas-phase irradiation experiment (RS-1) was somewhat similar to that of RS-2. However, additional fast-moving components were also observed. Some of the latter compounds may be less polar or more lipophilic in nature than amino acid amides.

The existence of a similarity between the products formed by irradiation with electrons and those formed by electrical discharges should not be surprising since both processes involve excitation and ionization phenomena by electrons. In fact, the products obtained in the decomposition of methane by electric glow discharges and low-energy electrons are almost identical and include hydrogen, ethane, ethylene, acetylene, and other hydrocarbons.[16] The irradiation of methane by high-energy electrons is also known to produce hydrogen, ethane, ethylene, propane, and butane.[17]

A radioautograph of a two-dimensional chromatogram of the products obtained from the solid-phase irradiation experiment (RS-4) is shown in Fig. 10-5. A careful comparison of this radioautograph with that of RS-2 (Fig. 10-4) will reveal a number of spots with identical Rf. This correlation can be carried back to the radioautographs of the experiments with electric discharges.[11]

---

16. J. E. Manton, and A. W. Tickner, Can. J. Chem. 38, 858 (1960).

17. F. W. Lampe, J. Am. Chem. Soc. 79, 1055 (1957).

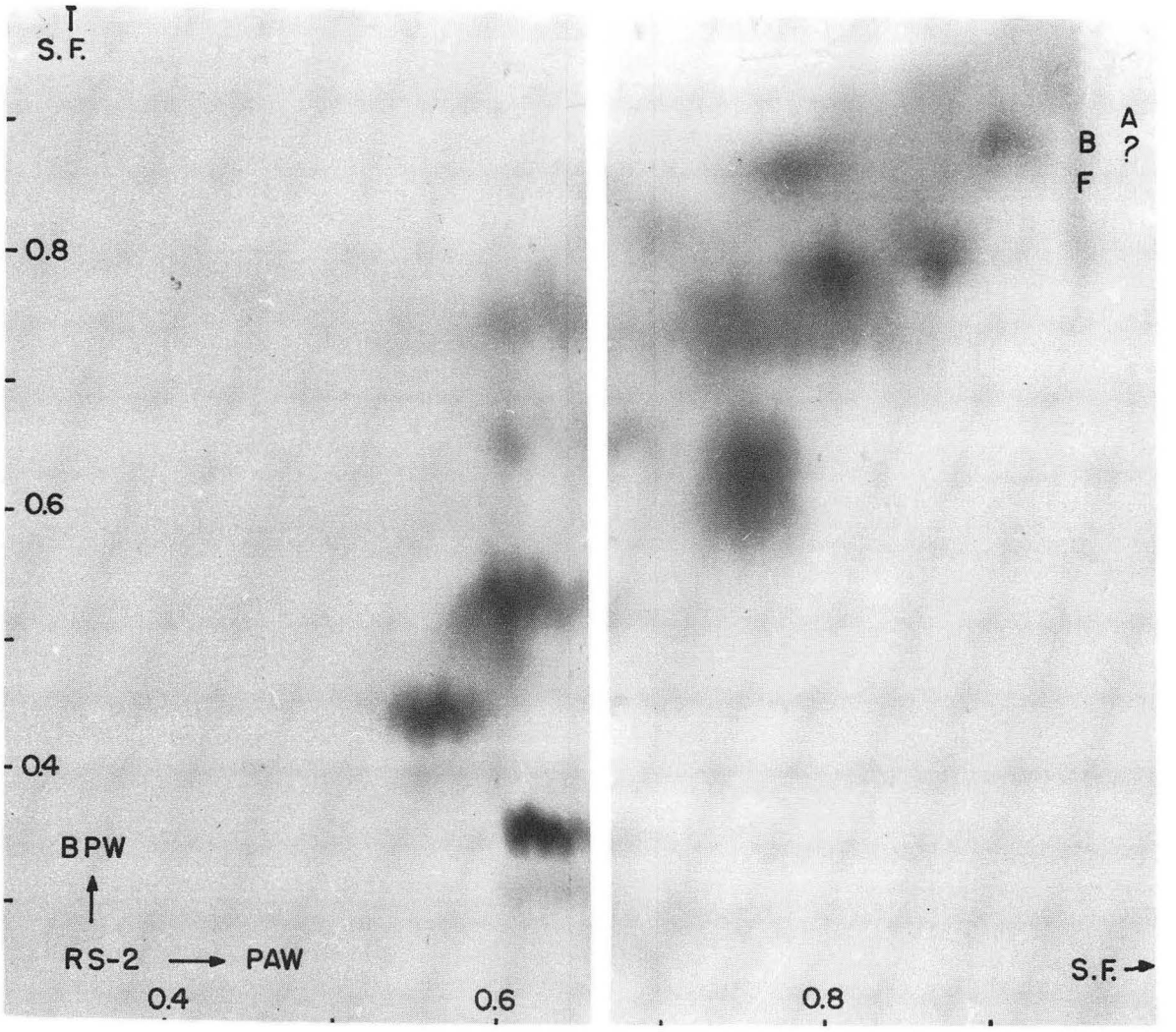

ZN-3563

Fig. 10-4. Radioautograph of a two-dimensional chromatogram of a gas-phase irradiation experiment (RS-2).

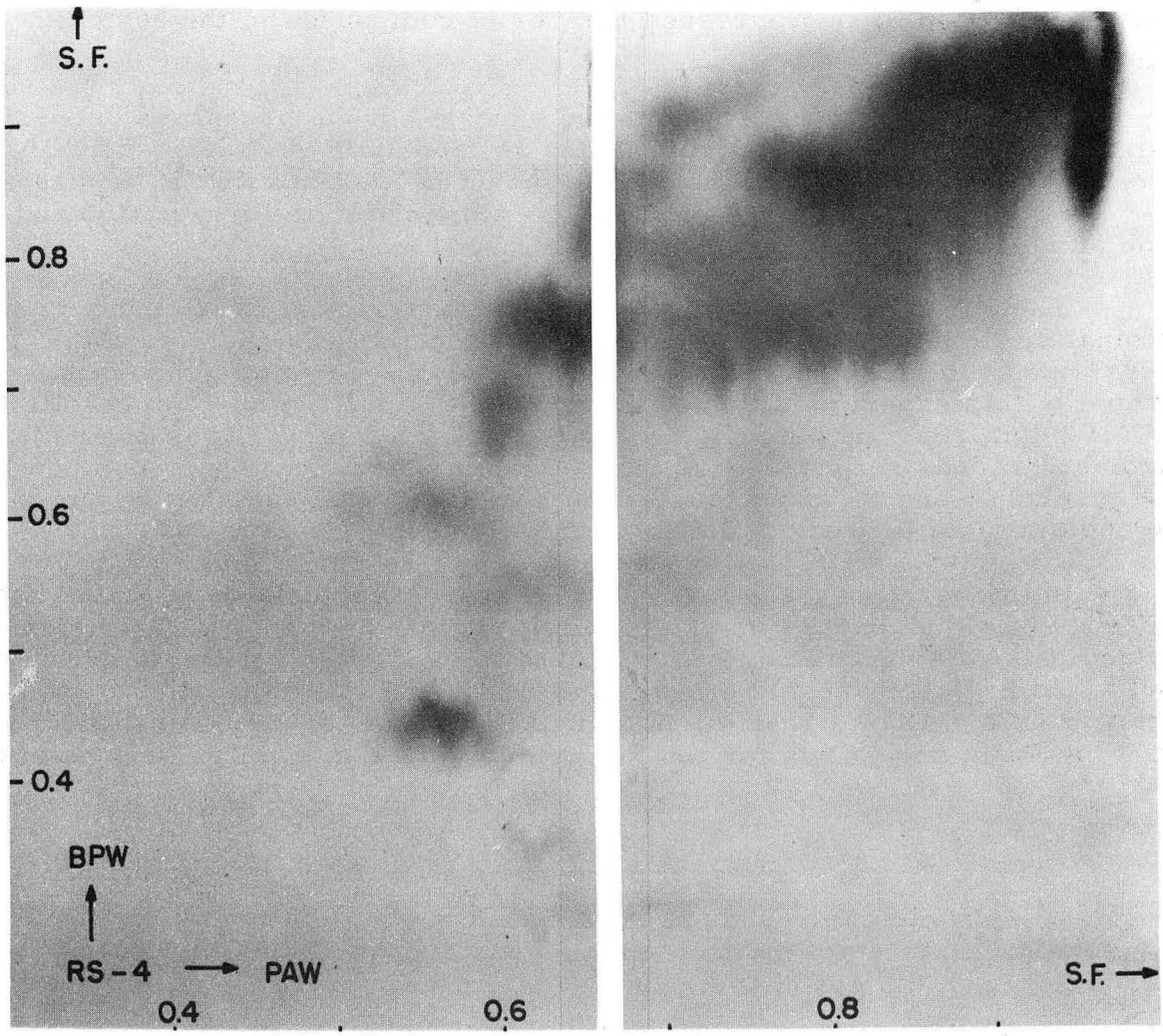

ZN-3562

Fig. 10-5. Radioautograph of a two-dimensional chromatogram of a solid-phase irradiation experiment (RS-4).

With the possible exception of what may be alanine, glycine, and glycinamide, it would appear that in general the compounds formed in the solid phase are of a less polar character than those formed in the gas phase. This is indicated by the increased number of compounds in the zone of higher Rfs.

This is probably what should be expected of the processes occurring in the solid phase, where hydrolytic and ammonolytic reactions should be very slow if not completely absent. It should be realized that it is possible that some hydrolysis has occurred between the end of the irradiation and the time at which the samples were analyzed.

The radioautograph of the irradiation experiment carried out in a predominantly liquid phase (RS-3) showed no detectable radioactive spots. It is uncertain, at the moment, whether any nonvolatile organic compounds were formed in this experiment, since the fixed ^{14}C activity was so small that only 3.8×10^4 dpm could be placed on the paper to carry out the two-dimensional chromatographic analysis. It would seem, however, that if any compound was formed in significant amounts it should have left a radioactive spot on the photographic film after five days of exposure.

In interpreting these last results, it appears very likely that in the presence of a high excess of water as compared to methane, the formation of OH radicals was the predominant effect of the radiation. This would, in turn, tend to oxidize methane and any organic compound, possibly all the way to formic acid and CO_2. This is, in fact, an extension of the mechanism proposed by Palm and Calvin for the formation of urea in similar experiments.[8]

Conclusions and Discussion

1. Organic compounds are formed in the irradiation by high-energy electrons of mixtures of methane, ammonia, and water not only when these reactants are in the gas phase, but also when they are in the solid phase.

2. The autoradiographic patterns of the compounds formed in the gas and solid phase are similar to those obtained by electric discharges. The compounds formed include amino acids, amino acid amides, amines, and other molecules of biological significance. By elution from paper chromatograms and co-chromatography in different solvents, it should be possible to establish definitely which of the compounds formed by electron irradiation are identical to those formed by electrical discharges. A more general analytical approach would involve the application of efficient column chromatographic methods to a sufficiently large sample of reaction product. As discussed elsewhere,[11] radioactive counting, uv-photometry, and other chemical tests should be carried out simultaneously with the effluent emerging from the column, to exclude the possibility of contamination.

3. On the basis of the results obtained here, and recognizing that the hydrides of C, N, and O (in the solid and gas phases) prevail in the universe, it is suggested that the radiation synthesis of organic compounds is a common natural process. If an appreciable radiation flux prevailed during the early evolution of the primordial solar nebula, an extensive synthesis of organic and biochemical compounds probably took place in the proto planets of the

solar system. The synthesis may also occur presently, at lower rates, in the atmospheres of the Jovian planets and in cometary bodies during perihelion orbital travel.

Acknowledgments

The author would like to thank Professor M. Calvin for providing the stimulus and laboratory facilities to carry out these experiments, and Dr. R. Lemmon for continued advice during the course of this investigation. The technical assistance of F. Woeller in some phases of this work is also gratefully acknowledged.

11. ULTRAVIOLET-ABSORBING COMPOUND(S) REPORTED PRESENT IN THE MURRAY METEORITE

John Oró

Introduction

Preliminary investigations from this laboratory[1-9] have shown that when a water extract of the Murray meteorite is applied to a column of Dowex 1 resin and eluted with water or with 0.05N hydrochloric acid, the eluates contain uv-absorbing compound(s).

Since some ion-exchange resins are known to yield water-soluble uv-absorbing substances,[10] the present study was undertaken to ascertain whether the compounds detected in meteorite extracts are indigenous to the meteorite or are the result of contamination by the analytical technique used.

The results presented here show that the uv spectra obtained from meteorite extracts passed through Dowex 1 and the spectra given by blank eluates from Dowex 1 are essentially identical. Observations concerning the presence of similar water-soluble uv-absorbing substances in Dowex 2 resin are also described.

---

1. S. K. Vaughn, in Bio-Organic Chemistry Quarterly Report, UCRL-8961, September 1959, p. 44.
2. S. K. Vaughn, in Bio-Organic Chemistry Quarterly Report, UCRL-9041, December 1959, p. 24.
3. S. V. Himes (nee Vaughn), in Bio-Organic Chemistry Quarterly Report, UCRL-9208, March 1960, p. 7.
4. S. V. Himes, in Bio-Organic Chemistry Quarterly Report, UCRL-9772, June 1961, p. 1.
5. M. Calvin and S. K. Vaughn, in Proc. 1st Space Sciences Symposium, Nice, France, 1960 (North Holland Publishing Co., Amsterdam, 1960), p. 1171.
6. M. Calvin, Chem. Eng. News 39, (21) 96, (1961).
7. M. Calvin, Ann. Internal Med. 54, 954 (1961).
8. M. Calvin, Chemical Evolution (University of Oregon Books, Eugene, Oregon, 1961).
9. M. Calvin, Perspectives Biol. Med. 5, 399 (1962).
10. D. Schwartz, Berkeley, 1962, private communication.

Summary of Previous Observations

The observations made by Vaughn[1-4] on the water extract from the Murray meteorite can be summarized as follows:

1. The spectrum obtained directly with the water extract of the meteorite showed no maxima in the uv region. A uniform absorption at the short-wavelength end of the spectrum and a very weak shoulder in the 260 to 280 mμ region were observed.[1,2]

2. No peak was found in the uv spectrum of the distillate obtained at 300°C in vacuum from the dry residue of the water extract.[1]

3. When the water extract was applied to a Dowex 1 column and the column eluated first with water and then with 0.05N hydrochloric acid, a small amount of uv-absorbing material was observed to emerge with the water eluate and a larger amount with the acid eluate.

4. The uv-absorbing spectra of the eluates, in particular of the acid eluate rechromatographed a second time through Dowex 1, showed (at pH 2) two absorption peaks—a strong one with a maximum at about 230 mμ and a smaller one with a maximum at about 273 mμ[2,3] (the maxima from the water eluate and from the first acid eluate were less well defined, yet in agreement with the above maxima).

5. At neutrality and under basic conditions (pH 9 to 10) the 230-mμ maximum shifted towards shorter wavelengths (about 222 mμ), while the 273-mμ maximum was very much decreased, and in some cases disappeared.

Experimental Procedure and Results

The Dowex 1 ion-exchange resin used here was obtained from a source identical to that of the resin that had been used previously in the meteorite studies.

A small column (5 cc) of Dowex 1 (200 to 400 mesh, × 8, Cl^- form) was eluted with 10 mliter of 0.1N hydrochloric acid at room temperature. The uv spectrum of the eluate was recorded in a Cary Model 11 spectrophotometer. Alternatively, an acid eluate of the same resin was obtained by passing 10 mliter of hot (90°C) 0.1N hydrochloric acid through a small column (1 cc) of Dowex 1. The uv spectrum of the eluate is shown in Fig. 11-1. A strong absorption peak at about 230 mμ and a smaller one at about 273 mμ can be observed in the two spectra.

The relatively larger uv absorption of the eluate obtained at 90°C compared with that obtained at room temperature indicates that the extraction of the uv-absorbing material from the resin is enhanced by the hot acid.

Elution of the same uv-absorbing material was also observed from samples of resin that were extracted with ether, regenerated with saturated sodium bicarbonate, washed with distilled water, and finally eluted with 0.1N hydrochloric acid. Figure 11-2 shows the spectrum of one such elute.[11]

---

11. Spectrum obtained by J. Ullrich.

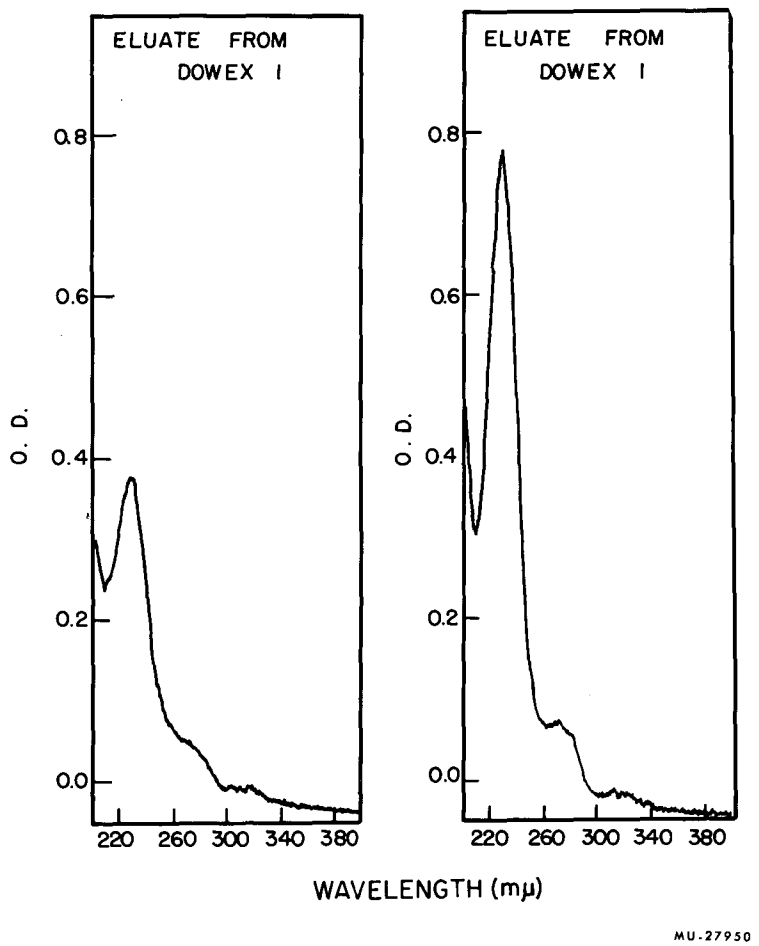

Fig. 11-1. Ultraviolet-absorption spectra of blank eluates from columns of Dowex 1 resin (Cl^- form). The eluates were obtained with 0.1N hydrochloric acid at room temperature (left) and 90° C (right).

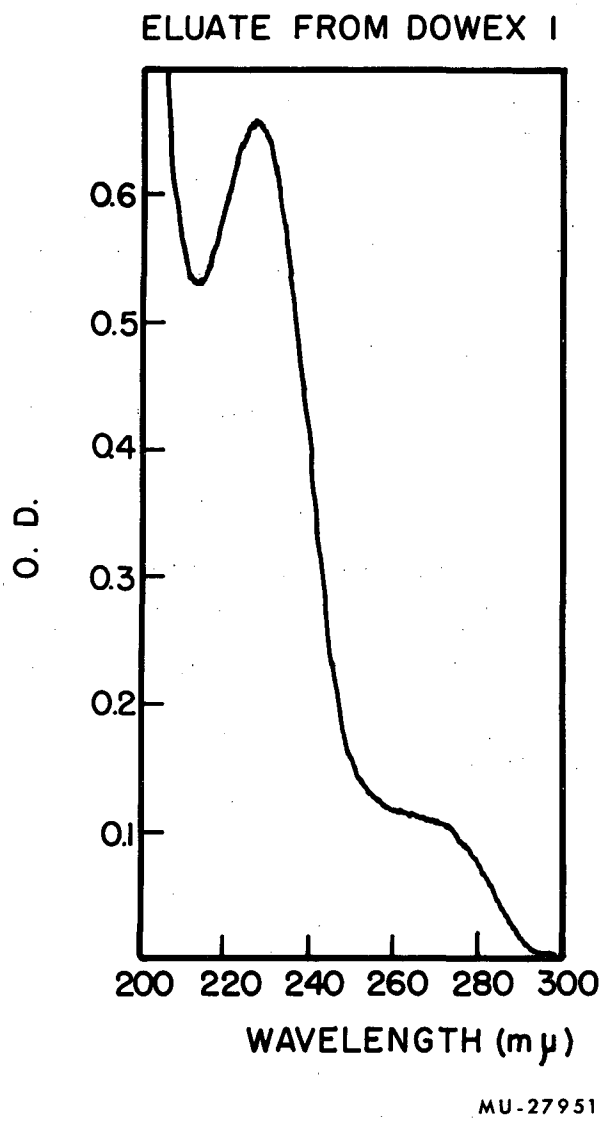

Fig. 11-2. Ultraviolet-absorption spectrum of a 0.1N hydrochloric acid eluate from a column of Dowex 1 resin. The resin had been extracted previously with ether, treated with saturated sodium bicarbonate, and washed with distilled water.

The fact that this uv-absorbing material is present after regeneration of the resin indicates that the uv-absorbing compounds are released from the inside of the resin beads. This observation is also in line with the results obtained in the extraction with hot acid.

Since Dowex 2 ion-exchange resin might be used in similar analytical applications, the presence of uv-absorbing compounds in the acid eluates from this resin was also studied.

A small column (5 cc) of Dowex 2 (200 to 400 mesh, ×8, OH^- form) was eluted with 10 mliter of 4N acetic acid. After evaporation of the acetic acid the residue was dissolved in 0.1 N hydrochloric acid. Figure 11-3 shows two of the typical spectra obtained from a number of Dowex 2 acetic acid eluates by this procedure.[12] The same two absorption peaks at about 230 and 273 mμ can be observed.

The identity of the absorption peaks obtained from resins of types 1 and 2 is not surprising. In fact it should be expected, since these two types of resins have the same structural polystyrene backbone and are manufactured following essentially the same procedure.[13]

The effect of pH change on the uv-absorption curve of a hydrochloric acid eluate from Dowex 2 is shown in Fig. 11-4. Curve A shows the uv absorption of the 0.1 N hydrochloric acid eluate, whereas curve B shows the uv absorption of the same eluate after it was made 0.1 N basic with sodium hydroxide. It can be seen that in 0.1N sodium hydroxide the 273-mμ absorption peak disappeared and the 230-mμ maximum was shifted to about 222 mμ. These changes are identical to those observed by Vaughn with the Dowex 1 eluates of a water extract of the Murray meteorite.[2]

When Dowex 2 (OH^- form) columns were eluted first with water and then with 4N acetic acid the uv-absorbing material was found in the water eluates as well as in the acid eluates, thus paralleling also the elution behavior described for the meteorite extracts.

Conclusions and Discussion

On the basis of the identity of the maxima, identity of shifts caused by pH changes, and similarity of elution pattern (observations 4, 5 and 3 of Vaughn, respectively), it is concluded that the uv-absorbing compound (s) detected in water extracts of the Murray meteorite after treatment with Dowex 1 came from the resin and not from the meteorite. This conclusion is also in

12. Spectra obtained by L. Engberg.

13. T. R. E. Kressman, in "Ion Exchangers in Organic and Biochemistry," C. Calmon and T. R. E. Kressman, eds. (Interscience Publishers, New York, 1957), p. 3, see also: Dowex: ION Exchange (The Dow Chemical Co., Midland, Michigan, 1958), p. 4.

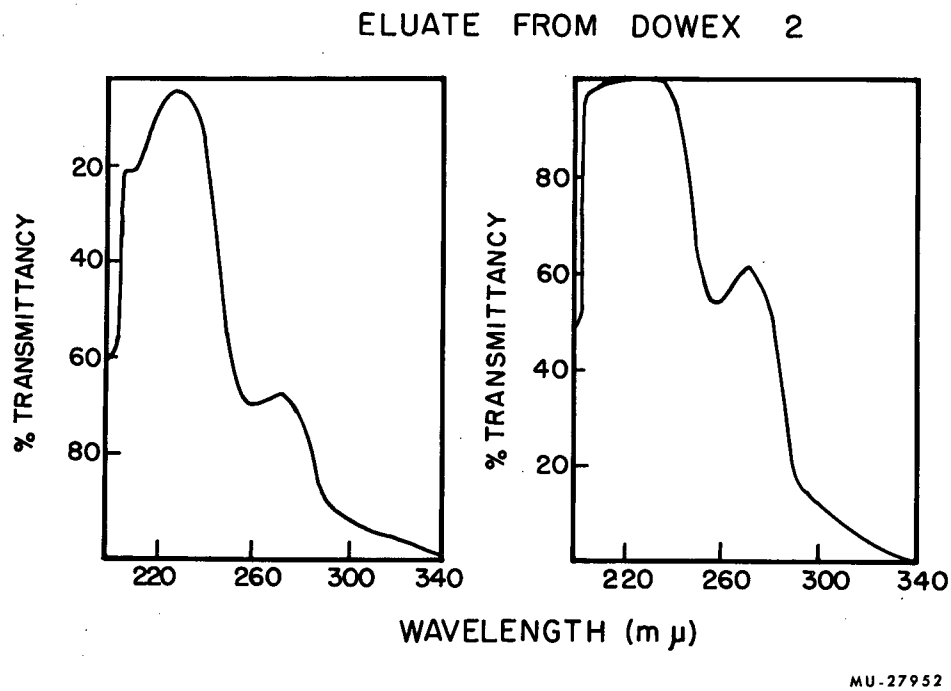

Fig. 11-3. Ultraviolet-absorption spectra of a 4N acetic acid eluate from a column of Dowex 2 resin (OH^- form). The acetic acid was evaporated and the residue dissolved in 0.1N hydorchloric acid.

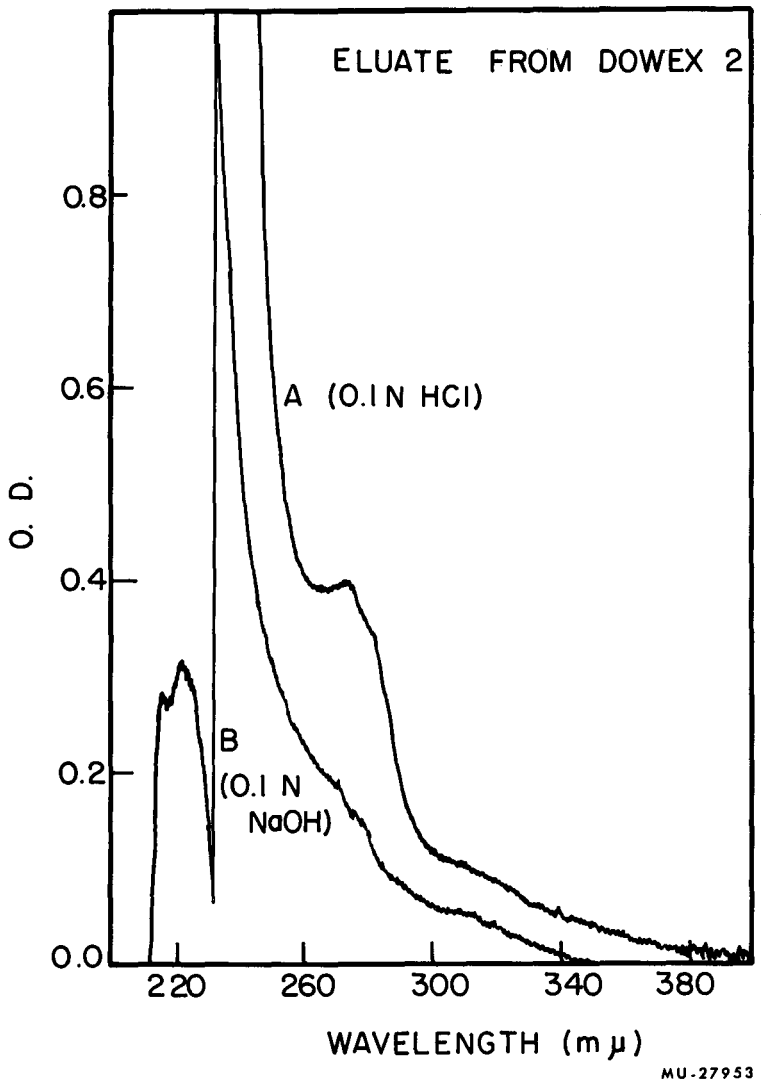

Fig. 11-4. Ultraviolet-absorption spectrum of a 0.1N hydrochloric acid eluate from a column of Dowex 2 resin (curve A) and spectrum of the same eluate after it was made 0.1N basic with sodium hydroxide (curve B).

line with the other observations[1,2] made by Vaughn. These results, however, do not exclude the possibility that some uv-absorbing compounds are present in the Murray meteorite. Vaughn's work[1] indicates the presence of such compounds because uv absorption was also found in extracts that had not come in contact with ion-exchange resins.

Acknowledgments

The author wishes to thank Professor M. Calvin for providing the laboratory facilities and the stimulus to carry out this work. The data provided by J. Ullrich and L. Engberg are also gratefully acknowledged.

This report was prepared as an account of Government sponsored work. Neither the United States, nor the Commission, nor any person acting on behalf of the Commission:

A. Makes any warranty or representation, expressed or implied, with respect to the accuracy, completeness, or usefulness of the information contained in this report, or that the use of any information, apparatus, method, or process disclosed in this report may not infringe privately owned rights; or

B. Assumes any liabilities with respect to the use of, or for damages resulting from the use of any information, apparatus, method, or process disclosed in this report.

As used in the above, "person acting on behalf of the Commission" includes any employee or contractor of the Commission, or employee of such contractor, to the extent that such employee or contractor of the Commission, or employee of such contractor prepares, disseminates, or provides access to, any information pursuant to his employment or contract with the Commission, or his employment with such contractor.